

# **BIOPHYSICAL CHARACTERISATION OF PLASMID FORMULATION**

**Supti Sarkar**

A thesis submitted in partial fulfillment of the requirements of the degree of Doctor of  
Philosophy of the University of London.

DEPARTMENT OF BIOCHEMICAL ENGINEERING  
UNIVERSITY COLLEGE LONDON

August 2005

UMI Number: U602804

All rights reserved

INFORMATION TO ALL USERS

The quality of this reproduction is dependent upon the quality of the copy submitted.

In the unlikely event that the author did not send a complete manuscript and there are missing pages, these will be noted. Also, if material had to be removed, a note will indicate the deletion.



UMI U602804

Published by ProQuest LLC 2014. Copyright in the Dissertation held by the Author.  
Microform Edition © ProQuest LLC.

All rights reserved. This work is protected against  
unauthorized copying under Title 17, United States Code.



ProQuest LLC  
789 East Eisenhower Parkway  
P.O. Box 1346  
Ann Arbor, MI 48106-1346

*To my family.*

# I. Abstract

DNA vaccination and gene therapy offer significant advantages in the treatment of many intractable diseases but many technical challenges must be overcome before the potential of these techniques are realised. A major challenge for non-viral vector particles is their physical instability in physiological conditions.

The delivery vector investigated was a Lipid-Peptide-DNA (LPD) complex. The initial system was composed of lipofectin, peptide 6 and a 6.9 kb plasmid DNA. The aim of this work was to study parameters with a view of optimising the biophysical characteristics of the system, namely with regard to storage and transportation.

The effects of ionic strength and pH on colloidal stability and structure of the gene delivery vector were investigated using dynamic and static light scattering. Results showed increased levels of aggregation at physiological concentrations (150mM NaCl), although a more stable system was observed in distilled water and at extreme salt conditions of 1M. The rates of aggregation were found to be related to the zeta potential of the system and could be predicted using Monte Carlo simulations.

Fractal dimension of complexes (where higher values correspond to more compact structures) showed values of 1.6 for 150 mM NaCl and 2.4 for 1M NaCl. Lipids, peptides and plasmid DNA were investigated to see the effect of chemistry and physical structure on the aggregation properties of the system. Lipid studies assessing the release of fluorescent calcein from a variety of lipids, over a range of pH found C14 Unsaturated + DOPE had the greatest level of release when observed at pH 5.0. The effect of increasing plasmid DNA size (number of base pairs 5.7-72) was also investigated, larger plasmid sizes showed greater stability although further investigation is required to confirm this.



## II. Acknowledgement

I would like to thank so many people that have made my time here at UCL over the last seven years, and more specifically the last three years, such a pleasant experience.

It is difficult to overstate my gratitude to my PhD supervisor, Professor Parviz Shamlou, for his genuine enthusiasm accompanied by his wealth of knowledge. I would also like to thank Dr Susana Levy, for stepping in so late in my PhD and taking over the supervisory role.

My appreciation also goes to Dr Stephen Hart, my advisor at the Institute of Child Health, who has always been patient and has allowed me to acquire a grasp of the very real biological issues associated with gene therapy. A special thanks to Dr Helen Hailes and Dr Alethea Tabor, for being so approachable and a pleasure to work with. I can't stress enough, how much I've enjoyed working in such a multi-disciplinary group, thank you for having me.

My gratitude to Dr Li Kim Lee, whose continued support, despite living abroad has helped with my work greatly. I would also like to thank Professor Nigel Titchener-Hooker and Dr Eli Keshavarz-Moore for always providing advice and encouragement throughout my stay at UCL.

If there's one thing that I'm going to miss it's definitely everyone in the Colonnades office, Helen, Roeb, James and Ihsan; it's not very often that coming to work is like meeting your best friends. Good Luck to all of you in whatever you choose to do, I hope we will always be in touch.

# III. Contents

I. ABSTRACT.....	1
II. ACKNOWLEDGEMENT .....	1
III. CONTENTS.....	2
IV. LIST OF FIGURES.....	6
V. LIST OF TABLES .....	12
VI. NOMENCLATURE.....	13
VII. PUBLICATIONS.....	15
CHAPTER 1 : INTRODUCTION .....	16
1.1 AIMS AND OBJECTIVES .....	17
CHAPTER 2 : LITERATURE REVIEW .....	19
2.1 INTRODUCTION .....	19
2.2 VIRAL GENE THERAPY .....	20
2.3 NON-VIRAL GENE THERAPY.....	23
2.3.1 Naked DNA .....	23
2.3.2 Cationic Lipid-DNA Complex (Lipoplex).....	25
2.3.3 Cationic Polymer-DNA Complex (Polypex) .....	26
2.3.4 Lipopolyplexes.....	26
2.3.5 Barriers.....	28
2.3.6 Serum Proteins .....	29
2.4 BIOPHYSICAL PARAMETERS.....	31
2.5 FORMULATION.....	32
2.6 PHYSICAL STABILITY.....	32
2.6.1 Aggregation.....	33
2.6.2 Electrical Double Layer Interaction .....	35
2.6.3 Coagulation Theory.....	35
2.7 MONTE CARLO .....	37
2.8 FRACTAL ANALYSIS .....	38
2.9 FUTURE OF GENE THERAPY .....	41
CHAPTER 3 : MATERIALS AND METHODS.....	42
3.1 MATERIALS .....	42
3.1.1 Materials .....	42
3.1.2 Peptides.....	43

3.1.3 Liposomes .....	44
3.1.4 Latex standards .....	44
3.2 SAMPLE PREPARATION .....	44
3.2.1 Preparation of Lipid/Peptide/DNA (LPD) Complexes.....	44
3.2.2 Lipid Preparation.....	45
3.2.3 Fractals Structures.....	46
3.3 MEASUREMENT TECHNIQUES .....	47
3.3.1 Dynamic Light Scattering (DLS) .....	47
3.3.2 Static Light Scattering (SLS) .....	48
3.3.3 Zeta Potential .....	48
CHAPTER 4 : LPD CONTROL EXPERIMENTS .....	50
4.1 INTRODUCTION .....	50
4.2 LIPID, PEPTIDE AND DNA COMPONENTS .....	50
4.2.1 Lipofectin.....	51
4.2.2 Integrin-Targeting Peptide .....	51
4.2.3 Plasmid DNA .....	53
4.3 LIPID/PEPTIDE/DNA COMPLEXES.....	53
4.3.1 Intermolecular forces in condensation .....	53
4.4 AGGREGATION OF LIPID COMPLEXES .....	55
4.5 VAN DER WAALS INTERACTIONS.....	59
4.6 STORAGE OF COMPLEXES .....	59
4.7 CONCLUSION .....	60
CHAPTER 5 : FRACTALS.....	61
5.1 INTRODUCTION .....	61
5.2 RESULTS AND DISCUSSION .....	63
5.3 CONCLUSION .....	76
CHAPTER 6 : AGGREGATION PROFILES.....	77
6.1 INTRODUCTION .....	77
6.2 RESULTS AND DISCUSSION .....	79
6.3 CONCLUSION .....	92
CHAPTER 7 : RATIONALE VECTOR DESIGN.....	94
7.1 INTRODUCTION .....	94
7.2 MODULAR STRUCTURE OF LPD.....	95
7.2.1 Lipid Optimisation .....	96
7.2.2 Peptide Optimisation.....	98
7.2.3 Plasmid DNA Optimisation .....	99

7.3	RESULTS AND DISCUSSION .....	100
7.3.1	Lipids .....	100
7.3.2	Peptide.....	104
7.3.3	Plasmid DNA .....	109
7.4	CONCLUSION .....	112
CHAPTER 8 : CONCLUSIONS .....		113
8.1	INTRODUCTION .....	113
8.2	FRACTALS.....	114
8.3	MONTE CARLO SIMULATIONS.....	114
8.4	RATIONALE DESIGN.....	114
8.5	RECOMMENDATIONS.....	115
CHAPTER 9 : APPLICATION TO INDUSTRY.....		116
9.1	INTRODUCTION .....	116
9.2	CURRENT COMMERCIALISATION FOR GENE THERAPY .....	116
9.2.1	Demand Uncertainty .....	117
9.2.2	Changes in Buyer Needs .....	118
9.2.3	Investment Specificity.....	118
9.2.4	Technological Discontinuities.....	118
9.2.5	Low Cost Imitation .....	118
9.3	SECOND MOVER BENEFITS .....	119
9.4	FIRST MOVER ADVANTAGE: WHEN DOES IT REALLY EXIST? .....	120
9.4.1	Market Change.....	121
9.4.2	Learning Curve .....	121
9.4.3	Switching Costs .....	121
9.4.4	Distribution Channels .....	122
9.4.5	Brand Reputation .....	122
9.4.6	Patent Protection .....	122
9.5	PHARMACEUTICALS .....	122
9.6	CASE STUDY: CLAMOXYL ANTIBIOTIC (GSK-FRANCE) .....	123
9.7	GENE THERAPY AND LPD COMMERCIALISATION .....	125
9.7.1	Learning Curve .....	125
9.7.2	Switching Costs .....	126
9.7.3	Brand Reputation .....	126
9.7.4	Brand Loyalty .....	126
9.8	RESEARCH AND DEVELOPMENT AND CURRENT LEGISLATION .....	127
9.9	CONCLUSION .....	130
CHAPTER 10 : REFERENCES .....		132

APPENDICES .....	149
PRE-EXPERIMENT .....	149
Performing angular scans on sample.....	149
SAMPLE PREP .....	150
Procedure .....	150
PAPERS .....	151

## IV. List of Figures

- Figure 4.1: Average particle size of lipofectin (1 mg/ml), in membrane filtered water (storage buffer) as a function of time. Mean sizes determined from intensity measurements of scattered light at 90 °. Data shown from a single representative sample.
- Figure 4.2: Particle size distribution of lipofectin in filtered water on the basis of the intensity of scattered light at 900. Sample measurement taken at 150 sec after preparation.
- Figure 4.3: Particle size distribution of LPD (7) in distilled water 240 sec (▲), 1800 sec (■), 3600sec (▼), 10800 sec (●).
- Figure 4.4: Lipid-DNA (LD) Aggregation profile in Phosphate Buffer Saline. Data show measurements for a single representative sample.
- Figure 4.5: Size distribution over time for an Integrin-Targeting Peptide/DNA (ID) complex. Measurements were only recorded for aggregates up to 3000 nm in size. Beyond this range the validity of the data cannot be verified since Brownian motion is no longer the only form of diffusion present in the system.
- Figure 4.6: Particle Size Distributions for LPD complexes in (A) 40 mM NaCl, symbols refer to time at min 1(!), 2min (7), 3 min (Λ), 4 min (,). (B) 150 mM NaCl at 4 min (!), 8 min (7), 12 min (Λ), 24 min (Ω ), 32 min (,), 36 min (ξ).
- Figure 5.1: Influence of salt concentration on the fractal dimension of latex particles at pH 3.0, 250mM NaCl (○) and 1M NaCl (8) for times at 2 hours and 9 days for 1M and 250mM, respectively The systems present exhibit aggregation in both the RLCA and DLCA regime. Insets show the time taken for the measured aggregate to form in each instance.

Figure 5.2: Particle size distributions of LPD complexes at a charge ratio of + 7.0 at, pH 7.2 in 150 mM NaCl, as a function of time after preparation: 0 min( $\square$ ), 4 min( $-$ ), 8 min( $\Delta$ ), 20 ( $\Xi$ ), 28 min(X), 32 min( $\psi$ ), 36 min( $\chi$ ). Size distributions were determined as mean of diameter based on the intensity of scattered light at 90°. The data shown was obtained from a three sample measurements.

Figure 5.3 Static light scattering curves for LPD particles, (scattering Intensity  $I(q)$  versus magnitude of the scattering vector ( $q$ ) obtained at successive times following the preparation of the lipopolyplexes in NaCl buffer, pH 7.2: (A) 100mM NaCl, (B) 150mM NaCl, (C) 250mM NaCl, (D) 750mM NaCl, (E) 1M NaCl times

Figure 5.4: Size distribution of LPD complexes as a function of time for varying electrolyte concentrations at pH 7.0: 40 mM ( $\nabla$ ), 80 mM ( $-$ ), 100 mM (8), 150 mM (X), 250 mM (M), 750 mM ( $\psi$ ), and 1 M ( $\square$ ). All measurements were taken using DLS

Figure 5.5: The fractal dimension ( $D_f$ ) of Lipofectin/integrin-targeting peptide/DNA (LPD) aggregates as a function of electrolyte concentration (mM). Data is given for the final  $D_f$  of the system.

Figure 5.6: Influence of buffer conditions on the dimensionless total energy of interaction between two spherical particles of a monomer hydrodynamic radius of 150 nm, as a function of the distance  $H$  (nm) between their surfaces; data generated using the DVLO theory of colloidal interactions. The total energy of interaction,  $V_T$ , between the particles was obtained by summing the van der Waals attractive potential,  $V_A$ , and the repulsive double layer electrostatic potential,  $V_R$ . (Zelphati et al., 1998; Sorensen. 2001).

Figure 5.7: Dependence of electrolyte concentration on the LPD system zeta potential. All systems were at pH 7.0. The zeta potential is calculated from the electrophoretic mobility of the particles in the buffer.

- Figure 5.8: Experimental dependence of stability ratio ( $W$ ) on electrolyte concentration. Stability values were determined from the Reerink and Overbeek approximation.
- Figure 6.1: Size distributions of: Lipid/Peptide/DNA (LPD) complexes as a function of time. Data are for different buffers (A) Phosphate Buffer Saline pH 7.4 (B) 20mM HEPES pH 7.2. (C) Distilled water pH 7.0. All measurements were taken using PCS techniques. The LPD system contained the  $(SD)_{HYD}$
- Figure 6.2: Polydispersity of LPD complexes in different buffers. Data refer to the  $(SD)_{HYD}$  in 150mM NaCl pH 7.5 (grey bars),  $(SD)_{HYD}$  in 75mM NaCl, pH 7.5 (grey bars),  $(SD)_{HYD}$  in PBS (pale bars), and  $(SD)_{GA}$  in HEPES pH 7.2 (black bars) The data shows the dependence of polydispersity on the buffer conditions which in turn controls the rate of aggregation.
- Figure 6.3: Influence of buffer conditions on the dimensionless total energy of interaction between two spherical particles of 150 nm in size as a function of distance  $H$ , between their surfaces.
- Figure 6.4: Comparison of Monte Carlo simulated data (-) of particle size distributions, with experimentally determined values ( $\nabla$ ), when placed in HEPES buffer pH 7.2, (A) 1920 sec, (B) 1200 sec (C) 1680 sec. The total number of events ( $k$ ) for a fixed cumulative time,  $t_k$  is stated for each time period.
- Figure 6.5: Data shows predicted size measurements using Monte Carlo Simulations (---) and actual experimental data ( $\blacksquare$ ). Systems shown are for (A) distilled water, (B) Hepes Buffer and (C) Phosphate Buffer Saline.
- Figure 6.6: The fitting parameter ( $\alpha$ ) used in particle size simulations shows a strong dependency on zeta potential.



- Figure 6.7: The average size of the vector particles obtained from Monte Carlo simulations (-), after a period of 30 minutes. Symbols refer to experimental data obtained from experiment under different conditions.
- Figure 6.8: Evolution of average particle size simulated by Monte Carlo techniques (- solid) and experimental data (symbols), data refer to (SD)<sub>HYD</sub>. PBS pH 7.4 (∇), 150mM NaCl, pH 7.5 (-), 75mM NaCl pH 7.5 (8), H<sub>2</sub>O (ψ). The Initial gradient of each system gives the severity of aggregation.
- Figure 6.9: The initial rate of aggregation of LPD particles is strongly dependent on zeta potential, and provides a powerful means of assessing the potential aggregation of a vector buffer system. (A): High-Moderate Aggregation. (B): Slow-No Aggregation.
- Figure 7.1: Size of aggregates 20 minutes after mixing. Data is given for saturated and unsaturated lipids, C14-C18 (C12 unsaturated only) in water and PBS in and not in the presence of DOPE.
- Figure 7.2: Percentage release of calcein from lipids across pH range 5.0-7.4 vertical bars indicate standard deviation, based on a set of three measurements.
- Figure 7.3: Average aggregate sizes in PBS, pH 7.4 as a function of time. Data refers to Peptide 6(■), MPM 108 (●), MPM 109 (7) and MPM 110 (ξ).
- Figure 7.4: (A) Average aggregate size as a function of time for different lysine chain length LPD complexes in PBS, pH 7.4. Data refers to K8 (∇), K16 (-), K24 (8) and K32 (ψ). (B) Zeta potential of K8, K16, K24 and K32. All measurements were conducted at a charge ratio of +7.
- Figure 7.5: Zeta potential measurements of LPD complexes with peptide component comprising of lysine series K8, K16, K24, K32. Measurements are shown for charge ratios +4, +7 and +10.
- Figure 7.6: Data shows LPD complexes (containing K16) at charge ratio + 4 (8), + 7 (-) and + 10 (∇).

Figure 7.7: Particle size distribution of LPD complexes in (A) distilled water, (B) 80 mM NaCl and (C) PBS. All complexes contain peptide 6 and lipofectin, with differing size plasmids, gWiz ( $\nabla$ ), psv $\beta$  ( $-$ ), pQR150 ( $\Delta$ ), p5180 ( $\psi$ ). All complexes were prepared at a charge ratio of +7.

Figure 7.8: Data shows plasmids: gWiz + H<sub>2</sub>O ( $\nabla$ ), gWiz + PBS (!), gWiz 80mM NaCl (8), psv $\beta$ +H<sub>2</sub>O (M), psv $\beta$  + PBS ( $\Omega$ ), psv $\beta$  + 80 mM NaCl ( $\Xi$ ), pQR150 + H<sub>2</sub>O ( $\xi$ ), pQR150 + PBS ( $\nu$ ), pQR 150 + 80 mM NaCl ( $\psi$ ), p5180 + H<sub>2</sub>O ( $\square$ ). All systems contain lipofectin and peptide 6 at a +7 charge ratio.

Schematic 2.1: Formation of lipopolyplex particles comprising lipofectin (L), cyclic integrin binding peptide (P) and plasmid DNA (D)

Schematic 2.2: Schematic 2.2: DNA uptake into the cell and intracellular transport: (1) cellular access to targeted cells followed by uptake through endocytosis (2) cytoplasmic trafficking of the transgene (3) fusion of vesicles with endosome compartment (4) release of plasmid from endosome into cytoplasm, dissociation from the synthetic vector, and entry into nucleus (5) after entering the nucleus, DNA must escape purging mechanisms and participate in transcription.

Schematic 2.3: Hypothetical potential energy barrier between two equal spherical particles. The net potential profile ( $V_T$ ) is a superposition of the van der Waal's potential ( $V_A$ ) and the repulsive double layer potential ( $V_R$ ). (Reproduced from Elimelech *et al.*, 1995).

Schematic 2.4: Constant Number Monte Carlo,  $N_1=N_2$ ,  $V_1<V_2$

Schematic 2.5: (A) Euclidean model used for the coalesced sphere model (CF) and (B) Fractal model for the coalesced fractal sphere (CFS). Where the smaller circles are the primary particles constituting the aggregates and the larger circles indicate the imaginary compact spheres, the volume of which is the same as the sum of the solid volumes in the aggregates.

Schematic 3.1: Peptides MPM 108, MPM 109 and MPM 110. Peptides were synthesised using standard solid phase synthesis methods.

Schematic 4.1: Modular vector components that make up Lipid/Integrin-Targeting Peptide/DNA.

Schematic 6.1: Hydrophobic linker space domain

Schematic 7.1: Peptides MPM 108, MPM 109 and MPM 110. Peptides were synthesised using standard solid phase synthesis methods.

Schematic 9.1: Generic Product Path.

Schematic 9.2: Success probability comparison between consumer and industrial goods.

## V. List of Tables

Table 5.1:	Zeta potential and dimensionless function of zeta potential at electrolyte concentrations 40 mM-1000 mM.
Table 6.1:	The total interaction, $V_T$ , between the particles obtained by summing the van der Waals attractive potential, $V_A$ , and the repulsive double layer electrostatic potential, $V_R$ , as outlined in (5.6) (5.7) and (5.8). The components used to calculate $V_T$ are shown.
Table 7.1:	Structure of C12-C18 saturated (0) and unsaturated lipids (1).
Table 7.2:	Average LPD complex size in distilled water, all experiments were conducted at 25 °C.

## VI. Nomenclature

AFM	Atomic Force Microscopy
DLCA	Diffusion-Limited Colloidal Aggregation
DLS	Dynamic Light Scattering
DNA	Deoxyribonucleic acid
DOPE	Dioeoyl phosphatidylethanolamine
DOTAP	1,2-dioleoyl-3-trimethylammonium propane
DOTMA	<i>N</i> -[1-(2,3-dioleyloxy)propyl]- <i>N,N,N</i> -trimethylammonium chloride
<i>E. coli</i>	<i>Escherichia coli</i>
FDA	Food and Drug Administration
GMP	Good Manufacturing Practice
h	hour
HEPES	<i>N</i> -[2-hydroxyethyl]piperazine- <i>N'</i> -[2-ethanesulphonic acid]
K	lysine
kb	kilobase
LPD	Lipid-Integrin Targeting Peptide-DNA
MW	Molecular weight
NaCl	Sodium Chloride
OTC	Ornithine transcarbamylase
PBS	Phosphate buffered saline (PBS)
PCS	Photon correlation spectroscopy
PLL	poly-L-lysine
RGD	Arg-Gly-Asp (arginine-glycine-aspartic acid)
RLCA	Reaction-Limited Colloidal Aggregation
SLS	Static Light Scattering
WHO	World Health Organization
$a$	Particle radius (m)
$A$	Hamaker constant (J)
$c$	Ionic concentration (mol/dm <sup>-3</sup> )
$D$	Diffusion coefficient (m <sup>2</sup> /s)
$D_f$	Fractal dimension (-)
$D_H$	Particle hydrodynamic diameter (m)
$e$	Elementary charge (1.6 x 10 <sup>-19</sup> C)

$H$	Separation distance between particles (m)
$K$	Boltzmann constant ( $1.381 \times 10^{-23}$ J/K)
$t$	Time (s)
$T$	Absolute temperature (298 K)
$V_A$	London-van der Waals (dispersion) energy (J)
$V_{\text{hyd}}$	Energy due to hydration forces (J)
$V_R$	Electrostatic interaction energy (J)
$V_T$	Total interaction energy (J)

## VII. Publications

Hurley, C.A., Sarkar, S., Floch, V., Writer, M., Wong, J.C., Lawrence, M.J., Tabor, A.B., Ayazi Shamlou, P.A., Hailes, H.C., Hart, S.H. 2004. Cationic lipid component analysis: Enhanced transfection with a ternary transfection vector. *In preparation*.

Sarkar, S., Levy, M.S., Hart, S.L., Hailes, H.C., Tabor, A.B., Ayazi Shamlou, P. 2004. The fractal structure of polycation-DNA complexes. *Biotechnology and Applied Biochemistry*, **40**, 1-10.

Sarkar, S., Zhang, H., Levy, M.S., Hart, S.L., Hailes, H.C., Tabor, A.B., Ayazi Shamlou, P. 2003. Prediction of size distribution of lipid-peptide-DNA vector particles using Monte Carlo simulation technique. *Biotechnology and Applied Biochemistry*, **38**, 95-102.

Sarkar, S., Levy, M.S., Hart, S.L., Wong, J.C., Hurley, C.A., Pilkington-Miksa, M., Hailes, H.C., Tabor, A.B., Ayazi Shamlou, P. 2003. Impact of biophysical and chemical properties of non-viral formulation on cell transfection. *AICHE Annual Conference Proceedings* 2003.

## Chapter 1 : Introduction

The complex mechanisms involved in gene therapy require a disciplinary approach to the challenges that can be categorised as *physical, chemical and biological*. To obtain a safe and efficient delivery vector, all of these challenges must be addressed. In the case of non-viral vectors, the physical stability of such vectors still remains to be fully explored, with the problem and aggregation problem being the most significant. The purpose of this thesis is to study the physical parameters that impact physical stability of the non-viral complexes and provide information on the biological behaviour of these systems. The results of this work give greater insight into these systems. It is important to note the behaviour of biological systems cannot be elucidated based on similar non-biological systems, whose behaviour is more predictable, nor do biological system conform to patterns observed with other less complex systems. The fundamental problem of aggregation has given rise to many previous studies included in the thesis. Physiological conditions, which have been mimicked through the use of Phosphate Buffer Saline and 150 mM NaCl have shown greater aggregation with increasing salt concentrations; concurrently increasing the salt concentration beyond this has shown a greater level of stability. It is however important to understand the mechanisms involved during aggregation and whether a slowly aggregating system really provides the optimum conditions for stability. The work on fractals conducted showed that rapidly aggregating complexes at 150 mM NaCl also formed the loosest structure. It is hypothesised that such a system may dissociate with greater ease in the endosome compared to the compact structure observed at 1M salt, or that these loose structures are more sensitive to shear damage during preparation and in delivery devices. The fractal dimensions of 1.6 and 2.4 for complexes prepared in 150 mM NaCl and 1M salt respectively are indicative of two different aggregation regimes, an important consideration when comparing different systems. The relationship between different physical parameters affecting aggregation of non-viral systems is important to establish. A low zeta potential indicated an unstable system resulting in aggregation. Monte Carlo, a statistical simulation tool was used in the



prediction of aggregate properties incorporating both size and zeta potential. In a similar way fractal dimensions were found to provide insight into mechanisms of aggregation.

The particular non-viral vector studied here is a lipopolyplex, a relatively advanced form of synthetic vector that contains all of the components commonly used in non-viral vector development, to provide safety and efficacy where viral vectors were deemed unable to. The components used are lipid, peptide and plasmid DNA, collectively described here as Lipid/ Integrin-Targeting-Peptide/DNA (LPD). Each component plays a different role in allowing the complex to be targeted and expressed in a cell. The modular structure of the lipopolyplex allows physical and chemical changes to be made to each component and its effect on biophysical parameters to be measured. The development of the lipopolyplex motivated my research on characterisation through improving the LPD complex by testing each component systematically. Addition of a hydrophilic spacer to the peptide reduced aggregation, with a 16 lysine peptide chain demonstrating greater stability than longer lysine chains, C14 Unsaturated + DOPE was the lipid that had the greatest release of calcein at pH 5.5.

## 1.1 Aims and Objectives

The aim of this work is to study the physical stability of LPD complexes with respect to aggregation, to examine the physiochemical properties of the system and consider the implications to biological functioning and model any effects on the stability of the system.

A common feature in many non-viral systems is the condensation of the plasmid DNA with a polycation. A condensed DNA particle is thought to be of a suitable size for penetrating cellular membranes. Important features of a condensed complex include its size and zeta potential, which will affect how the particle behaves *in vivo*. The size, fractal dimension and zeta potential will be measured using dynamic, static light scattering and LASER Doppler velocimetry, respectively.

Properties of the system are highly susceptible to changes in electrolyte salt concentration therefore an understanding of the aggregation profiles and the zeta potential of the system is desirable. It is also important to be able to find a means of relating size and zeta potential, since they are both characteristics of any given system.

Being able to quantify the levels of aggregation is critical to providing a means of distinguishing between different systems and providing a quantitative description of system stability rather than the qualitative approach to describing aggregation as has been adopted to date.

Although size is an important indicator of aggregation, it alone does not provide any information on the mechanisms involved in forming the aggregate, or if all aggregates are structurally identical regardless of size. Fractal measurements using static light scattering will study these structures to determine their fractal dimensionality. Structural information will also allow further investigation into aggregation kinetics to take into account fractal models.

To develop and improve the current LPD vector (containing lipofectin, peptide 6 and psv $\beta$ ), other materials will need to be systematically investigated. This may lead to the formation of trends as a result of altering each component chemically or physically and measuring the resulting biophysical output, it may also be possible that an optimal set of components exist that provide high stability and transfection efficiencies and only the logical testing of a variety of structures will identify this.

The employed particle characterisation techniques of static and dynamic light scattering, doppler velocimetry and flurometry will help provide a better understanding of the physical nature of the complexes. These established techniques ensure accuracy in providing process and product reproducibility on the scale of the experiments conducted here and also those carried out in future on a large manufacturing scale.

## Chapter 2 : Literature Review

### 2.1 Introduction

Gene therapy refers to the practice of applying genes to the treatment of diseases, including cancers and viral infections. The genetic material can be either DNA or RNA, and the altered function can be an increase or a decrease in the production of a protein (Godbey *et al.*, 2001). Gene therapy is regarded by many as a potential revolution in medicine; this is because gene therapy is aimed at treating or eliminating the causes of disease, whereas most current drugs treat only the symptoms. This radical improvement is possible because the gene-based approach can provide targeting. Hence, in comparison with the other form of therapy, it will permit biological effects that are more subtle and better localised to the most appropriate cells. Ultimately, this will translate into substantial improvements in therapeutic effect and cure-rate for diseases that are presently untreatable or poorly managed. Gene therapy also has the important advantage of being a broad platform technology, applicable to a wide range of diseases ranging from inherited diseases such as cystic fibrosis and cancer to acquired diseases such as AIDS (Deshmukh *et al.*, 1995; Pappas *et al.*, 1996).

In theory there are two types of gene therapy: *somatic* and *germ line*, however, due to the ethical issues (Pappas *et al.*, 1996) of germ line techniques research is at present only based on somatic treatments. Somatic gene therapy treatment involves the manipulation of an individual's genetic material, adding the normal or wild type copies of a mutant gene to cells thus restoring the correct functioning of cells, producing normal gene products and treating the symptoms of the genetic disease (Pappas *et al.*, 1996). Unfortunately unlike germ line gene therapy this treatment will not cure the disease from the population, as any progeny will still inherit the disease but it does provide hope for many people who suffer from genetic diseases.

Genes or nucleic acid molecules that regulate gene expression must be delivered into cells of the appropriate organ or tissues affected by the disease, tumour etc., (Hart *et al.*, 1999). The use of gene therapy for the treatment of diseases of both genetic and infectious origins is now becoming a reality. Crucial to the success of any gene therapy strategy is the efficiency, with which the gene is delivered, which is in turn is dependent on the type of delivery vector used. Many vectors have been developed based on either recombinant viruses or non-viral vectors (Cristiano *et al.*, 1998).

## 2.2 Viral Gene Therapy

Viruses are effective at transferring genes into cells because they have evolved specialised mechanisms that allow them to bind to specific types of cells and deliver their material efficiently into the cellular interior (Felgner *et al.*, 1997; Safinya *et al.*, 2001). Yet the therapeutic use of viruses as gene delivery vehicles, or vectors, entails problems, as some viruses can disrupt the DNA of the cells they infect, with potentially harmful results. Furthermore, weakened viruses can conceivably change inside the body and regain their pathogenic activity (Felgner, 1997). An additional serious limitation is that a patient may generate an immune response to the microbe. Fighting infection by bacteria and viruses is among the key functions of the immune system. So, bacteria (plasmids) and viruses or parts of them promptly trigger an ‘innate’ immune response as soon as they enter the body, causing cytokine production and an influx of nonspecific inflammatory cells (macrophages, dendritic cells, NK (natural killer) cells, and others).

‘Adaptive’ immunity is stimulated later, when antigen-presenting cells (APCs) carrying antigens from the microorganisms migrate to the lymph nodes. It includes the production of neutralizing antibodies circulating in the blood that are specific of the vector or transgene antigen, and a cell-mediated response involving T cells and NK cells. Adaptive immunity not only contributes to eliminating the vectors and infected cells from the body but also results in a memory response that undermines further attempts to use the same vector or transgene.

Viral vectors are the most likely to induce an immune response, especially those derived from adenovirus and adeno-associated virus (AAV), which express immunogenic

proteins within the organism. The innate inflammatory response is high with adenoviral vectors, and almost nil with AAV vectors. Plasmid DNA vectors, because of the presence of CpG dinucleotides, also tend to stimulate the innate inflammatory response.

Specific ‘adaptive’ immune responses are due to capsid antigens in adenoviruses and AAV. Viral gene-encoded proteins in adenoviruses can also be immunogenic.

In the case of retroviral vectors, the immune response is mainly directed at the transgenes located within the vector rather than the antigens in the vector itself. Nonetheless, when used *in vivo*, they are inactivated in the serum by complement activation and can also trigger a cytotoxic response, in which cells containing the vector are killed (Ho, 2005). This makes repeat dosing a major challenge for viral vector systems. As with all drug-induced toxicities, the degree to which viral vectors induce harmful immune mediated and inflammatory responses and other toxic side effects is a question of vector dose studies in the immuno-privileged rodent brain (in which innate immune response can be studied in isolation from adaptive cellular immune responses) have shown that inflammatory response to the adenovirus capsid increase linearly with an escalation in vector dose, but the situation could be more complicated in other organs, particularly if the vector particles become disseminated into the circulation. Dose-escalation studies have shown that the relationship between adenovirus dose and direct cellular toxicity is characterised by a threshold effect, cellular toxicity occurs over a narrow dose range and often no symptoms are observed until a slightly higher vector dose is administered which induces severe cellular injury (Thomas *et al.*, 2003).

The disadvantages of viral delivery include (Kreiss *et al.*, 1999; Templeton *et al.*, 1999): Generation of an immune response to expressed viral proteins that subsequently kill the target cells producing a therapeutic gene product.

- Random integration of some viral vectors into the host chromosome.
- Clearance of viruses delivered systemically.
- Difficulty in engineering viral envelope or capsids to achieve specific delivery to cells other than those with natural tropism for the virus.
- Possible recombination of the viral vector with DNA sequences in the host chromosome that generate a replication-competent, infectious virus.
- Inability to administer certain viral vectors more than once.
- High cost in producing large amounts of high-titre viral stocks for use in the clinic.

- Limited size of the nucleic acid that can be packaged and used for viral gene therapy

There have been known cases of work conducted in the developmental stages with viral vectors. A new system involving the inhalation of an aerosol that contains a viral vector, adeno-associated virus (AAV) carrying a functional copy of the gene to be found at the root of Cystic Fibrosis (CF) symptoms is being developed at Stanford University (Bradley *et al.*, 1999). Nevertheless it is likely that ultimately gene therapy will require repeat treatments (Davies *et al.*, 2001) and so taking into consideration many of the fears associated with the use of viral vectors, nonviral vectors seem to be a more realistic route for research into gene therapy (Kwoh *et al.*, 1999; Nishikawa *et al.*, 2001).

There are some formulations that combine the merits of both viral and non-viral vectors, such as virus-cationic liposome DNA and cationic lipid DNA mixed with G glycoprotein from the vesicular stomatitis virus envelope. Cell surface integrins are interesting potential targets for gene delivery by polycation-DNA complexes since they are exploited for cell entry by a number of viruses including adenovirus and echovirus (Nishikawa *et al.*, 2001).

One of the landmarks in clinical gene therapy using viruses took place in 1997 when such a method was used to treat patients with Ornithine transcarbamylase (OTC) deficiency. It was part of a highly reputable gene therapy program at the University of Pennsylvania, and was designed to be a Phase I dose escalation safety trial involving patients with mild to moderate disease that were relatively healthy and stable. In this case, the gene transfer vector was a recombinant adenovirus designed to express the wild type OTC gene. This vector was delivered directly to the liver of patients using injection via the hepatic artery; this particular delivery route was deemed to be acceptable by the Food and Drug Administration (FDA). Other federal bodies reviewing gene therapy trials, namely the Recombinant DNA Advisory Committee (RAC) and the National Institutes of Health (NIH), had suggested that the vector be administered by a safer route intravenous route. As widely reported in the scientific and popular press, this trial ended with a spectacular tragedy (Boyce *et al.*, 1999). The first hint of a problem came when a moderate toxicity was seen at intermediate vector doses, and contrary to the clinical protocol the trial was not halted and the FDA and RAC were not consulted. One patient Jesse Gelsinger was enrolled at this point even though there were some questions as to whether he met the criteria. This patient received the highest vector dose and died four days later from a

massive inflammatory response to the vector. For this reason, regarding safety and some of the other potential problems with viral vectors, scientists have begun studying possible alternative vectors in the form of non-viral or synthetic vector gene therapy vehicles.

Another safety issue concerns the delivery to the right target cells. In the late 1990s a gene therapy trial was undertaken to treat several children who suffered SCID (severe combined immune deficiency syndrome) and were forced to live in a germ-free environment thereby assuming the moniker, 'bubble boy'. The gene therapy trial was intended to restore the function of a crucial gene, gamma C, to the cells of the immune system. The trial was successful. However, two children developed leukemia as a result of mis-incorporation of the gene in a second target. Those cells went out of control causing leukemia. The children were treated with chemotherapy but the situation raises a very real safety issue (Boyce *et al.*, 1999).

## 2.3 Non-Viral Gene Therapy

Non-viral approaches to gene transfer, utilising synthetic gene delivery systems, have been the focus of intensive study over the past several years. Ongoing research and development of various non-viral vectors for commercial products testify to the significant potential of these systems. The advantages of non-viral systems such as excellent targeting, low immunogenicity, and reliable large-scale manufacture at relatively reduced costs, make them very attractive alternatives to the viral approach (Mountain, 2000).

### 2.3.1 Naked DNA

“Naked” plasmid DNA without any viral or non-viral association is the simplest form of gene delivery, and gives virtually insignificant expression in cell culture transfection experiments. Nevertheless, naked DNA injected *in vivo* demonstrates activity, especially in muscle (Wolff *et al.*, 1990). Furthermore, transfection efficiencies can be high, if not higher than those observed with equivalent non-viral gene delivery systems (Huang *et al.*, 1996). Physical methods of gene delivery, usually mechanical and electrical procedures, tend to have limited applicability compared to other gene transfer approaches. However, several of the available techniques such as needle free injectors and electroporation are promising (Mountain, 2000). Despite being laborious and time consuming, microinjection of DNA directly into the tumour cell nucleus has long been employed in *in vitro* studies

where individual cell manipulation is necessary. Electroporation, which employs strong electrical pulses to transiently create pores in the target cell; and thus allowing the DNA to enter the target cells, is a more efficient approach for *in vitro* applications (Lockie *et al.*, 1999). The most recent “gene gun” approach, or biolistic particle delivery, entails the use of electrical currents and magnetic properties to accelerate DNA coated micro-particles of gold or tungsten into cells (Luo *et al.*, 2000).

Since free DNA as a gene delivery system is unsuitable for targeting a large number of cells and tissues, its applications are limited to superficial layers of the body are available for direct injection such as the skin, or cancer gene therapy where the expression vector DNA can be injected directly into the tumour. The most encouraging applications of naked DNA at present are the injection or gene gun delivery in preventative vaccination against infectious diseases, and the delivery of naked DNA containing genes promoting angiogenesis for cardiovascular disorders (Donnelly *et al.*, 1997). The mechanism by which *in vivo* delivery of naked DNA to the cells occurs is still unknown (Lockie *et al.*, 1999). Powder Ject Pharmaceutical has developed a ‘needleless’ system which delivers medicines and vaccines to the patient transdermally, but without breaking the skin. Using Powder Ject’s hand held delivery device, dry powder formulations of microscopic solid particles are propelled across the skin into the target tissue layer. The particles are accelerated to supersonic speeds (Mach 2-3) with a helium gas jet, which is generated momentarily inside the device. Powder Ject currently manufactures vaccines a number of uses including meningitis and influenza (Chiron Vaccines, 2005), their very successful technology could be used in future to administer plasmid DNA in cells.

Non-viral vectors, based on polycation/DNA complexes provide an attractive alternative to recombinant viral vectors as discussed earlier. Non-viral vectors being relatively easy to produce in large quantities and potentially less toxic in comparison to viral vectors (Sudimack *et al.*, 2000, Uduehi *et al.*, 2001;). Many of the same techniques used to produce and analyse recombinant protein pharmaceutical are readily applied to the production of plasmid DNA for gene therapy (Marquet *et al.*, 1995). Cationic liposomes are clinically well tolerated with few side effects but have relatively poor *in vivo* transfection efficiency (Hart *et al.*, 1995). With few exceptions such as muscle and to a lesser extent lung, many organs *in vivo* show limited ability to express transgenes following administration of naked DNA. The formation of electrostatic complexes



between plasmid DNA and cationic polymers (polyplex) or liposomes (lipoplex) improves this low transfection efficiency (Uduehi *et al.*, 2001).

### 2.3.2 Cationic Lipid-DNA Complex (Lipoplex)

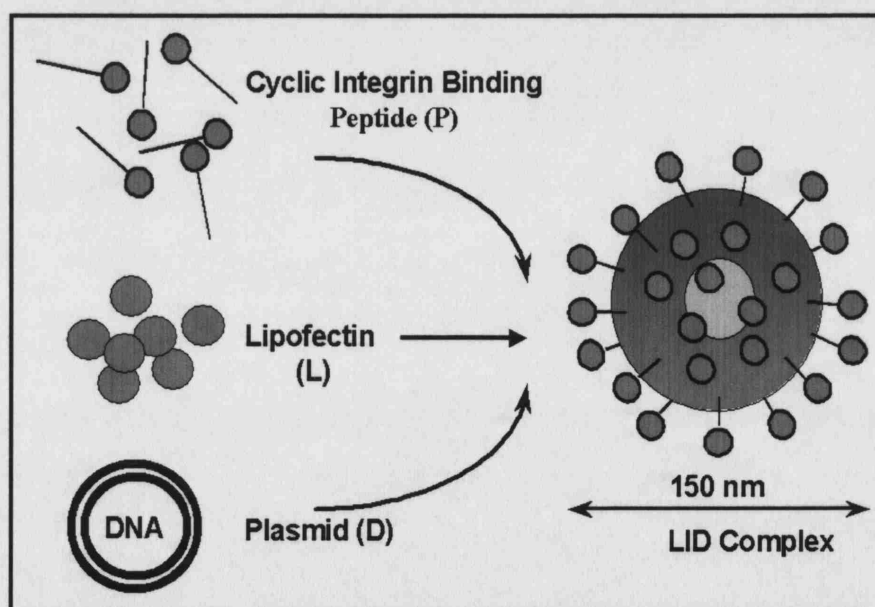
Liposomes, phospholipid bilayer membranes vesicles, have been widely investigated as a drug carrier for drug delivery systems (DDS). However, it is rather difficult to realise controlled release, especially stimuli-induced release of entrapped water-soluble substances from the liposomes composed of phospholipids (Hara *et al.*, 2001). Studies have shown the fluorescence from liposome compositions containing DOPE (dioleoylphosphatidyl ethanolamine) was able to penetrate deeper into the stratum corneum than that from liposome without DOPE (Kirjavainen *et al.*, 1996). Liposomes composed of oleic acid and phosphatidylethanolamine that aggregate can be stabilised below pH 6.5 in 150 mM NaCl. The endocytotic pathway has been shown to be the primary route by which negatively charged liposomes are internalised by cultured mammalian cells. Acidification of endosomes containing liposomes appear to enhance the membrane permeability of encapsulated fluorescent markers that are weakly acidic and to enable such molecules to gain access to the cytoplasm. It may also be possible to improve the cytoplasmic delivery of membrane-impermeable and pH sensitive liposomes which may fuse with or destabilise transiently the endosome membrane (Düzgüneş *et al.*, 1985). Cationic lipids can be used to enhance the delivery and expression of plasmid DNA *in vitro* and *in vivo* (Wheeler *et al.*, 1996; Subramanian *et al.*, 2000). The addition of cationic lipids to plasmid DNA decreases its negative charge and facilitates its interaction with cell membranes. Neutral lipids such as dioleoylphosphatidylethanolamine (DOPE) or cholesterol are generally added as ‘helper lipids’ in cationic lipid-DNA complex to facilitate the release of plasmid DNA from the endosome after endocytic uptake of the complex. Incorporation of cationic polymer such as poly-L-lysine and protamine, into cationic liposome DNA complexes leads to a tight condensation of DNA and prevents the complex from aggregation and nuclease degradation (Nishikawa *et al.*, 2001). The structure and function of liposome/DNA ionic complexes have been extensively studied (Sakurai *et al.*, 2000; Son *et al.*, 2000; Pedrosa *et al.*, 2001). At low ionic/DNA ratios, liposomes adhered to DNA as ‘beads on a string’; while at high ratios the DNA strands are either intercalated between the lipid bilayers or is coated by the liposomes (El Ouahabi *et al.*, 1997; Son *et al.*, 2000).

### 2.3.3 Cationic Polymer-DNA Complex (Polypex)

Although the predominantly used synthetic vector in recent years is lipopolyplexes, many workers are using cationic polymers. High molecular weight cationic polymers are more effective in condensing DNA than cationic liposomes and have been used as a delivery system for DNA including poly-L-lysine (PLL) and poly-L-ornithine. These polymers can enhance the cellular uptake of plasmid DNA by non-specific adsorptive endocytosis, as cationic lipids do. The disadvantages of PLL include polymer heterogeneity, toxicity, and potential immunogenicity (Mumper *et al.*, 1999; Han *et al.*, 2000).

### 2.3.4 Lipopolyplexes

Vectors that combine the safety parameters of non-viral vectors with the transfection efficiency of viral vectors are desirable. The difficulty in targeting lies in the recognition of the desired cell, which varies from one genetic disorder to another, for example the cell required to express the DNA in Cystic Fibrosis is very different to the cell that needs to be targeted for lung cancer i.e. for cases of tumour specific gene therapy (Frederiksen *et al.*, 1999). One approach to enhance the transfection efficiency of non-viral vectors is to incorporate targeting elements that bind efficiently to cell surface receptors (Liang *et al.*, 2000; Varga *et al.*, 2000) including integrins (Hart *et al.*, 1995). Integrins are heterodimeric cell surface glycoproteins consisting of  $\alpha$  and  $\beta$  subunits that are expressed on many cells including airway fibroblasts, epithelial cells and myeloid cell lines.



Schematic 2.1: Formation of lipopolyplex particles comprising lipofectin (L), cyclic integrin binding peptide (P) and plasmid DNA (D).

Their physiological functions relate to cell-cell and cell-matrix interactions (Jenkins *et al.*, 2001); similarly the intracellular bacterial pathogen (*Yersinia pseudotuberculosis*) is internalised after binding of the bacterial protein invasin with high affinity to cell membrane integrins (Hart *et al.*, 1995). Peptides provide a convenient and extensive source of integrin ligands. Integrin binding peptides ligands are usually short, as few as six amino acid residues. Peptides containing the highly conserved arginine-glycine-aspartic acid (RGD) motif bind to a range of integrins including  $\alpha_5\beta_1$ ,  $\alpha_v\beta_3$ ,  $\alpha_v\beta_5$  which are widespread in their tissue distribution (Hart *et al.*, 1999). Integrin-mediated peptide/DNA transfection efficiencies were enhanced more than 100 fold *in vitro* by the incorporation of a precisely defined amount of lipofectin (L) into complexes along with integrin targeting peptide (P) and plasmid DNA to form LPD complexes (Schematic 2.1). The LPD vector consisting of a cationic liposome (L), an integrin targeting peptide (P), with a sixteen lysine tail, and plasmid DNA (D), combined in optimal proportions form an electrostatic complex which has been previously shown to transfect a number of cell types *in vitro* (Hart *et al.*, 1998).

Lipoplexes have been shown to have greater levels of transfection in comparison to lipoplexes which do not contain a peptide component, it is though that the transfection efficiency is dependent on the amount of integrin-targeting ligand in complexes containing varying proportions of isoleucine and lysine peptides. A 34% reduction in integrin mediated transfection efficiency of LPD complexes was achieved with a  $\alpha_5\beta_1$  monoclonal antibody (Hart *et al.*, 1999). It was demonstrated that cationic liposomes could complex and condense DNA, Felgner and collaborators proposed the use of cationic liposomes as efficient carriers for the intracellular delivery of DNA. These authors prepared liposomes composed of the cationic lipid 2,3-bis(oleoyl)oxipropyltrimethylammonium chloride (DOTMA) and dioleoylphosphatidylethanolamine (DOPE), which became commercially available as a transfection reagent designated Lipofectin®. The ability of this system to mediate transfection was attributed to the recognition of certain properties, namely: (1) a spontaneous electrostatic interaction between the positively charged liposomes and the negatively charged DNA, which results in an efficient condensation of the nucleic acids (Adami *et al.*, 1998; He *et al.*, 1999; Ramsay *et al.*, 2000), (2) the fact that the resulting cationic liposome/DNA complexes could exhibit a net positive charge that promotes their association with the negatively charged cell surface and (3) the fusogenic properties exhibited by the cationic liposome formulation that can induce fusion and/or

destabilization of the plasma membrane, thus facilitating the intracellular release of complexed DNA. These assumptions paved the way to pursue studies aimed at improving the biological activity of lipopolyplexes, which have allowed the identification of several critical parameters that affect their efficacy (Pedroso de Lima *et al.*, 2001).

Development of an efficient method for introducing a therapeutic gene into target cells *in vivo* is the key issue in treating genetic and acquired diseases by gene therapy. Cationic vectors sometimes attract serum proteins and blood cells when entering into blood circulation. To reach target cells, non-viral vectors should pass through the capillaries, avoid recognition by the mononuclear phagocytes, emerge from the blood vessels to the interstitium, and bind to the surface of the target cells. They need to be internalised, escape from endosomes and then find a way to the nucleus, avoiding cytoplasmic degradation (Nishikawa *et al.*, 2001). Endocytosis is a multi-step problem involving binding, internalisation, formation of endosomes, fusion with lysosomes, and lysis. The extremely low pH and enzymes within the endosomes and lysosomes usually bring about degradation of entrapped DNA and associated complexes. Crucial to the success of DNA as a pharmaceutical is transfection efficiency; in general practice too few cells receive and express the exogenous DNA. Efficiency of transfection is dependent on both the efficiency of DNA delivery (i.e. fraction of DNA molecules getting into the nucleus) and efficiency of DNA expression (i.e. fraction of nuclear DNA molecules that undergo transcription). In addition transfection efficiency *in vitro* and *vivo* do not correlate, making translation of positive results in cell culture into animals more difficult (Lou *et al.*, 1999).

### 2.3.5 Barriers

Most DNA delivery systems operate at one of three general levels: DNA condensation and complexation, endocytosis, and nuclear targeting/entry. Negatively charged DNA molecules are usually condensed and/or complexed with cationic transfection reagents before delivery. These complexes are taken up by cells usually through endocytosis, (Wattiaux *et al.*, 2000; Girao da Cruz *et al.*, 2001). It is proposed that after the cationic lipid-nucleic acid complex is internalised by endocytosis, it destabilises the endosomal membrane, the destabilisation includes flip-flop of anionic lipids from the cytoplasmic facing monolayer, which laterally diffuse into the complex and form a charge neutral ion-pair with the cationic lipids. This results in displacement of the nucleic acid from the cationic lipid and subsequent release of the nucleic acid into cytoplasm of the cell (Szoka

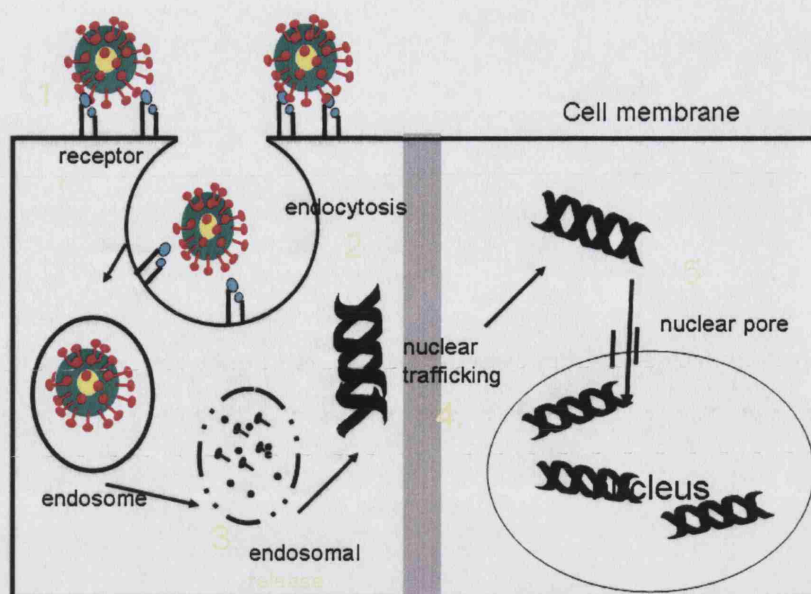
*et al.*, 1997). Finally, if the DNA has survived both the endocytotic processing and also the cytoplasmic nucleases, it must then dissociate from the condensed complexes either before or after entering the nucleus. Entry is thought to occur through nuclear pores which are ~10 nm in diameter, or during cell division. Once inside the nucleus, the transfection efficiency of delivered DNA is mostly dependent on the composition of the gene expression system (Luo *et al.*, 1999). There are many factors that influence the extent and duration of gene expression following administration of a successful gene medicine. The significance of each biological barrier will depend on the intended route of administration of the gene medicine and on the location of target cells.

Clearance of DNA and lipoplexes has been investigated along with other macromolecules (Takakura *et al.*, 1996). The hepatic clearance of naked DNA was very close to the plasma flow rate through this organ, which indicates that DNA is cleared substantially on the first pass of the liver. The uptake of DNA was thought to be by non-parenchymal cells, probably Kupffer cells, followed by interaction of DNA with scavenger receptors for polyanions. The liver also cleared liposome-DNA complexes rapidly, in this case by Kupffer cells (phagocytosis); this could be explained by the instability of cationic particulate systems. In addition there is a rapid degradation of the DNA by plasma nucleases, giving rise to significant rates of urinary excretion of partially degraded DNA. Cationic polymer/DNA complexes also show short plasma circulation times, with rapid hepatic uptake, also with accumulation or deposition in organs such as skin and intestine.

Since these organs are known to possess very fine capillary structures, it is possible that the deposition results from physical trapping of the complexes, perhaps following their aggregation or binding to serum components such as albumin. The pattern of deposition and of plasma clearance is partially influenced by the charge ratio of complex formation (Pouton *et al.*, 2001).

### **2.3.6 Serum Proteins**

In cell culture development the presence of serum proteins in culture media has been shown to reduce the delivery efficiency of non-viral vectors (Zelphati *et al.*, 1998; Smisterova *et al.*, 2001). Serum components bound to the complex may lead to an increase in particle diameter and entrapment in the capillary bed (Sakurai *et al.*, 2001), poor complex accessibility to cells or increased clearance by the reticuloendothelial system (RES) (Zelphati *et al.*, 1998).



Schematic 2.2: DNA uptake into the cell and intracellular transport: (1) cellular access to targeted cells followed by uptake through endocytosis (2) cytoplasmic trafficking of the transgene (3) fusion of vesicles with endosome compartment (4) release of lasmid from endosome into cytoplasm, dissociation from the synthetic vector, and entry into nucleus (5) after entering the nucleus, DNA must escape purging mechanisms and participate in transcription.

The possible explanations for serum inhibition are the coating of the complex with serum components and dissociation of the complex by serum components. The first explanation for the inhibition of delivery relates to non-specific interactions between the cationic lipids and serum proteins, this interaction leads to neutralisation of the positive charges and/or increase in size of the complex. These results suggest a polyelectrolyte charge interaction occurring between the positively charged surface of the complex and negatively charged serum components. The non-specific interactions with serum components alter the size and surface charge and cause the complex to aggregate, resulting in rapid clearance from the circulation (Zelphati *et al.*, 1998; Mok *et al.*, 1999). Incubations of polyplexes with albumin yield a decline of the zeta potential of the complexes to negative values, making an electrostatic mechanism in the dominant lung uptake less likely (Verbaan *et al.*, 2001). The coating of particles (in this case the coating of particles with plasmas proteins) is referred to as *opsonization*. It seems likely that components will bind to cationic lipoplexes. Experiments performed using a phase partitioning method indicated that several hours were required for polyethylene glycol (PEG) coated liposomes to adsorb significant amounts of protein that were otherwise adsorbed to the surface of conventional liposomes within a minute. It is thought that the

surface charge and hydrophilicity of PEG may play an important role in prolonging the circulation time of these PEG grafted liposomes (Bedu-Addo *et al.*, 1995). While it is believed that the PEG increases circulation time, it is known to reduce transfection efficiency.

## 2.4 Biophysical Parameters

Cationic lipids and polymers form complexes with DNA via electrostatic interaction. When formed, a DNA complex has its unique particulate characteristics depending on the properties of the components used. Of the various properties particle size is an important factor determining the tissue distribution process, such as passage through the capillaries (about 5µm) and through the fenestrae between discontinuous epithelial cells (30-500µm). The entrance of a particle via endocytosis is also a size limiting process. The electrical charge of the complex also greatly affects its bio-distribution. The cell surface membrane is negatively charged because of the abundant presence of glycoproteins and glycolipids, this negatively charged membrane is a good target for cationic complexes to induce cellular uptake. Non specific interaction is also a hurdle for cell specific delivery of DNA after local or systemic administration (Nishikawa *et al.*, 2001).

Gene delivery and expression are dependent on various physiochemical factors related to the formulated DNA complexes. In order to improve the effectiveness of gene transfer, it is important to understand the properties of DNA complexes which impact gene transfer. The methods of characterising DNA complexes are critical in assessing whether the complexes have reproducible physical properties and in predicting of transfection efficiency. Additionally, to proceed into advanced clinical trials, regulatory agencies including the World Health Organisation (WHO) and the US Food and Drug Administration (FDA) have specified that it is necessary for gene therapy products to be assessed in the same pharmaceutically rigorous fashion as other (pharmaceutical) products (Marquets *et al.*, 1997). The accurate characterisation of DNA formulations as a drug substance for therapeutic use involves establishing, among other things, formulation purity, particle size, charge, morphology, stability in physiological salt and transfection efficiency (Mahato *et al.*, 1999).

## 2.5 Formulation

The key components in a non-viral preparation are purified DNA, lipids (usually a mixture of cationic and neutral lipids) and an appropriate buffer. Typically an additional agent is required to protect and perhaps condense the DNA. The buffer plays a significant role in the electrostatic interaction between the various components of the formulation and DNA. It can also directly influence the efficacy as well as stability (Smith *et al.*, 1997; Atkinson *et al.*, 2001). According to the Deryaguin-Landau-Verwey-Overbeek (DLVO) theory of colloidal stability, these dispersions can be destabilised by reducing the repulsive energy barrier between the particles (Napper *et al.*, 1989).

The lack of control over the biophysical and molecular parameters influencing complex formation represents a limitation to consistently obtaining a well-defined, stable and monodisperse formulations with reproducible biological activity (Zelphati *et al.*, 1998). While stable non-viral vectors are being developed, it is doubtful that liquid formulations can be rendered sufficiently stable to resist stresses inherent in shipping and storage. Lyophilisation has been proven to be an effective method for the large-scale production of dried pharmaceuticals. The lyophilisation process basically consists of three steps: <sup>(1)</sup>freezing the solution; <sup>(2)</sup>primary drying to remove the majority of bulk water by sublimation removal of ice; <sup>(3)</sup>secondary drying to reduce the solid-associated moisture content of the final product to 1-4% range by vacuum drying. The dry cake that has a volume of the original solution after a majority of mass is removed suggests a highly porous. Since typical lyophilisation does not involve droplet formation, the dry cake can only be reduced to particles when subjected to a secondary dispersive force such as mechanical milling or grinding. Although the particle size and distribution are primarily controlled by the input energy, the properties of the lyophilised cake also play a role. These properties include the porosity, pore size and distribution, and the chemical composition of the cake. The advantages of lyophilisation include high yield, an aseptic and convenient process. The disadvantages include the expensive nature of the technique and the formation of irregular sized and broad sized particles (Maa *et al.*, 2000). Transfection rates upon rehydration are closely correlated with the maintenance of particle size (Allison *et al.*, 2000).

## 2.6 Physical Stability

Many cationic agents are being developed for use in non-viral delivery vehicles, but studies have demonstrated marked instability of such systems (Kay *et al.*, 1997).



Typically, separate solutions of cationic agent (such as liposomes) and DNA are mixed to form a heterogeneous suspension of complexes. However the resulting Lipid-DNA complexes tend to aggregate over time, resulting in reduced rates of gene delivery (Gustaffson *et al.*, 1995). [To circumvent the problem, clinical studies employing the non-viral vectors used complexes mixed by doctors immediately before injection]. Although preparations in current clinical trials are more stable, instability continues to represent a significant problem for both lipid-DNA complexes and vectors composed of non-lipid materials.

Isotonic liquid formulation that could be drawn into a syringe and injected into a patient would be the most convenient for the clinician. Several studies have attempted to improve the stability of non-viral vectors in aqueous suspension. Hong *et al.*, 1997 incorporated polyethylene glycol-lipid conjugates into complexes and demonstrated that such preparations are stable at 4 °C for two months.

Attempts to stabilise non-viral vector formulations are hampered by the dearth of information regarding their active (native) state. For example, if protection is simply a matter of preventing aggregation, formulations can be designed to trap active vectors in a glassy matrix, minimising contact between particles. On the other hand, if a specific individual structure must be preserved, formulation scientists could focus on developing strategies to achieve that end. A better understanding of the physical characteristics that determine whether a vector is active would not only aid in stabilisation, but would greatly facilitate efforts to engineer more efficient gene delivery vehicles. Unfortunately, physical characterisation of non-viral vectors is complicated by many factors including an insufficient understanding of the mechanics of the gene delivery process (Anchordoquy *et al.*, 1999).

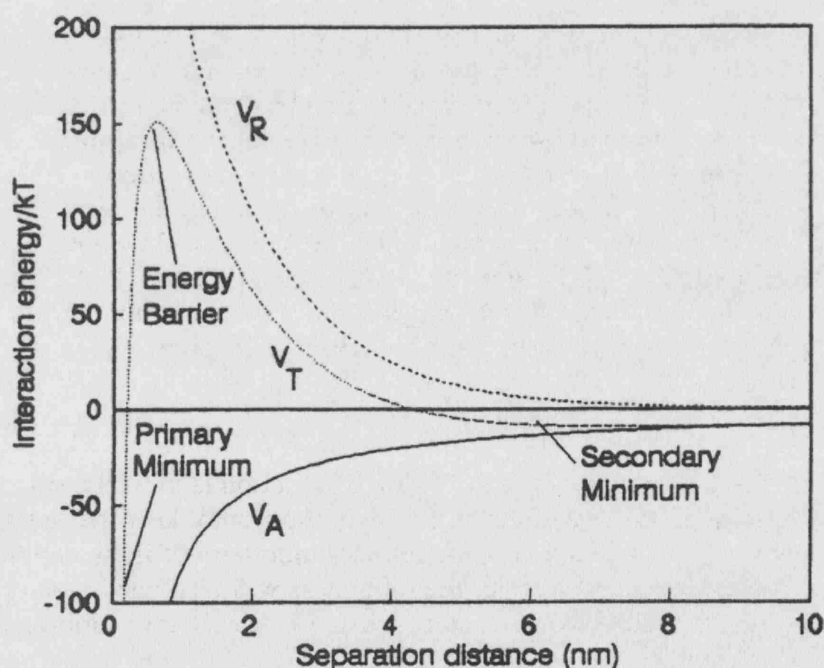
### 2.6.1 Aggregation

One of the fundamental problems in gene therapy is the aggregation of complexes when prepared and/or stored under physiological conditions. The drawback of cationic lipid formulations transfer is colloidal instability, which leads to the formation of large aggregates. This creates difficulties for *in vivo* and clinical trials, which require complexes with size compatible with *in vivo* delivery (Scherman *et al.*, 1998). There are a number of parameters associated with the various forms of aggregation, which many papers have discussed. In the 1940s, two groups of scientists concurrently and

independently developed a theory of colloidal stability now known as the DLVO theory (named after the proponents, Derjaguin, Landau, Verwey and Overbeek). For particles of like charge, an electrostatic repulsion occurs when the diffuse layers overlap while attraction is due to the van der Waals energy. In the DLVO theory, it is assumed that these long-ranged forces (van der Waals and electrostatic) control the stability of colloids. However, the DLVO theory does not always provide accurate predictions of colloid stability (Elimelech *et al.*, 1995; Popescu *et al.*, 1996).

For colloids with a surface charge, the electrostatic repulsion energy gives rise to an energy barrier at intermediate separations (Schematic 2.2), the energy barrier has been used to quantitatively predict colloidal stability. The DLVO theory allows for the calculation of the critical coagulation concentration (CCC), which is the theoretical electrolyte concentration where fast aggregation should occur (Baldwin *et al.*, 2001).

In colloidal systems, the first interaction to be taken into account is the van der Waals dispersion forces. For spherical particles of radius  $a$  separated by a centre-to-centre distance  $R$ , the interaction has the following expression:



Schematic 2.3: Hypothetical potential energy barrier between two equal spherical particles. The net potential profile ( $V_T$ ) is a superposition of the van der Waals potential ( $V_A$ ) and the repulsive double layer potential ( $V_R$ ). (Reproduced from Elimelech *et al.*, 1995).

$$U_A = -\frac{H}{6} \left[ \left( \frac{2a^2}{R^2 - 4a^2} \right) + \frac{2a^2}{R^2} + \ln \left( \frac{R^2 - 4a^2}{R^2} \right) \right] \quad 2.1$$

where  $H$  is the Hamaker constant for two particles acting across the medium. On the basis of the Lifshitz theory,  $H$  is always positive for two identical particles hence the interaction  $U_A$  is always attractive.

### 2.6.2 Electrical Double Layer Interaction

Electrically charged particles in aqueous media are surrounded by counterions and electrolyte ions, namely, the screening double layer. As two particles approach each other, the overlapping of double layers leads to long-range repulsive forces due to entropic effects. The profile of the interaction depends on the ratio between the particle size and the Debye screening length  $\kappa^{-1}$ . The Debye parameter ( $\kappa^{-1}$ ) has the dimensions of reciprocal length and plays a very important part in electrical interaction between colloidal particles (Elimelich *et al.*, 1995). For two identical particles with surface potential  $\Psi_0$  the repulsive interaction is:

$$U_R = 2\pi\epsilon\psi_0^2 a \left( \frac{2a}{R} \right) \exp[-\kappa(R-2a)], \kappa a \leq 5 \quad 2.2$$

For a  $z$ - $z$  electrolyte,  $\kappa = (\epsilon k_B T / 2z^2 e^2 n_b)^{-1/2}$  where  $e$  is the electronic charge and  $n_b$  is the density number of ions in the bulk (Quemada *et al.*, 2001). Where  $\epsilon$  is the permittivity of the medium,  $k_B$  is the Boltzman constant and  $T$  is the absolute temperature.

### 2.6.3 Coagulation Theory

The classical coagulation theory first developed by Smoluchowski (Smoluchowski, 1917) described aggregation with the following equation:

$$\frac{dn_k}{dt} = \frac{1}{2} \sum_{i=1, i+j=k}^{k-1} \beta_{ij} n_i n_j - n_k \sum_{k=1}^{\infty} \beta_{ik} n_i \quad 2.3$$

where  $i, j, k$  are size classes,  $\beta_{ij}$  is the flux of  $j$  particles on an  $i$  reference particle (a second-order rate constant) giving a particle of size  $k$ ;  $n_i$  is the number concentration of the particles in size class  $i$ . Smoluchowski derived the following values of  $\beta$  for different forms of aggregation :

(1) *Perikinetetic aggregation* (due to Brownian motion)

$$\beta_{p_{ij}} = \left( \frac{2KT}{3\mu} \right) \left[ \frac{(a_i + a_j)^2}{a_i a_j} \right] \quad 2.4$$

where K is the Boltzman constant, T the absolute temperature,  $a_i$  is the particle radius and  $\mu$  the viscosity of the fluid.

(2) *Orthokinetic aggregation* (due to shear flow)

$$\beta_{oi} = \frac{4}{3} G (a_i + a_j)^3 \quad 2.5$$

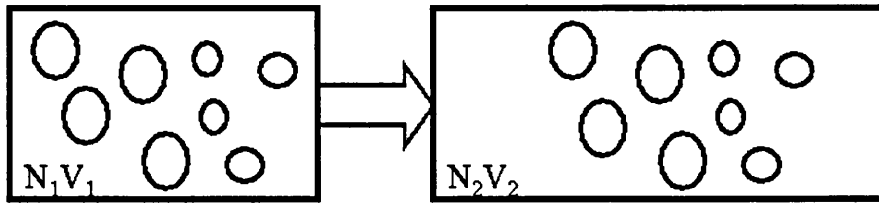
(3) *Differential sedimentation*

$$\beta_{dij} = \left( \frac{2\pi g}{9\mu} \right) (\rho_p - \rho_w) (a_i + a_j)^3 (a_i - a_j) \quad 2.6$$

where g is the acceleration due to gravity,  $\rho_p$  is the particle density and  $\rho_w$  that of the fluid. The equations were developed for the hard sphere model, neglecting hydrodynamic interactions and colloidal forces. These effects were later studied and were generally introduced in the Smoluchovsky equations by multiplying  $\beta$  by an aggregation efficiency factor  $\alpha$  (Atteia *et al.*, 1998).

The collision efficiency  $\beta$  is a function of the mode of flocculation i.e. perikinetic, orthokinetic or differential sedimentation. The collision efficiency  $\alpha$  (taking values from 0 to 1) is a function of the degree of stabilisation; the greater the degree of destabilisation, the greater the value of  $\alpha$ . Thus, in effect,  $\beta$  is a measure of the transport efficiency leading to collisions, whilst  $\alpha$  represents the percentage of those collisions leading to attachment (Thomas *et al.*, 1998). The collision efficiency cannot be expected to provide a comprehensive account of the inter-particle forces involved in flocculation.

Substantial developments have been made in defining the influence of van de Waals attraction and hydrodynamic forces. In particular, the inclusion of hydrodynamic forces has led to a marked reduction in both the expected rates of flocculation and the significance of mixing intensity. The conventional kinetic approach to flocculation modelling discussed so far essentially relies upon the calculation of collision frequencies and collision efficiencies based on the knowledge of particle velocities and surface potentials. The validity of this approach is questionable when systems become

Schematic 2.4: Constant Number Monte Carlo,  $N_1=N_2$ ,  $V_1<V_2$ 

concentrated such that collisions between more than two particles are likely (Thomas *et al.*, 1998).

The coagulation kernel for Brownian diffusion is given by:

$$k_{ij} = \frac{1}{4} \left[ 2 + \left( \frac{M_i}{M_j} \right)^{\left( \frac{1}{3} \right)} + \left( \frac{M_j}{M_i} \right)^{\left( \frac{1}{3} \right)} \right] \quad 2.7$$

This expression presumes that the particles are spherical and that instantaneous coalescence follows each coagulation event. The characteristic coagulation time being (Smith *et al.*, 1998):

$$\tau_c = \frac{3\mu}{8kBTC_0} \quad 2.8$$

## 2.7 Monte Carlo

Another technique which may be used to predict aggregation of particles is the Monte Carlo simulation, developed by tracking a sample of the population whose size (number of particles in the sample) is kept constant throughout the simulation, the constant number Monte Carlo, amounts to expanding or contracting the physical volume represented by the simulation so as to continuously maintain a reaction volume that contains constant number of particles.

The growth and disintegration of dispersed systems and the evolution of their size distribution is a problem that arises in several areas of scientific and engineering interest. The use of Monte Carlo methods in the application of growth processes has been used successfully in the past. Monte Carlo utilises probabilistic tools to sample a finite subset

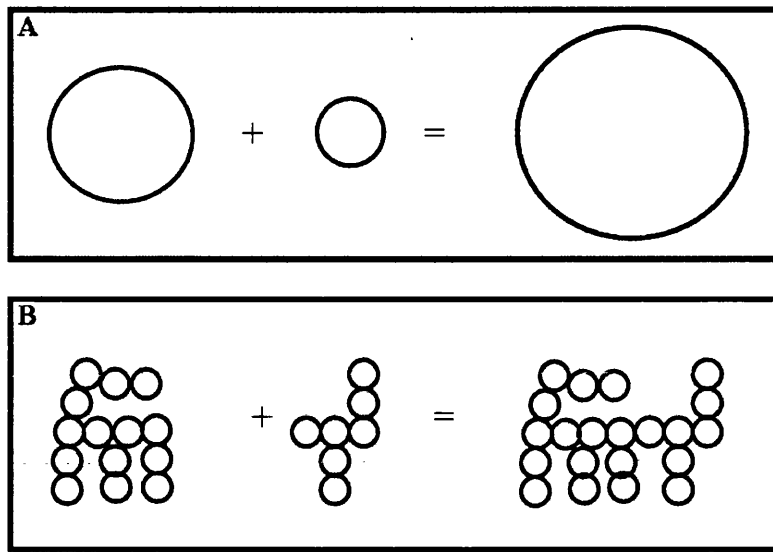
of a system in order to infer its properties. Its discrete character makes it a natural choice for the simulation of processes that are inherently discrete. The finite number of particles used in the simulation introduces certain limitations. In coagulation for example two particles are combined to form a new one, resulting in the net loss of one particle per coagulation event. If the simulation begins with  $N_0$  particles (initially), then after  $(N_0 - 1)$  coagulation events, all of the system mass is concentrated onto a single particle, at which point the simulation must be terminated. A serious consequence of the depletion of the particle array is the continuous decrease of accuracy. Thus, in practice the simulation must be terminated well before the formation of a single particle. The use of constant number (*constant-N* Monte Carlo) is a concept where there is a constant re-filling of the array, selecting a particle from the array at random and placing its copy in the position vacated by coagulation. All particles have the same probability to be chosen to fill the vacancy, thus on average, this operation leaves the size distribution intact. This method amounts to using a sample of  $(N-1)$  particles to produce a sample of constant size  $N$ . This approach views the simulation box as a finite sample of the actual population and has a simple physical interpretation (Smith *et al.*, 1998).

## 2.8 Fractal Analysis

Fractals are disordered systems whose disorder can be described in terms of non- integral dimension (Avnir *et al.*, 1990). Aggregates are now recognised as fractal objects. If for a large number of aggregates, the mass is plotted against aggregate size (diameter, for example), the plot may be linear, but with a non-linear slope. For regular three-dimensional objects the slope of such plots is 3. A lower fractal dimension corresponds to a more open (or stringy) aggregate structure. The relation between aggregate mass ( $M$ ) and size ( $L$ ) is as follows:

$$M \propto L^{d_f} \quad 2.9$$

The size  $L$  can be defined in various ways and in fundamental studies it is often taken as the radius of gyration of the aggregate (Gregory *et al.*, 1995). A fractal dimension of 3.0 represents a uniformly distributed structure or more commonly a compact structure.



Schematic 2.5: (A) Euclidean model used for the coalesced sphere model (CF) and (B) Fractal model for the coalesced fractal sphere (CFS). Where the smaller circles are the primary particles constituting the aggregates and the larger circles indicate the imaginary compact spheres, the volume of which is the same as the sum of the solid volumes in the aggregates.

Fractal theories applied to particle aggregation studies have been mainly used as quantifying tools for describing the structure of the aggregates. Fractal theories are also believed to apply to particle aggregation kinetics as well as the morphology of the structure (Lee *et al.*, 2002). The coalesced sphere (CS) assumption in conventional coagulation kinetic models can be depicted as above (Schematic 2.5 (A)).

A new approach (Lee *et al.*, 2000) is the coalesced fractal sphere (CFS) assumption for modelling fractal particle aggregation (Schematic 2.5 (B)). The model incorporates the effects of the purely fractal nature of aggregates by using a packaging factor of unity to eliminate shape effects. The CFS assumptions are stated below:

- All aggregates consist of a single type primary particle that is a compact spheres. All aggregates in the particular system have coalesced fractal sphere from which a fixed fractal dimension is deduced, independent of aggregate size.
- When two aggregates collide and combine, the newly formed aggregate has the same fractal dimension as the colliding aggregates, with the solid volume of the new one being the some of the solid volumes of the colliding aggregates.

The CFS assumption is a generalisation of the CS assumption, because the CFS assumption reduces to the CS assumption when the fractal dimension is 3.0. It is known that the presence of salt plays a significant role in the type of mass fractal formed. The effects of salt concentration on the aggregate structure can be explained qualitatively by the DLVO theory. At low salt concentrations the energy barrier against particle aggregation into the primary potential energy is very significant; only those particles that have sufficient thermal energy can overcome this energy barrier. Thus an incoming particle can penetrate deeper into the interior of the aggregate structure, resulting in a denser aggregate. In contrast at high salt concentrations the energy barrier against aggregation is completely removed and particles stick to each other on every collision. Thus, an incoming particle is likely to be intercepted before it can reach the interior of the aggregate, leading to an open aggregate structure. As the initial particle concentration increases, inter-particle concentration increases. Higher particle collision frequencies will reduce the time available for a particle to wander around an aggregate in its attempt to find the most favourable energy position before it is permanently locked by incoming particles. As a result, less structural rearrangements can take place and hence more open aggregates are expected with increasing particle concentration. Since restructuring can only occur if there are no strong attractive forces between the particles, the particle concentration effect will only be significant at low salt concentrations (Yan *et al.*, 2002).

Fractals give the proper mathematical framework for the treatment of irregular, seemingly complex shapes found in nature from the small-scale structures for disordered systems such as aggregate clusters to macrostructures such as clouds. One of the common features of fractal objects is that they are similar (scale invariant). This means that if part of them is cut out, and then blown out, the resulting object will look the same as the original object (Raper *et al.*, 1993).

For aggregation due to Brownian motion, two well-defined regimes of irreversible colloidal aggregation have been identified, those of diffusion limited colloid aggregation (DLCA) and that of reaction-limited colloid aggregation (RLCA). The regimes are determined by the collision mechanisms, for example a sticking probability (between monomers) equal to one leads to the DLCA, while values much smaller than one give rise to the RLCA. The addition of electrolytes into suspensions results in a decrease in the repulsive force between the particles and results in an increase in the sticking probability. DLCA occurs when there are negligible repulsive forces between the colloid particles,



causing particles to stick upon contact and form highly tenuous structures. In contrast to DLCA, a substantial repulsive force remains between particles during RLCA, so that the particles may collide many times before sticking and the sticking probability approaches zero.

Experiments have shown universality with respect to the aggregate fractal nature and the reaction kinetics in the regimes of DLCA and RLCA. Theory and computer simulation predict that the fractal nature of aggregates are close to 1.8 for DLCA and 2.1 for RLCA (Tang *et al.*, 2000).

The growth of aggregates can be simulated by making simple assumptions concerning transport of particles to the growing agglomerate and the events which occur when a primary particle or cluster collide with the growing aggregate. The mass fractal dimension, together with the aggregate size, and primary particle size yield a partial description of a mass fractal aggregate that is sufficient for the study of some aspects of growth and some properties, especially those related to mass/volume ratios.

## 2.9 Future of Gene Therapy

Not with standing an enthusiastic take-off, gene therapy has not fulfilled all the expectations of the beginning. It is hard to say how many of 3000 patients recruited worldwide, taking part in nearly 300 clinical protocols, really benefit from gene therapy. Some evidence of clinical improvement has been proved for one adenosine deaminase (ADA) patient, two patients with familial hypercholesterolemia and two patients with Faconi's anemia (Raper *et al.*, 1997). The real obstacle to the development of gene therapy as a powerful therapeutic tool remains the targeted and long-term regulated expression of the transgene (Palu *et al.*, 1999). The desirable properties of non-viral gene delivery systems include biocompatibility (low toxicity, non immunogenicity and *in vivo* stability), efficient nucleic acid delivery with high functionality, and manufacture in a commercially acceptable form amenable to scale up and storage stability. Although the perfect system does not currently exist, recent studies suggest that there have been significant improvements made over the past few years. The advancement on individual issues now need to be integrated into systems that exploit their combined attributes without suffering losses due to the creation of the system.

## Chapter 3 : Materials and Methods

### 3.1 Materials

All solutions were prepared from deionised Milli-Q water (resistivity  $\approx 18.2 \text{ M}\Omega$ ) (Millipore Ltd, Bedford, MA, USA) and cleaned with  $0.2 \text{ }\mu\text{m}$  pore size Millipore filters to remove particulates. HEPES (N- [2-hydroxyethyl] piperazine-*N'*- [2-ethanesulfonic acid]) (Sigma-Aldrich, Poole, Dorset, UK) was deionised with NaOH to pH 7.4. Phosphate Buffer Saline (PBS, containing no calcium or magnesium) was obtained from Sigma-Aldrich (Poole, Dorset, UK). Particle free water was supplied by Fresenius Kabi Ltd (Warrington, UK). All other buffers were made using Milli-Q water concentration adjusted by adding varying levels of sodium chloride and pH adjusted using NaOH. Zeta potential standards were obtained from Malvern Instruments (Malvern Instruments Ltd, Malvern, Worcester, UK). Nanosphere™ size standards were purchased from Duke Scientific Corporation (Palo Alto, CA, USA). Due to the limited availability of materials, all experiments were conducted in low volume disposable cuvettes from Malvern Instruments Ltd (Malvern, Worcester, UK). Tryptone and yeast obtained from Oxoid (Basingstoke, Hampshire, UK), and sodium chloride obtained from Sigma- Aldrich (Poole, Dorset, UK) were used to make up LB broth in the fermentation of *E. coli*.

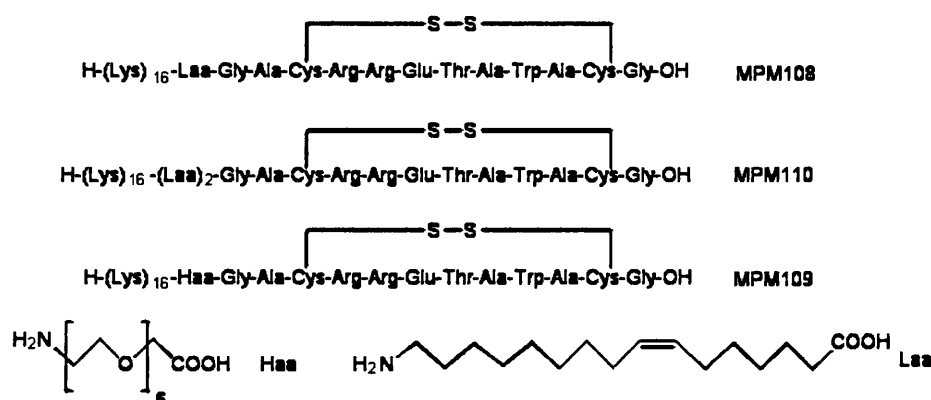
#### 3.1.1 Materials

The 6.9 kb plasmid, pSV $\beta$  (Promega Corp., Madison, WI, USA), containing the bacterial  $\beta$ -galactosidase gene, is a common plasmid used extensively at the Dept. of Biochemical Engineering, UCL. The plasmid was transformed and propagated in *Escherichia coli* DH5 $\alpha$  (Life Technologies, Inc., Gaithersburg, MD, USA) and grown in LB broth; further details are given in Levy *et al.*, (2000). The plasmid DNA was purified by the alkaline lysis process whereby bacterial cells are lysed and the plasmid DNA are then adsorbed onto an ion-exchange column. The eluted plasmid DNA was isopropanol precipitated, washed with 70% (v/v) ethanol, air dried, and re-suspended as stated in the supplier's

protocol (Qiagen Plasmid Giga kit, Qiagen Ltd, West Sussex, UK). Concentration and quality were assessed by spectrophotometric analysis at 260 nm and 280 nm. The DNA concentration was determined using a value of 50 µg DNA per one absorbance unit at 260 nm. The plasmid had 260 nm/280 nm absorbance ratio greater than 1.8 (Ayazi Shamlou *et al.*, 2003). The final purified plasmid DNA was re-suspended in either sterile TE buffer (10mM TrisCl pH 8.0, 1mM EDTA) at a concentration of 1.5mg/ml.

### 3.1.2 Peptides

The integrin-targeting peptide, peptide 6 [K]<sub>16</sub>GACRRETAWACG (3331.5 MW), was of a purity > 80% and was purchased from Zinsser Analytic (Maidenhead, Berkshire, UK). The peptide was dissolved in deionised water to 2 mg/ml and stored at -20 °C. Peptide series K8-K32 were kindly provided by Dr Stephen Hart (Molecular Immunology Unit, Institute of Child Health). Peptides MPM 108, MPM 109 and MPM 110 were synthesised from protected forms of the amino acids Haa and Laa, using standard solid phase synthesis methods. **Haa:** The hydrophilic amino acids (Haa) used were PEG chains with an amino group on one end and a carboxylic acid on another. The idea here was twofold: (i) PEG linkers are normally very good spacers in biological systems, so this was one potential way of putting the integrin-recognition headgroup sticking out from the LID complex; (ii) PEG-coated liposomes have greater stability towards serum and plasma proteins, so a complex made up with PEG units should be more stable *in vivo*. **Laa:** The lipophilic amino acids were designed to have an alkyl group in the middle to imitate the structure of the DOTMA lipid – and hence to pack better into an ordered lipid bilayer, thus causing the headgroup to stick out beyond the lipid (Tabor *et al.*, In preparation). The structures are shown in Schematic 3.1.



Schematic 3.1: Peptides MPM 108, MPM 109 and MPM 110. Peptides were synthesised using standard solid phase synthesis methods.

### 3.1.3 Liposomes

The transfection reagent Lipofectin, a 1:1 (w/w) mixture of the cationic lipid *N*-[1-(2,3-dioleoyloxy)propyl]-*N,N,N*-trimethylammonium chloride (DOTMA) and the neutral lipid dioleoyl phosphatidylethanolamine (DOPE), from Invitrogen Life Technologies (Palo Alto, CA, USA). Calcein encapsulated lipids: C12 Saturated + DOPE; C14 Unsaturated ± DOPE; C16 Unsaturated ± DOPE and C18 Unsaturated ± DOPE were very kindly provided by Department of Chemistry. Calcein was purchased from Sigma, Poole, Dorset, UK.

### 3.1.4 Latex standards

The latex particles were purchased originally as size calibration standards (Duke Scientific, CA, USA).

## 3.2 Sample Preparation

This section describes the sample preparation that is common to all of the experiments conducted in chapters 4-7, as well as the preparation of samples specific to chapter 5 (Fractals) and 7 (Rationale Vector Design).

### 3.2.1 Preparation of Lipid/Peptide/DNA (LPD) Complexes

Lipopolyplexes were prepared by mixing LPD complexes at a weight ratio of 0.75:4:1 (L-P-D). The relation for the charge ratio of these complexes is given below (Equation 3.1). Based on these the following values, 0.75 µg Lipofectin, 4µg integrin-targeting peptide and 1µg DNA were mixed, the charge ratio of the lipopolyplexes is approximately 6.8.

$$CR = \left[ \frac{(\text{moles of lipofectin}) + (\text{moles of peptide})}{\text{moles of DNA}} \right] \quad 3.1$$

Note that the calculation of the charge contribution by Lipofectin was performed on the charged lipid, DOTMA.

In all of the experiments the L-P-D ratio of 0.75:4:1 were maintained to give a ratio of positive to negative charge equivalents of +7 (6.8). The concentration of each component in the feed stock solution was as follows: Lipofectin (Life Technologies, Paisley, U.K.) 1 mg/ml; peptide, 2 mg/ml; and plasmid DNA 1.6mg/ml. 56µl of lipofectin was mixed with 15 µl of peptide; similarly 4µl of DNA was added to 248µl of the desired buffer.

The DNA and the lipofectin-peptide solutions were mixed directly by pipetting the two solutions into a low volume disposable Malvern cuvette (Malvern Instruments Ltd, Worcestershire, U.K.) placed in position in a Malvern Zetasizer (Model 3000, Malvern Instruments Ltd, Worcestershire, UK). This protocol allowed in-situ measurements of particle size and zeta potential ( $\zeta$ ) as a function of time accurately and reproducibly. When experiments were conducted with LD and PD the ratio of combination of the components were mixed in the same weight ratio as LPD, i.e. 0.75:1 (L:D) and 4:1 (P:D). A mixture of lipid and peptide were added to a mixture of DNA and buffer, pipetted for 5 seconds and placed in a low volume cuvette, volume 0.5 ml. Size and zeta measurements were all made in the Zetasizer 3000 (Malvern Instruments).

For static light experiments, 0.5 ml of solution was added to a glass cell (RR85C Malvern Instruments Ltd). Prior to taking sample readings toluene measurements were taken to ensure that that count rate at 90 °, was half that at 30 ° and 150 °. Non-encapsulated calcein was removed by dialysis at 25 °C (Peribo Sciences UK Ltd, Tattenhall, Cheshire, UK) against several changes in 0.01 M phosphate buffer saline, (0.0027 M potassium chloride, 0.137 M NaCl Sigma Poole, Dorset, UK).

### 3.2.2 Lipid Preparation

Calcein was encapsulated in liposomes at a concentration of 80 mM (phospholipid concentration between 1-2  $\mu$ M), at which concentration its fluorescence is self quenched. Leakage of calcein from the liposomes and its dilution in to the buffer results in an increase in fluorescence. Eighty microlitres of calcein-loaded liposomes was added to 40 ml of MES-buffered saline (140 mM NaCl, 10 mM MES) at various pH values (pH 5.0-7.4). The effect of pH was taken into account and all samples were brought up to pH 7.4 before fluorescence measurements were taken. 100% leakage was measured by sonicating a sample at pH 7.4, for 90 seconds, 10 cycles on, 10 cycles off, using a sonicator (Soniprep 150, Integrated Services, TCP Inc, PO Box 106, Palisades Park, New Jersey 07650, USA). Calcein fluorescence was measured at  $\lambda_{ex} = 490$  nm and  $\lambda_{em} = 520$  nm, using a Fluoromax-3 flurometer (Jobin Yvon Horiba, Middlesex, UK). The percentage leakage of calcein from the lipid was measured using the formula below:

$$\%Leakage = \left[ \frac{I_{pH} - I_0}{I_{100} - I_0} \right] \times 100 \quad 3.2$$

Where  $I_0$  is the fluorescence at neutral pH,  $I_{pH}$  is the fluorescence of the pH range tested (after correction) and  $I_{100}$  the totally released calcein from the sample at pH 7.4 after sonication.

### 3.2.3 Fractals Structures

Since there are no reported measurements of fractal dimensions for gene delivery particles, in order to provide comparative data a series of initial tests with latex particles (Duke Scientific, CA, USA) were performed. The latex particles were purchased originally in a surfactant-stabilised state as standard calibration particles ( $220 \text{ nm} \pm 5 \text{ nm}$ ) for the particle-sizing instrument. The particles were suspended in either 250 mM or 1M NaCl, pH 3.0 solutions for static light scattering studies.

In the fractal experiments, the scattered intensity  $I(q)$  from the randomly oriented particles in suspension is measured as a function of the scattering angle,  $\theta$ . The magnitude of the scattering vector,  $q$ , measured in reciprocal length, is given by:

$$q = \left[ \frac{4\pi n \sin\left(\frac{\theta}{2}\right)}{\lambda} \right] \quad 3.3$$

where  $n$  is the refractive index of the solution (1.33) and  $\lambda$  the incident wavelength of the light in a vacuum (532 nm). The scattered intensity  $I(q)$  may be described as the product of the form factor,  $P(q)$ , which is the scattered intensity function of the elementary (scatterer) particles of radius  $a$  and the structure function,  $S(q)$  which accounts for the scattered intensity arising from the spatial distribution of the scatterer particles within the aggregates, having a characteristic maximum length  $l$ . Thus:

$$I(q) \propto S(q)P(q) \quad 3.4$$

In the intermediate regime of the wave number, which is of interest to the present study, i.e. in the range  $l^{-1} < q < a^{-1}$ , the form factor,  $P(q)$ , is assumed to be constant and independent of  $D_f$  (Yates *et al.*, 2001). Importantly, in this regime, theoretical considerations lead to the following mathematical statement between the structure function,  $S(q)$ , and the wave number ( $q$ ) (Tang *et al.*, 1999; Tirado-Mirando *et al.*, 2000). Thus:

$$S(q) \propto q^{-D_f} \quad 3.5$$

Therefore, in the intermediate regime, letting  $P(q) = 1.0$  and using equations (3.4) and (3.5), leads to the following relationship (Amal *et al.*, 1993; Schmidt *et al.*, 1989):

$$I(q) \propto S(q) \propto q^{-D_f} \quad 3.6$$

According to equation (5.5), a plot of the scattered intensity (photocounts),  $I(q)$ , or the form factor  $S(q)$ , against the wave number,  $q$ , on a log-log co-ordinates would be expected to yield a straight line with a negative slope equal to  $D_f$ . To ensure the accuracy of results, the angular range  $10^\circ \leq q \leq 30^\circ$  experiments ( $0.1 < qa < 1$ ) in experiments involving the latex particles and LPD were used.

### 3.3 Measurement Techniques

Dynamic light scattering and zeta potential measurements were used only in Chapters 4-7. Static light scattering measurement techniques were used in Chapter 5.

#### 3.3.1 Dynamic Light Scattering (DLS)

Analysis of the time dependence of the intensity fluctuations yield the diffusion coefficient of the particles from which, via stokes Einstein equation (Bhattacharya *et al.*, 1999; Li *et al.*, 2004), knowing the viscosity of the medium, the hydrodynamic radius or diameter of the particles can be calculated. In Photon Correlation Spectroscopy (PCS) the intensity fluctuations of scattered LASER light determined by the vector particles are measured. Under Brownian motion and using a scattering angle  $90^\circ$ , a speckled pattern is observed. A correlator is used to analyse changes in the fluctuating signals continuously. The time dependence of the intensity fluctuation is most commonly analysed using a digital correlator. Such a device determines the intensity autocorrelation function that can be described as the ensemble average of the product of the signal with a delayed version of itself as a function of the delay time. Analysis of the autocorrelation function in terms of particle size distribution is done by numerically fitting the data with calculations based on assumed distributions. Sample size was analysed by the unimodal cumulants method (monomodal analysis) using the software supplied by the manufacturer.

Before each measurement the calibration of the instrument was checked against standard mono-sized Latex particles (Duke Scientific Corporation, Palo Alto, CA, USA). At least 10 readings were taken, with each reading consisting of 10 sub runs over a minimum

period of 20 minutes. Each experiment was carried out a minimum of two times on different days.

### **3.3.2 Static Light Scattering (SLS)**

Fractal properties of the vector particles were obtained from static light scattering measurements using a Malvern 4800 computer controlled spectrophotometer (Autosizer 4800, Malvern Instruments Ltd, Worcestershire, UK). The light source used was a 50 mW 532 nm Uniphase Micro Green laser. The scattered light was collected by an avalanche photodiode detector positioned at angle  $\theta$  relative to the forward direction of the incident beam. All experiments were performed at the constant temperature of 25 °C. The spectrometer was calibrated by performing angular measurements of intensity on toluene. The toluene count rate was taken at 30 °, 90 ° and 150 °, to ensure that the count rate at 90 ° was half that at 30 ° and 150 °. Angular scans were performed from  $\theta = 10^\circ$  to  $40^\circ$ , with a measurement made every  $4^\circ$  (31 steps) for an acquisition time of 10 seconds (sample acquisition time  $\geq 230$  seconds). The intensity measurements were repeated at different times following sample preparation. The ability to measure the intensity of scattered light at angles less than  $20^\circ$  on a goniometer system will depend on the degree of flare that the laser produces as it enters the cuvette. The refractive-index difference between the glass of the vat and the liquid contained in the vat will aggravate this situation. To reduce this flare, toluene can be used in the vat. However if the system is very well aligned and the vat and fluid are exceptionally clean, there is no reason why measurements made at angles lower than  $20^\circ$  cannot be performed (Malvern Instruments). The way to validate the suitability of the system for measurements at such forward angles is to perform angle scans with a suitable solvent such as toluene. If the system is well aligned and cleaned, the standard angle scan will produce a flat response. This measurement was always performed in our experiments prior to measurements of the samples to ensure that the system was suitable for data collection.

### **3.3.3 Zeta Potential**

The zeta potential ( $\zeta$ ) of the LPD particles was calculated from the electrophoretic mobility of the particles in each buffer using an optical technique based on LASER Doppler velocimetry (Malvern Zetasizer, Model 3000, Malvern Instruments Ltd, UK). The instrument was calibrated using a  $-55$  mV standard (DTS5050; Malvern Instruments) between sample measurements. Typically after sizing measurements, the sample was diluted further with relevant buffer to maintain an acceptable photomultiplier signal. In



these measurements the lipopolyplex (LPD) DNA concentrations were approximately 20 g/ml. The zeta potential was averaged from 10 measurements with temperature maintained at 25 °C.

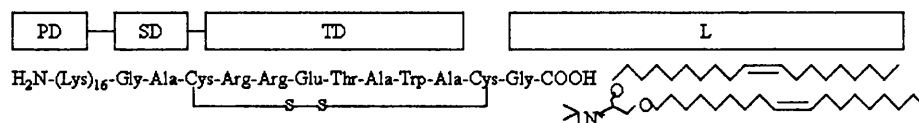
## Chapter 4 : LPD Control Experiments

### 4.1 Introduction

The ability to safely and efficiently transfer foreign DNA into cells is a fundamental goal in biotechnology (Luo *et al.*, 1999) and rapid advances have recently been made in the understanding of mechanisms for DNA stability and transport within cells. Most current systems address only one of the obstacles of DNA delivery by enhancing DNA uptake. In fact, the effectiveness of gene expression is also dependent on several additional factors, including the release on intracellular DNA, stability of DNA, unpackaging of DNA-vector complex, and the targeting of DNA to the nucleus; delivery systems of the future must fully accommodate all these processes. In order to develop a better delivery system, it is important to have knowledge of the original LPD vector. The information required includes parameters such as hydrodynamic size under non-aggregating conditions, complex behaviour over a length of time, the role each of the components plays on the final structure and the likelihood of free components being present in solution. The suitability of PCS as a measuring technique is investigated along with the role other commonly used techniques play in providing additional information on LPD complexes. The goal of this work is to elucidate the behaviour of the complex as a gene therapy vector, by assessing its biophysical behaviour. The aim of this chapter is to establish some of the characteristics of the individual components and basic properties of the complex that will pave the way for later findings and discussions.

### 4.2 Lipid, Peptide and DNA Components

This section looks at each of the components individually with a view to understanding how each one is detected and how these measurements differ from when they form a complex.



Schematic 4.1: Modular vector components that make up Lipid/Integrin-Targeting Peptide/DNA.

#### 4.2.1 Lipofectin

Figure 4.1 shows the size of lipofectin over time in its storage buffer (filtered water), although it was not found to aggregate, it was seen to form two distinct peaks at approximately 300 nm and 1600 nm as shown. Figure 4.2 show a snapshot of the distribution, the peaks being too large to represent the individual lipofectin components DOTMA and DOPE, which have molecular weights of 699.5 Da and 774 Da, respectively. Private communication with Invitrogen confirmed that the two components form a mixture and the peaks present are typical of those formed from a mixture of DOPE and DOTMA. Figure 4.1 shows the average size of lipofectin with time when in filtered water.

#### 4.2.2 Integrin-Targeting Peptide

It has been shown that Dynamic Light Scattering (DLS) is unable to measure the size of individual peptide components, the scattering from the peptide with poly-L-lysine (Lai *et al.*, 2001) is only slightly above that measured from background solvent scattering. This was confirmed in the experiments with peptide 6 and poly-L- lysine using the Zetasizer 3000 (data not shown). Alternative methods of observation include Atomic Force Microscopy (AFM) and Cryo-Electron microscopy techniques. However, the preparation technique involved is thought to interfere with the physical structure of the sample and subsequently alter the true nature of the particles. Therefore, this method of measuring peptides was not employed. Previous studies measuring the size of LPD particles using AFM in water has shown measurements in the region of 40 nm (White *et al.*, 2003); such measurements are inconsistent with the data obtained from PCS that measure all of the particle sizes and yield a distribution of particle sizes from a static environment. AFM size measurements are based on individual particle measurements and not on a distribution. On the contrary, photon correlation spectroscopy (PCS), a non-invasive technique does not alter the sample, in anyway, during preparation. PCS is also the only technique that allows real time measurement and a distribution of particle sizes to be observed.

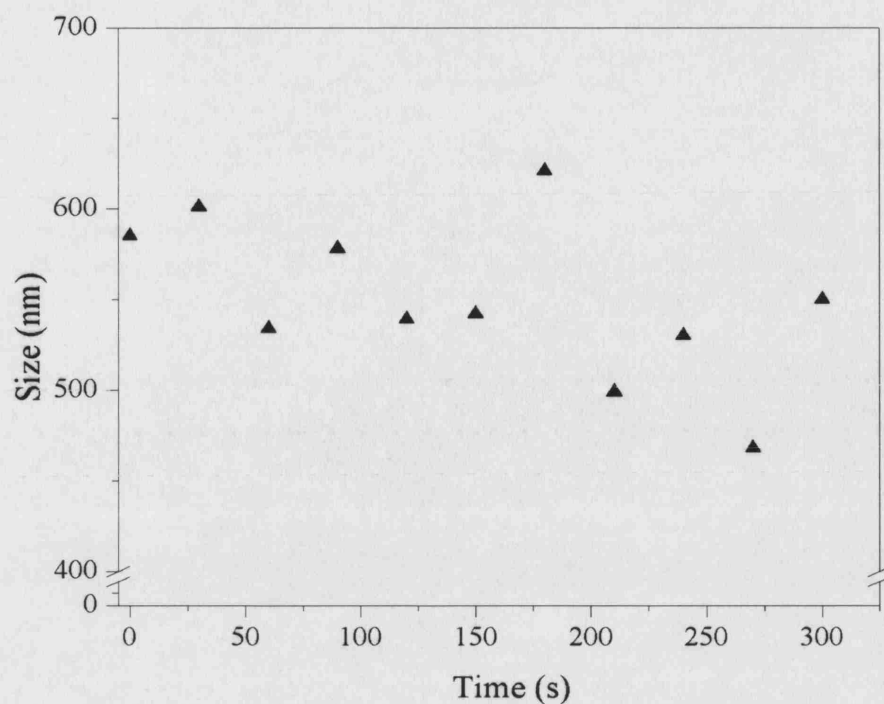


Figure 4.1: Average particle size of lipofectin (1 mg/ml), in membrane filtered water (storage buffer) as a function of time. Mean sizes determined from intensity measurements of scattered light at  $90^\circ$ . Data shown from a single representative sample.

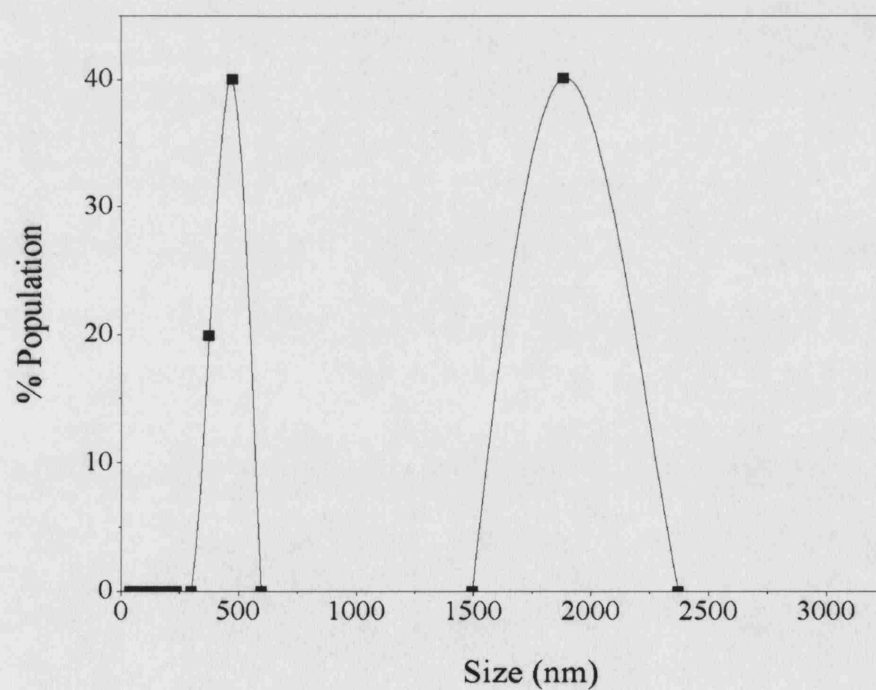


Figure 4.2: Particle size distribution of lipofectin in filtered water on the basis of the intensity of scattered light at  $90^\circ$ . Sample measurements taken at 150 sec after preparation.

### 4.2.3 Plasmid DNA

The PCS technique employed in this study was not able to detect the (uncondensed) DNA molecules in solution. It has been reported previously that the loose structure of the (uncondensed) DNA molecule does not allow sufficient light scattering to facilitate such measurements (Private communication, Dr Mike Kaszuba, Malvern Instruments). This is due to the wormlike random coil shape of the molecule. [Electrostatic interactions between DNA segments cause condensation by excluding the volume of the worm-like coil by causing localised bending or distortion of the helical structure (Bloomfield *et al.*, 1998) the complex can be measured.].

## 4.3 Lipid/Peptide/DNA Complexes

The individual components lipid (L), peptide (P) and plasmid DNA (D) come together electrostatically to form a LPD particle. PCS data show (Figure 4.3) that there is no scattering due to the presence of free lipid molecules present after the addition of peptide and lipid to plasmid DNA; this suggests the binding of plasmid DNA to lipid and peptide form a condensed structure. There are also no observed peaks at 300 nm and 1900 nm in the PCS data (those seen for free lipofectin) (Figure 4.2). Additionally, AFM studies (private communication Dr S.L. Hart) show that there are no free lipid, peptide or DNA particles present in suspension (data not shown). For this purpose AFM has been used only to demonstrate the condensation and formation of the complexes and not as a technique for measuring size. Unless otherwise stated, all experiments were conducted at a Lipid:Peptide:DNA weight ratio of 0.75:4:1 resulting in a +7 charge ratio. These studies demonstrate that the presence of a negatively charged condensing agent, such as the peptide 6 or the Lipofectin, causes the DNA molecule to collapse on itself forming a condensed structure in association with the components in the condensing reagent, it has been suggested, for example, that the reduction in the size of the DNA molecule facilitates its transport across the cell wall membrane while the complex structure formed through binding of the DNA and the components in the condensing agent has been implicated in the cellular trafficking processes that lead to transfection.

### 4.3.1 Intermolecular forces in condensation

DNA condensation arises from a complex interplay of interactions. These include: <sup>(1)</sup> *entropy*, loss upon collapse of the expanded worm-like coil, <sup>(2)</sup> *stiffness*, which sets limits on tight curvature, <sup>(3)</sup> *electrostatic repulsions* which must be overcome by high salt

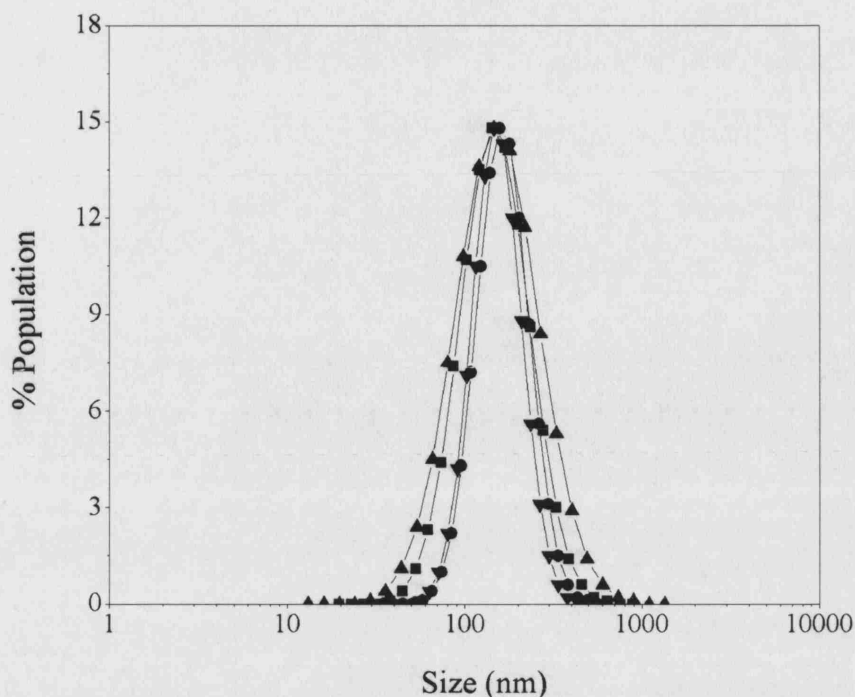


Figure 4.3: Particle size distribution of LPD (7) in distilled water 240 sec (▲), 1800 sec (■), 3600sec (▼), 10800 sec (●).

concentration or by the correlated fluctuations of territorially bound multivalent cations, <sup>(4)</sup> *hydration* which must be adjusted to allow mutual accommodation of the water structure surrounding surface groups on the DNA helices as the approach, and <sup>(5)</sup> *repulsive excluded volume* interactions with other polymers in the solution. Attractive free energy may also come by bridging through condensing ligands, and by inter-helical binding between bases whose normal intra-duplex pairing and stacking have been disrupted by interactions with solvent or ligand. Recent attention has largely focused on counterion fluctuations and hydration forces, because at close range both hydration and ionic forces appear to depend on the effect of apposing surface lattices on the fluctuating correlations of ions and water molecules between them; the two types of force may prove difficult to disentangle (Bloomfield, 1996).

DNA condenses in the presence of multivalent cations when (89-90) % of its charge is neutralised (Wilson *et al.*, 1979). This is true not only in water, but also in aqueous solutions in which the dielectric constant is lowered by alcohols or raised by osmolytes. The counter-ions not only screen coulombic repulsions between the DNA phosphates, they also produce attraction through correlated fluctuation of the ion atmosphere. Although DNA condensation and aggregation require multivalent cations,

mononucleosomal DNA has been found to aggregate at a critical concentration that increases with added NaCl.

The addition of peptide 6, to the LD complex creates a further reduction in size of the LD complex, suggesting there is an increase in condensation of the DNA by the addition of peptide 6, this is expected since the peptide has a greater overall positive charge (+17), which promotes condensation after charge neutralisation of the DNA. Neutral polymers, such as PEG, at high concentrations and in the presence of adequate concentrations of salt, can provoke DNA condensation through an excluding volume mechanism. The condensation of such DNA molecules has been observed by AFM (Minagawa *et al.*, 1994; Vasilevskaya *et al.*, 1995; Yoshikawa *et al.*, 1995). When DNA is condensed with cationic liposomes composed of a mixture of cationic and fusogenic lipids, the complex become a very efficient agent for transfection of eukaryotic cells (Felgner *et al.*, 1997), with considerable potential interest for gene therapy. Part of the efficacy of liposome complexes is presumably due to the compact state of the DNA, which protects it from nucleases and allows it to pass more easily through small openings. The lipid coating on the DNA may also increase its permeability through cell membranes, although there is evidence (Zhou *et al.*, 1994) that membrane penetration occurs predominantly by endocytosis rather than fusion.

The structure of these complexes appear to depend on the type of microscopy used to view them, as well as their lipid composition and preparative details this is a major disadvantage of using microscopy. Conventional electron microscopy (EM) studies suggest that cationic liposomes initially form clusters along the uncondensed DNA. At a critical density, these clusters coalesce by DNA-induced membrane fusion, and the DNA shows liposome complexes and bi-layer covered DNA, with the DNA tubules connected to the liposome complexes (Zhou *et al.*, 1994). Cryo-EM shows an excess of lipid charge, plasmids are trapped between lamellae in clusters of aggregated multilamellar structures (Gustaffson *et al.*, 1995).

#### 4.4 Aggregation of Lipid Complexes

Figure 4.4 suggests that there is evidence of aggregation by LD complexes in physiological conditions as observed in PBS buffer (Figure 4.4), however the rate of

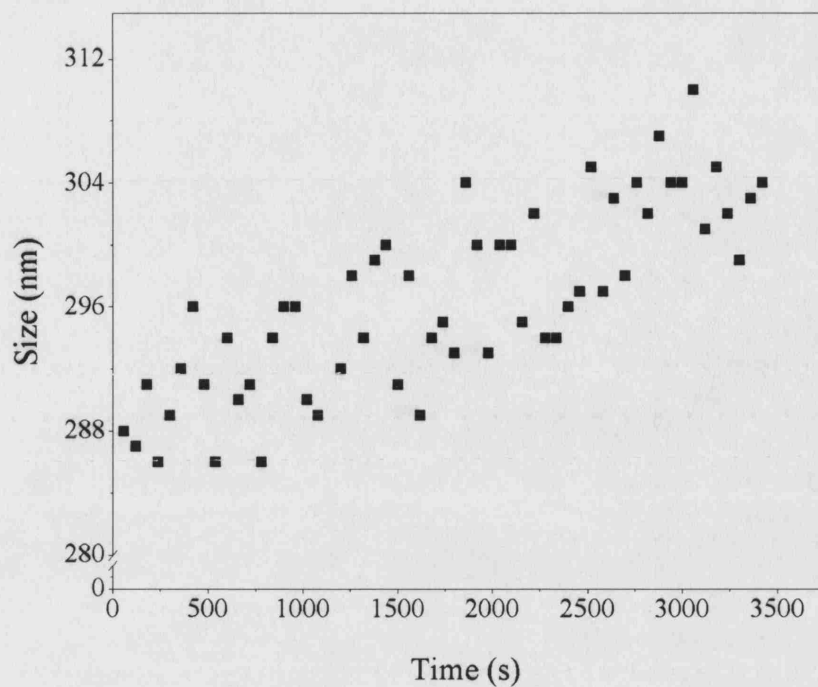


Figure 4.4: Lipid-DNA (LD) Aggregation profile in Phosphate Buffer Saline. Data show measurements for a single representative sample at a charge ration of +0.2.

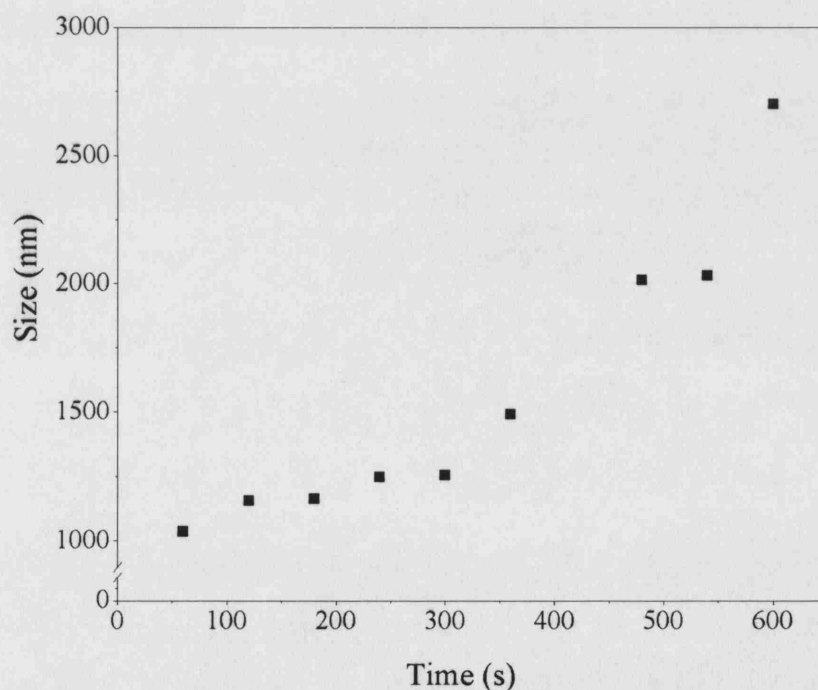


Figure 4.5: Size distribution over time for an Integrin-Targeting Peptide/DNA (ID) complex in PBS. Measurements were only recorded for aggregates up to 3000 nm in size. Beyond this range the validity of the data cannot be verified since Brownian motion is no longer the only form of diffusion present in the system.



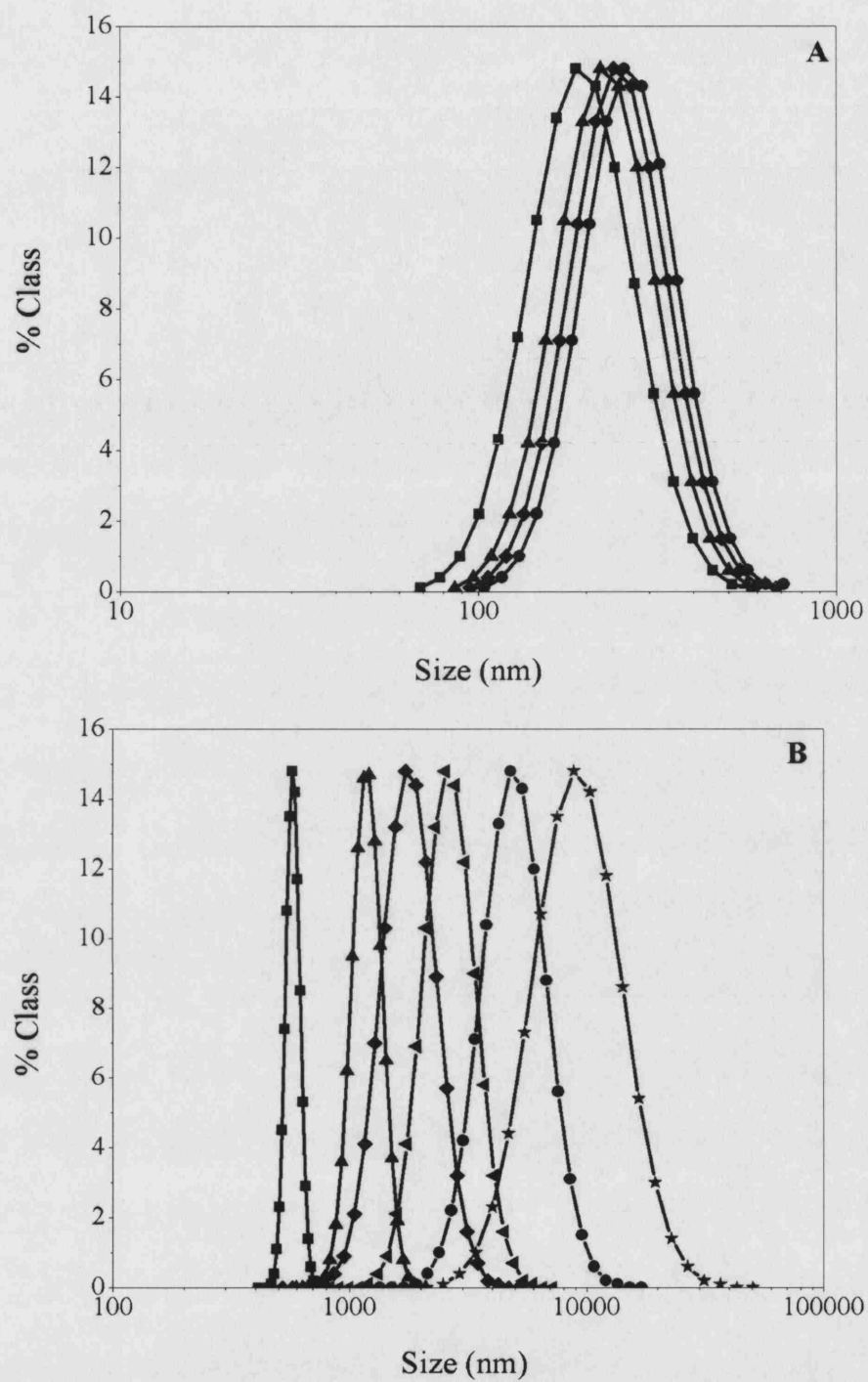


Figure 4.6: Particle Size Distributions for LPD complexes in (A) 40 mM NaCl, symbols refer to time at min 1(!), 2min (7), 3 min ( $\Delta$ ), 4 min (.). (B) 150 mM NaCl at 4 min (!), 8 min (7), 12 min ( $\Delta$ ), 24 min ( $\Omega$ ), 32 min (.), 36 min ( $\xi$ ).

aggregation is far greater for the PD complexes when the samples are mixed at the same charge ratio as shown in Figure 4.5.

Charge neutralization renders the condensed DNA molecules susceptible to aggregation; the rate and extent of aggregation are critically controlled by the buffer conditions (ionic strength and pH). Figure 4.6 (A) is an example of LPD in a 40 mM NaCl buffer, aggregation here is observed, with an increase in the shift of size distribution towards higher values, unlike in Figure 4.3. The rate of aggregation is further still as demonstrated in Figure 4.6 (B) as the concentration of salt is nearly quadrupled. This is the expected aggregation behaviour, although above a certain salt concentration other forces may come into play (Chapter 5). There is as yet no consensus of opinion on the precise molecular mechanisms by which the components in the condensing agent interact (associate) with the DNA molecules, although a number of hypotheses have been suggested (Lai *et al.*, 2001).

It is emphasised that size measurements due to the scattering of light only become detectable upon condensation of the DNA. Considering the rapidly aggregating nature of the condensed DNA particles, controlled experiments were devised to establish the size of the scatterer particles. In the case of LPD system, we showed that mixing of the DNA and Lipid and Peptide in distilled water induced DNA condensation, but did not cause aggregation. In all other buffers, condensation was followed by rapid aggregation. We therefore used measurements in water to define a nominal (notional) “scatterer” size of 150 nm (Figure 4.3) for the LPD particles.

LPD complexes are subject to varying levels of aggregation when placed in salt conditions, as demonstrated previously with PLL/DNA complexes (Lee *et al.*, 2001; Mount *et al.*, 2003).

The two most familiar kinds of colloidal interaction are *van der Waals attraction* and *electrical double layer repulsion*, which form the basis of the well-known DLVO theory of colloidal stability. While these enable a large amount of experimental aggregation and deposition data to be explained, at least in a semi-quantitative manner, there are many cases where other types of interaction have to be invoked. Initially, these were lumped together under some general heading, such as ‘structural forces’, but recent advances have given considerable insight into these ‘extra’ or ‘non-DLVO’ forces and it is now

possible to give a more detailed classification. In aqueous systems, various kinds of hydration effects can be important, especially at close approach of surfaces. These are often associated with the hydration of ions at the particle or deposition surfaces and usually give an extra repulsion. It is now known that hydrophobic effects can also be important, mostly giving an extra attraction between particles. Other important effects arise from the presence of adsorbed polymers, giving either repulsion ('steric' interaction) or an attraction ('polymer bridging'). Quantitative discussion is focused on interaction of spherical particles with similar and dissimilar particles and macroscopic surfaces.

#### 4.5 Van der Waals Interactions

The fact that an attractive force always exists between colloidal particles of the same material has long been recognized but a detailed understanding of these forces took a long time to emerge (Israelachvili *et al.*, 1992). This attraction between two closely separated surfaces is generally called the *London-van der Waals force*. The force arises from spontaneous electrical and magnetic polarizations, giving a fluctuating electromagnetic field within the media and in the gap between them. Essentially there are two theoretical approaches to the evaluation of London-van der Waals attraction. In the classical (or microscopic) approach, due largely to Hamaker (1937), the interaction between two macroscopic bodies is obtained by the pair wise summation of all the relevant intermolecular interactions. All expressions obtained in this manner may be split into a purely geometrical part and a constant A, the Hamaker constant, which is related only to the properties of the interacting macroscopic bodies and the medium. Generally A is assumed to have a value of  $5 \times 10^{-21}$  J, which is within the range recommended for biological materials (Gregory *et al.*, 2003).

#### 4.6 Storage of Complexes

There was no change in the size of LPD complexes containing psv $\beta$ , peptide 6 and lipofectin over a period of two weeks when stored at room temperature (data not shown). Previous work (Lee, 2002) showed the same for complexes of Poly-L-lysine and DNA complexes.

## 4.7 Conclusion

Experiments presented in this chapter confirm that PCS is a reliable technique for measuring particle size distributions of colloidal aggregation. The individual peptide and DNA components on their own could not be detected by PCS, only lipofectin could be measured. AFM data have shown LPD complexes to form at a charge ratio of +7, with no free lipid present in solution. The nominal scatterer size was measured to be 150 nm and is found to be stable in distilled water, changing the ionic strength of the buffer made the particles susceptible to aggregation. The peptide component (peptide 6) was largely responsible for the high levels of aggregation observed in physiological conditions. The storage of LPD over a month and at - 20 ° C did not alter the physical stability of the complexes.

## Chapter 5 : Fractals

### 5.1 Introduction

The stability of a colloidal system is generally imparted by the presence of some surface charge on the particles which results in the DLVO electric double repulsion. Aggregation of these fine particles into large aggregates can be achieved by the addition of inert electrolyte. However, much of the early work on particle aggregation was only concerned with the kinetics of the aggregation process and very little was known about the structure of the aggregates formed (Bushnell *et al.*, 2002). The lack of development in the understanding of the aggregate structure stemmed from the fact that, until approximately two decades ago, there was no suitable method for properly describing the complex structure of particle aggregates. The nature of particle aggregates makes the conventional symmetry approach inapplicable to the description of their complex structures. The breakthrough came in the mid 1970s, when fractal geometry emerged with the publication of Mandelbrot's work (Mandelbrot *et al.*, 1975). The development of the idea of fractal mathematics breathed new life into floc characterisation efforts with the realisation that when many colloidal systems aggregate, mass fractal structures are generated. This allows the representation of the apparently wild, complex structures of aggregates by simple parameters known as *fractal dimensions*.

Considerable research has been devoted to establishing the causes of poor transfection and the size of plasmid DNA complexes has been identified as an important factor. When polycations are mixed with nucleic acids, the ensuing electrostatic interactions result in the collapse of DNA into a compact structure. Previous work at UCL (Lee *et al.*, 2001; Mount *et al.*, 2003; Sarkar *et al.*, 2003) and elsewhere (Rolland *et al.*, 1998; Zelphati *et al.*, 1998) has shown that aggregation of these compacted DNA-polycation complexes occurs under most physico-chemical conditions, including physiological conditions. There is a tendency for aggregation of these systems that is governed by their physio-

chemical properties and is described by the DLVO theory (Lee *et al.*, 2001). The kinetics of aggregation of these complexes using Monte Carlo simulations is described in Chapter 6. The properties of aggregates of DNA complex have also been investigated in numerous studies using a variety of techniques including light scattering, centrifugation, gel electrophoresis, electron microscopy, X-ray diffraction and atomic force microscopy (Zelphati *et al.*, 1998; Ferrari *et al.*, 1998; Kreiss *et al.*, 1999; Ross *et al.*, 1999; Wolfert *et al.*, 1996). However, these techniques provide no information on the mechanisms of aggregation and give no indication of the morphology of the resulting aggregates. The spatial distribution of DNA complexes within the aggregates may vary considerably with time and/or as a result of changes in the physio-chemical and preparation conditions. The three-dimensional structure of the aggregates may vary from a loosely bound, open structure to a tightly packed, dense structure. The impact of these structures on transfection efficiency may be significant, but has not been investigated because it has proven difficult to quantify these structures.

The concept of fractals has been used previously to describe the morphology of many structures resulting from naturally occurring growth processes. The formation of a fractal structure starts when primary nano-particles or clusters of such particles in a liquid medium collide continuously to form larger self-similar structures; depending on the detailed kinetics of the collisions between the particles the final structure may vary from a 1-dimensional linear structure to a 2- or 3-dimensional branched, porous or solid structure. Mass fractals are formed in this way and may be characterised by their fractal dimension,  $D_f$ , which relates the size ( $R$ ) to the mass ( $M$ ) of the structure. Thus:

$$R = \alpha(N)^{1/D_f} \quad 5.1$$

where  $\alpha$  is a constant and  $N$  is the number of the primary particles in the structure.  $D_f$  is typically in the range  $1 \leq D_f \leq 3$ . Experimental studies combined with theoretical analysis have identified two primary mechanisms by which mass fractal structures form. Reaction-limited colloidal aggregation (RLCA) has been reported to occur at low particle concentrations and/or low sticking probability where only a small fraction of encounters between particles leads to aggregation. These conditions lead to the formation of compact fractal structures with a high value of fractal dimension ( $D_f \geq 2.1$ ). In contrast, diffusion-limited colloidal aggregation (DLCA) occurs at high particle concentrations. In this case it is hypothesised that all particle-particle collisions cause aggregation, corresponding to a

sticking probability of unity. The result is the formation of loose structures with fractal dimensions close to 1.8 (Lin *et al.*, 1989).

In biotechnology, many growth processes including growth of filamentous micro-organisms and microbial colonies have been shown to have fractal properties (Großkinsky *et al.*, 2002). For example, it has been demonstrated that the fractal dimensions of bacterial colonies and the branching ability of filamentous micro-organisms are sensitive to changes in nutrient concentration. Other examples of fractal aggregation also include aggregation of particles with adsorbed antibody fragments, coagulation of waste water sludge and many non-biological systems (Magazu *et al.*, 1989; Amal *et al.*, 1993; Ayazi Shamlou *et al.*, 1996; Bohr *et al.*, 1997; Molina Bolívar *et al.*, 1998).

To date there has been no study that has been reported in the literature on the fractal properties of vector delivery systems. In the present investigation a hypothesis that the aggregation of DNA complexes leads to the formation of fractal structures and provide new experimental data will be tested. The fractal dimension of aggregates of DNA complexes using static light scattering (SLS) are measured and demonstrate that the fractal dimension provides insight into the spatial distribution of DNA complexes within the aggregate. The fractal dimension of these aggregates is shown to be sensitive to changes in physico-chemical properties of the system and thus fractal methods may be used as a new tool for monitoring the quality of gene delivery vectors during preparation and storage.

## 5.2 Results and Discussion

Figure 5.1 shows the variation of the scattered intensity,  $I(q)$ , of light as a function of the scattering angle,  $\theta$ , with time as a parameter. The data refer to experiments with the latex vector particles. The scattering vector,  $q$ , was calculated from Equation 2 with  $n = 1.33$  (for water) and  $\lambda = 532$  nm. For clarity of presentation only some of the data points are shown. The conditions of the experiments always satisfied the basic requirements of the Rayleigh-Debye model but for accuracy the calculations were confined to data in the range  $10^\circ \leq \theta \leq 30^\circ$  for LPD corresponding to  $0.2 < qa < 1.0$  LPD and latex, where

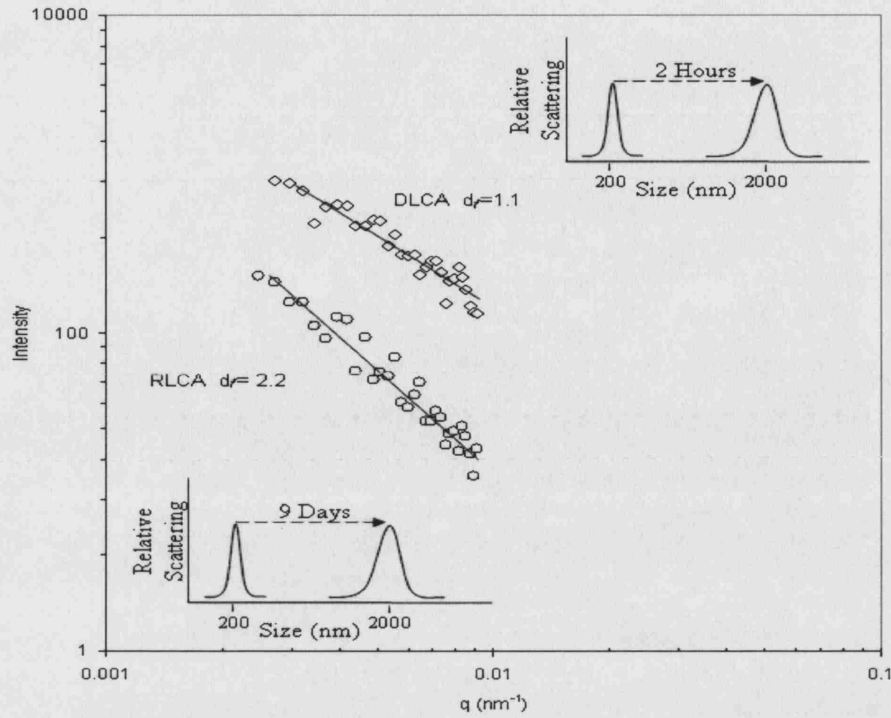


Figure 5.1: Influence of salt concentration on the fractal dimension of latex particles at pH 3.0, 250mM NaCl ( $\circ$ ) and 1M NaCl ( $\diamond$ ) for times at 2 hours and 9 days for 1M and 250mM, respectively. The systems present exhibit aggregation in both the RLCA and DLCA regime. Insets show the time taken for the measured aggregate to form in each instance.

the radius,  $a$ , of the scatterer within the aggregates was taken to be 200 nm (Latex) and 150 nm (LPD). Based on the power-law dependence of the scattered intensity on the scattering vector,  $I(q) \propto q^{-D_f}$ , we applied linear regression analysis to the data points in Figure 5.1.

Theoretical considerations based on statistical physics of diffusion-limited colloidal aggregation (DLCA) and reaction-limited colloidal aggregation (RLCA) suggest that the latex particles exhibit both forms of aggregation at given salt concentrations. The latex particles were initially stabilised in a buffer that prevented aggregation of any form, it is only upon the addition of high concentrations of salt and an increase in acidic conditions to pH 3.0, that aggregation was induced. A  $D_f$  of 2.2 can be seen for RLCA, a  $D_f$  of  $2.1 \pm 0.1$  has been cited (Lin *et al.*, 1989) and confirmed by computer simulations (Ball *et al.*, 1987) for RLCA. A  $D_f$  of 1.1 was observed for latex particles in 1M indicative of DLCA regime. In the absence of any previous data on fractal dimension of plasmid vector particles, we performed experiments for comparison with latex plasmid vector particles,



we performed experiments for comparison with latex particles aggregating under both DLCA and RLCA conditions. The Latex Particles follows the classical DLVO theory; the increase in ionic strength gives rise to a reduction of the electrical double layer around the particles, given by the Debye-Hückel length (Gregory *et al.*, 1993).

Fractal dimensions of LPD complexes were taken in the region 10 °-30 ° as LPD particles remained effectively unchanged despite the fact that the aggregate size distribution shifted continuously towards larger sizes throughout the period of measurement, as shown in Figure 5.2. Figure 5.2 shows an LPD complex at various time points when placed in physiological conditions, measurements were taken using DLS, at 90° based on the intensity of scattered light. Taken together, these observations support the view that the addition of peptide and lipid (lipofectin®) rapidly induces condensation of the plasmid DNA by charge neutralisation (Bloomfield, 1996). As discussed earlier in section 4.3.2. The decrease in the repulsive interaction force arising from the electrical double layers of the complexes, caused by the electrolyte in the medium, resulted in the aggregation of the self-assembled complexes. A constant fractal dimension that was unaffected over time is evidence of little restructuring of the aggregates. A shift towards larger size distributions with time is typical of a LPD complex in salt conditions, the broadening of the distributions over time is responsible for the increase in system polydispersity from a value of 0.144 in distilled water to 1.0 in Phosphate Buffer Saline, this is the case in Figure 5.2 where the polydispersity changes from 0.177 at 0 min to 1.0 at a period of 36 minutes after preparation. The speed at which a completely heterogeneous system is established is dependent on the rate of aggregation.

Scattering from aggregates is accounted for by the sum of the distribution of scattering density over the  $N_0$  individual particles. For simplicity, it is assumed that the primary particles of which the aggregates consist are identical, rigid (hard), and of spherical symmetry. The scattering intensity  $I(q)$  from an aggregate of  $N_0$  of such primary particles is given by (Tang *et al.*, 1999).

$$I(q) = N_0 V_0^2 (\Delta\rho)^2 P(q) S(q) \quad 5.2$$

Where  $V_0$  is the volume of each primary particle,  $\Delta\rho$  the difference of the scattering-length densities between the particles and the solvent, and  $q$  the wave number which is

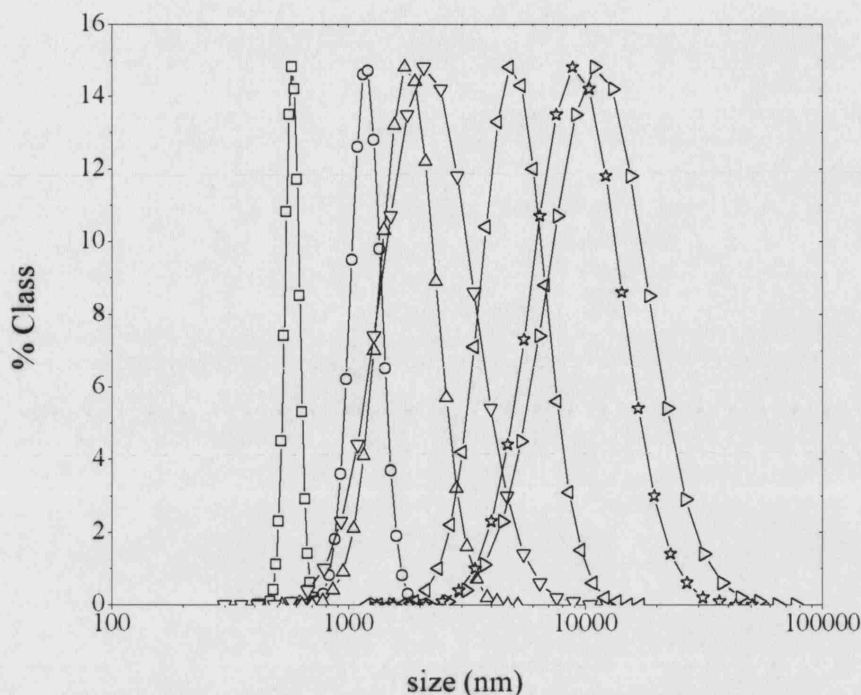
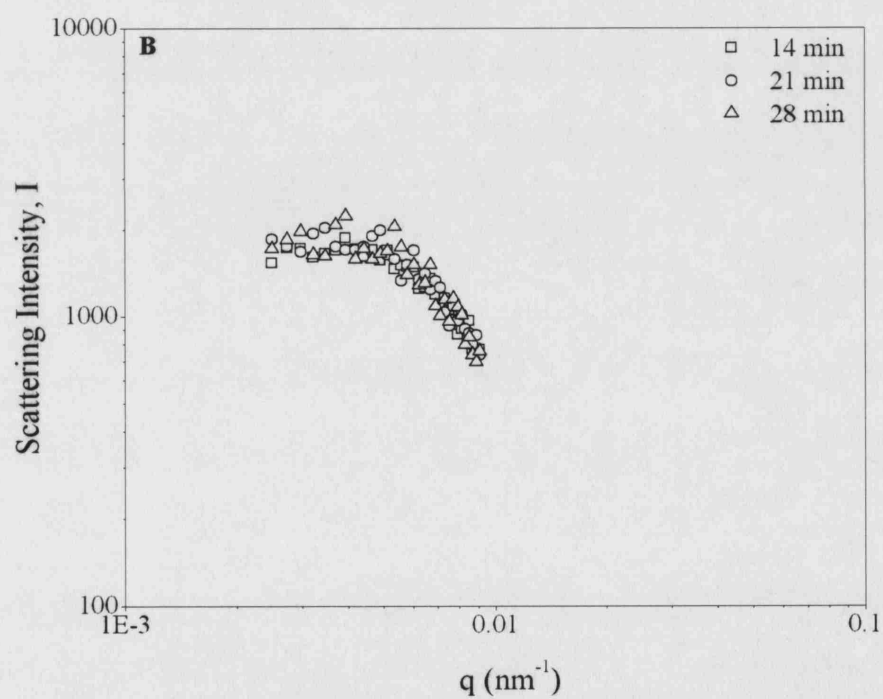
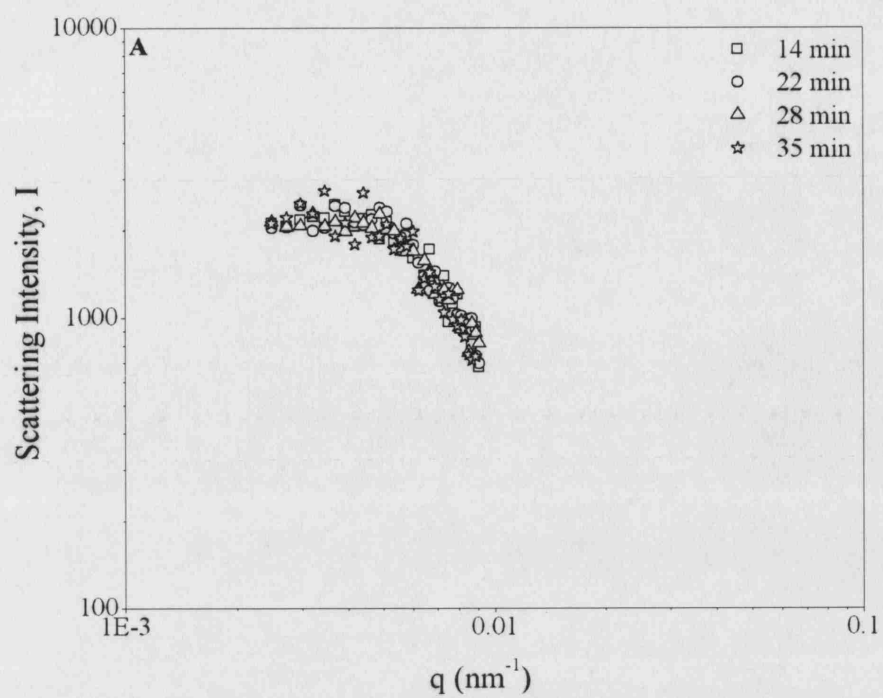
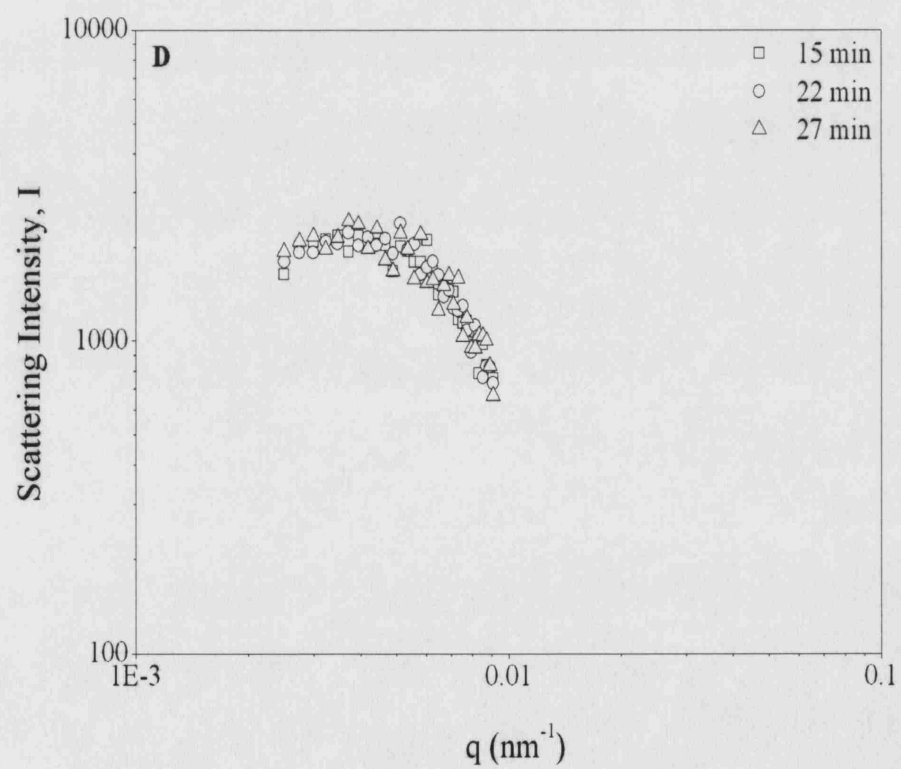
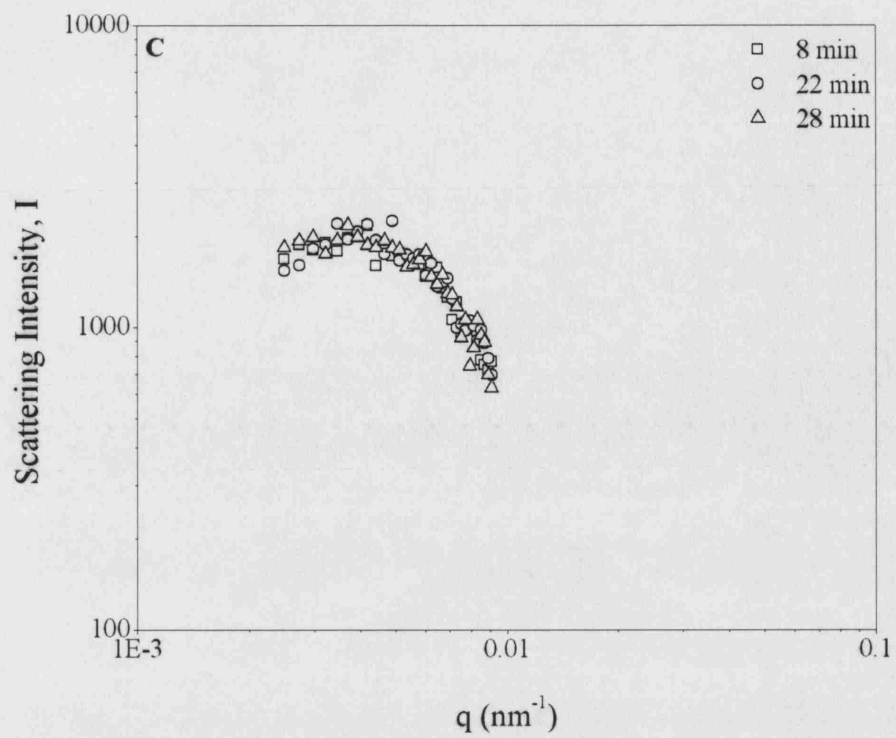


Figure 5.2: Particle size distributions of LPD complexes at a charge ratio of + 7.0 at, pH 7.2 in 150 mM NaCl, as a function of time after preparation: 0 min( $\square$ ), 4 min( $-$ ), 8 min( $\Delta$ ), 20 ( $\Xi$ ), 28 min( $\times$ ), 32 min( $\psi$ ), 36 min( $\chi$ ). Size distributions were determined as mean of diameter based on the intensity of scattered light at  $90^\circ$ . The data shown was obtained from a three sample measurements.

defined by  $q = (4\pi n/\lambda) \sin(\theta/2)$ , where  $\theta$  is the scattering angle,  $\lambda$  the wavelength of the incident laser light, and  $n$  the refractive index of medium.  $P(q)$  denotes the form factor of the primary particles, and  $S(q)$  is the inter-particle structure factor. Scattering Intensity-  $I(q)$ - can be classified into three regions according to the magnitude of the wave number  $q$  (Guinier *et al.*, 1955):  $q \leq 1/l$  (Guinier region);  $1/l < 1/r_0$  (fractal region) and  $q > 1/r_0$  (asymptotic region), where  $l$ , is the correlation cut-off range (equal to the aggregate characteristic length here) and  $r_0$  the radius of the primary particles.

In the Guinier region, the object is likely to be uniform and scattering intensity  $I(q)$  is independent of wave number  $q$ . In the intermediate region  $1/l < 1/r_0$ , the form factor  $P(q)$  is independent of fractal dimension  $D$ , the structure factor  $S(q)$  is approximately proportional to  $q^{-D_f}$ . Therefore, the scattering intensity from mass aggregates has a power law correlation with the wave number  $q$ :  $I(q) \propto q^{-D_f}$ . A graph of  $I(q)$  against  $\log q$  gives a gradient of  $-D_f$ . Figure 5.3 shows some typical examples.





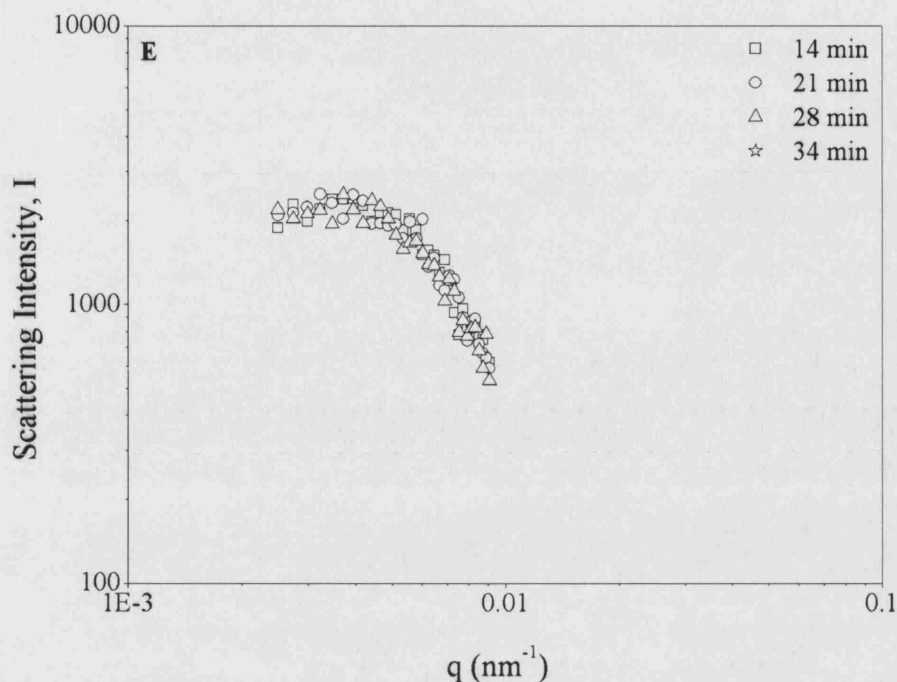


Figure 5.3: Static light scattering curves for LPD particles, (scattering Intensity  $I(q)$  versus magnitude of the scattering vector ( $q$ ) obtained at successive times following the preparation of the lipopolyplexes in NaCl buffer, pH 7.2: (A) 100mM NaCl, (B) 150mM NaCl, (C) 250mM NaCl, (D) 750mM NaCl, (E) 1M NaCl times.

The rate of aggregation of the complexes aggregate is shown in Figure 5.4. Measurements above  $3\ \mu\text{m}$  were not recorded since they fall beyond the detection range of the machine. The results indicate the greatest severity of aggregation at 150 mM NaCl (physiological conditions), and a reduction in aggregation above this value. Figure 5.4 shows the aggregation value of the complexes in varying levels of salt concentration. Examination of the data indicates that aggregation slows down at both low and high electrolyte concentrations. Crucially, aggregation rate is at its maximum for an electrolyte concentration of 150 mM corresponding to physiological conditions.

A decrease in fractal dimension, indicating, loose more open structures is seen for complexes from 80 mM to 150 mM (Figure 5.5). At higher salt concentrations, an increase in fractal dimensionality is observed. At electrolyte concentrations of 750 mM and 1000 mM, the fractal dimension increased to 2.1 and 2.4 respectively, indicating more compact structures. In contrast, we obtained a fractal value of 1.7 for aggregation occurring at an electrolyte concentration of 40 mM, indicating the formation of loose

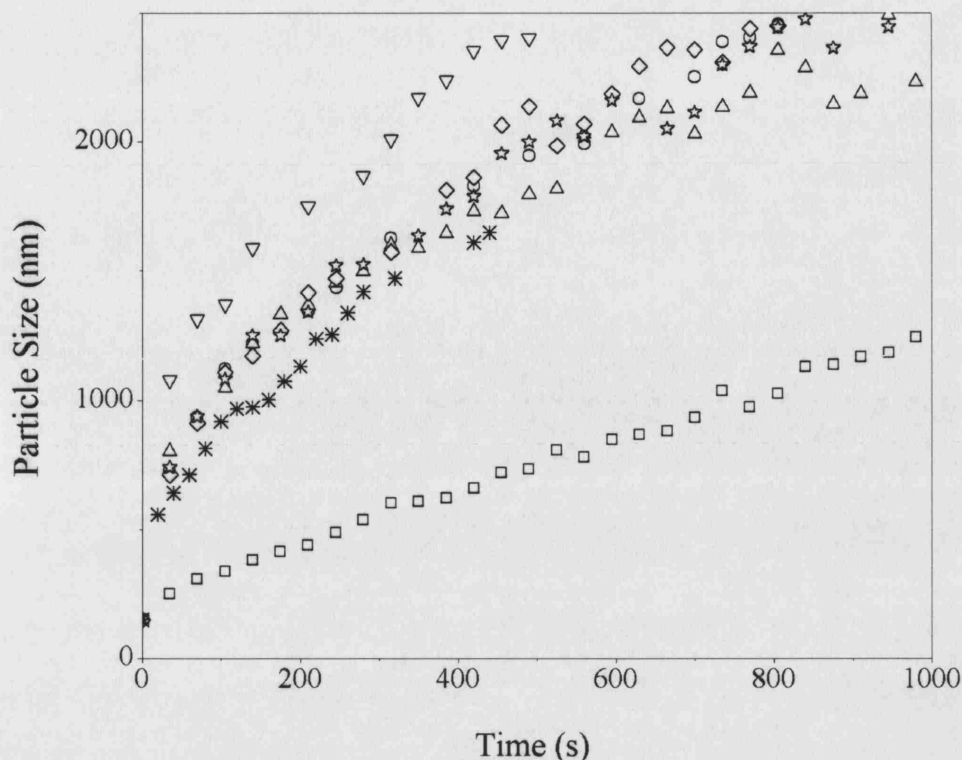


Figure 5.4: Size distribution of LPD complexes as a function of time for varying electrolyte concentrations at pH 7.0: 40 mM ( $\nabla$ ), 80 mM ( $-$ ), 100 mM ( $\circ$ ), 150 mM ( $\times$ ), 250 mM ( $M$ ), 750 mM ( $\psi$ ), and 1 M ( $\square$ ). All measurements were taken using DLS.

structures, as expected for growth in the DLCA regime, for which a theoretical value of fractal dimension of 1.8 has been reported (Lin *et al.*, 1989; Meakin, 1988). Although the results are not as expected from classical DLVO theory as explained in chapter 4. Based on the aggregation profiles in Figure 5.4 we expect the most open structure at 150 mM NaCl and the most compact structure at 1M electrolyte solution as observed in Figure 5.5. The lower than expected fractal value for the complex at 40 mM NaCl suggests there may be a more complicated explanation into the formation of aggregates than just reaction limited and diffusion limited aggregation at electrolyte concentrations close to the critical coagulation concentration.

The energy plots for the different systems shown in Figure 5.6 confirm that at the extremes of electrolyte concentrations (750 mM and 1000 mM), the energy barrier is highest for the particles (non DLVO theory). This suggests that the regime present is reaction limited, since there is a barrier to coagulation. The experiments were not conducted at higher concentrations than 1M, but it may be possible to speculate based on

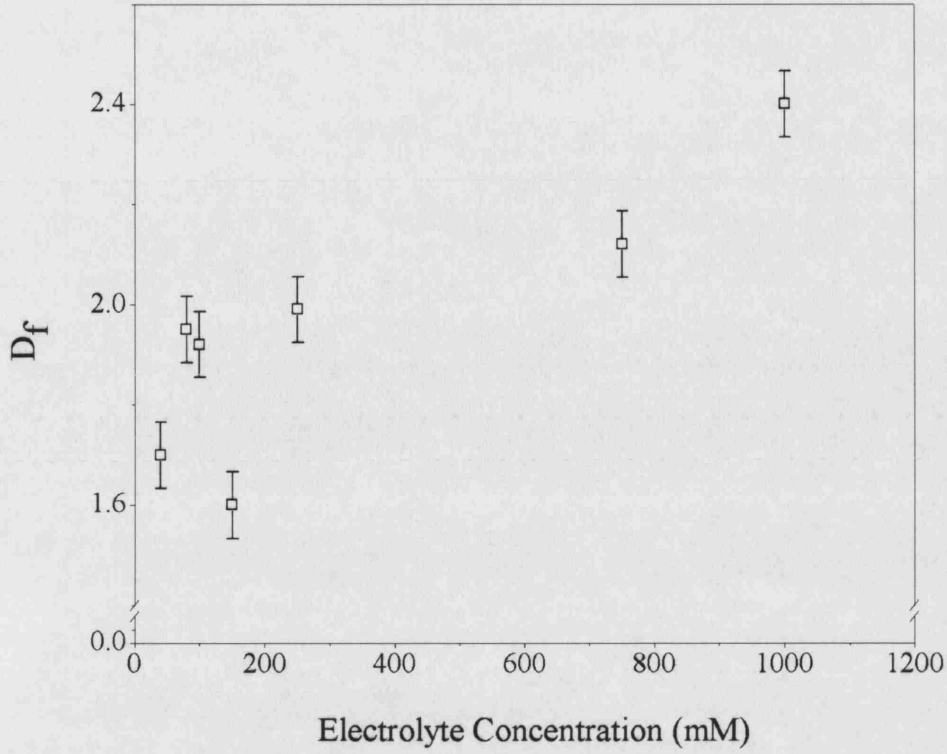


Figure 5.5: The fractal dimension ( $D_f$ ) of Lipofectin/integrin-targeting peptide/DNA (LPD) aggregates as a function of electrolyte concentration (mM). Data is given for the final  $D_f$  of the system.

the current data, that a further increase in the electrolyte concentration would continue to raise the barrier to aggregation.

$$V_A = -\frac{A}{12} \left[ \frac{y}{x^2 + xy + x} + \frac{y}{x^2 + xy + x + y} + 2 \ln \left( \frac{x^2 + xy + x}{x^2 + xy + x + y} \right) \right] \quad 5.3$$

where  $x = (H/a_1 + a_2)$  and  $y = a_1/a_2$ ,  $A$  is the Hamaker constant, assumed to have a value of  $5 \times 10^{-21}$  J.  $H$  is the separation distance between the surfaces of two spherical particles of radii  $a_1$  and  $a_2$ . The electrical double-layer repulsion force calculated from the following expression (Zelphati *et al.*, 1998):

$$V_R = \frac{64\pi\epsilon a_1 a_2 K_B^2 T^2 \gamma_1 \gamma_2}{(a_1 + a_2) e^2 z^2} \exp[-\kappa H] \quad 5.4$$

where  $\epsilon$  is the permittivity of the medium,  $K_B$  the Boltzmann constant,  $T$  the absolute temperature (Appendix C),  $\kappa$  the Debye-Hückel reciprocal length has a value of  $2.4 \times 10^9$

$m^{-1}$  and  $e$  is the elementary charge (Appendix C). The dimensionless functions,  $\gamma_1$  and  $\gamma_2$ , of the zeta potentials  $\zeta_1$  and  $\zeta_2$ , respectively, are given by:

$$\gamma_i = \frac{\exp[ze\zeta / 2kT] - 1}{\exp[ze\zeta / 2kT] + 1} \quad 5.5$$

These observations may be explained via the concepts of the critical coagulation concentration (ccc) and the critical stabilisation concentration (csc), both of which have found application in the analysis of aggregation data for biological and non-biological systems. The repulsive behaviour of certain hydrophilic particles in hydrophobic environments of high ionic strengths contradicts the classical DLVO theory which predicts strong adhesion or coagulation in a primary minimum (Israelachvili *et al.*, 1992). This colloidal stability, not completely understood, can be explained by the existence of a repulsive structural force known as the *hydration force*. Several workers have found that the hydration forces, which are exponentially repulsive, play an important role in the

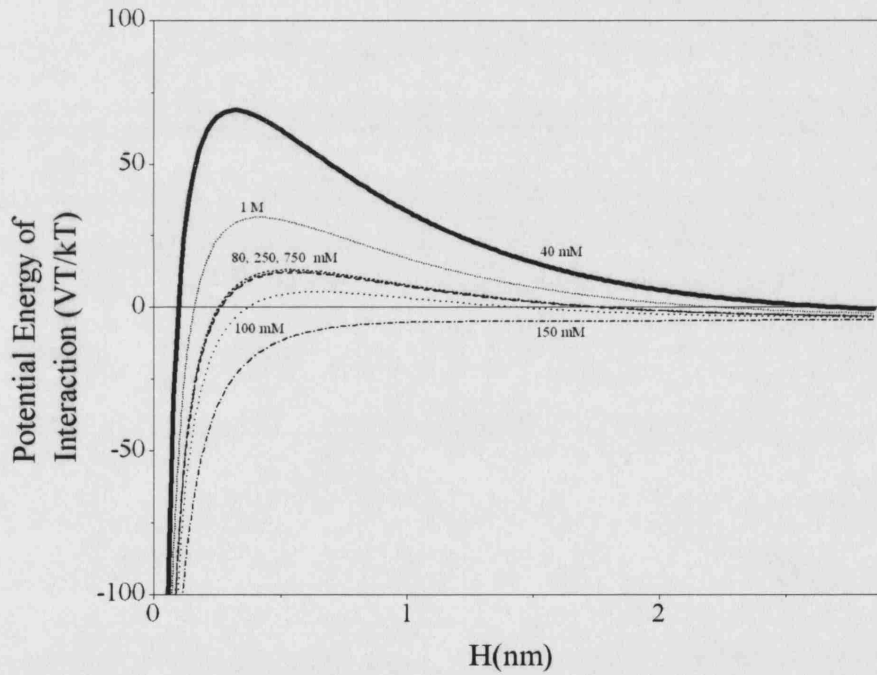


Figure 5.6: Influence of buffer conditions on the dimensionless total energy of interaction between two spherical particles of a monomer hydrodynamic radius of 150 nm, as a function of the distance  $H$  (nm) between their surfaces; data generated using the DVLO theory of colloidal interactions. The total energy of interaction,  $VT$ , between the particles was obtained by summing the van der Waals attractive potential,  $VA$ , and the repulsive double layer electrostatic potential,  $VR$  (Zelphati *et al.*, 1998; Sorensen. 2001).



stabilisation of colloidal systems, particularly those containing particles with hydrophilic surfaces (Molina- Bolivar *et al.*, 1999). These hydration forces originate from the water molecules that bind to the surface of charged macromolecules such a lipid bilayers and biological membranes, as well as any ionic, zwitterionic or H-bonding peptides, polysaccharides and other functional groups at the surface of these materials. For these particles to contact or approach each other closely, some dehydration of their surfaces and ionic groups must occur. This raises the free energy of the system, leading to an anomalous repulsion between the particles even when they are exposed to high electrolyte concentrations. The hydration effects can be significant, acting as ranges comparable to the electrical double layer repulsion, even in very high salt environments (Butt, 1991; Healy *et al.*, 1978).

The hydration force between two spherical particles can be approximated by:

$$V_h = na\lambda_h^2 P_0 \exp\left(-\frac{H}{\lambda_h}\right) \quad 5.6$$

The inclusion of hydration forces in the classical DLVO theory results in the following equation for the total potential energy of interaction between two particles:

$$V_T = V_R + V_A + V_h \quad 5.7$$

Previous studies have shown the hydration forces generally exist between negatively charged biological entities only (Pahley, 1981; Paetsev *et al.*, 2000). This is not supported by the zeta potential data shown in Figure 5.7. It can be seen at pH 7 that the lipopolyplex growth is extremely sensitive to NaCl concentration in the range 40 mM to 1M. Initially

Electrolyte concentration (mM)	Zeta potential, $\xi$ (mV)	$\gamma_1 \gamma_2$
40	34.4	0.323
80	22.8	0.218
100	20.6	0.198
150	15.0	0.145
250	22.9	0.219
750	23.1	0.221
1000	27.6	0.262

Table 5.1: Zeta potential and dimensionless function of zeta potential at electrolyte concentrations 40 mM-1000 mM.

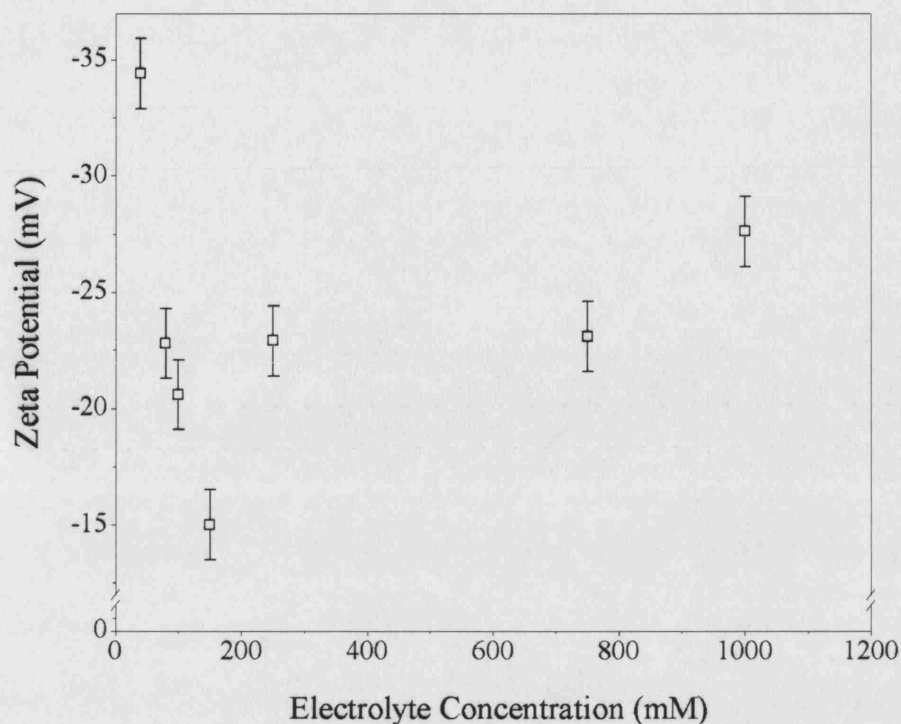


Figure 5.7: Dependence of electrolyte concentration on the LPD system zeta potential. All systems were at pH 7.0. The zeta potential is calculated from the electrophoretic mobility of the particles in the buffer.

an increase in the small molecule electrolytes,  $\text{Na}^+$  and  $\text{Cl}^-$ , balanced the surface charge on the polyplex and thus reduced the repulsion between them. This effect is altered above NaCl concentrations above 150 mM as demonstrated in Figure 5.4.

The raw data is shown in Table 5.1 for the zeta potentials at the electrolyte concentrations shown in Figure 5.4 along with the dimensionless function of zeta potential.

As the electrolyte concentration is increased, the electrical double layer surrounding the particles diminishes reducing the electrostatic repulsive force between the colliding particles. Theoretically, the electrolyte concentration at which the double layer force becomes zero is known as the *critical coagulation constant* (ccc). The impact of electrolyte concentration on the stability of the particles and the ccc for a particular system may be determined in terms of the stability ratio,  $W$ .

According to the DLVO theory, an increase in electrolyte concentration leads to a reduction in the sticking probability following collision between particles. As a result,

only a fraction,  $1/W$ , of the encounters between particles leads to a permanent contact.  $W$  is known as the stability ratio and may be obtained in a number of ways (Shaw *et al.*, 1992). A useful equation for the estimation of  $W$  is the Reerink and Overbeek approximation (Reerink *et al.*, 1954], given by:

$$W \approx \frac{1}{2\kappa a} \exp \left[ \frac{V_{\max}}{K_B T} \right] \quad 5.8$$

where  $\kappa = 3.288\sqrt{[\text{NaCl}]}$  nm<sup>-1</sup> is the Debye-Hückel parameter (e.g.  $1.27 \times 10^{-9}$  for 150 mM NaCl),  $a$  is the radius of a primary particle (i.e. 150 nm for the LPD system),  $K_B$  is Boltzmann's constant ( $1.38 \times 10^{-23}$  J/K) and  $T$  is the absolute temperature (taken to be 298 K).

The energy barrier,  $V_{\max}$ , determined when  $dV/dH = 0$ , is obtained from Figure 5.6. Figure 5.8 shows the stability ratio ( $W$ ) as a function of electrolyte concentration. As the salt concentration is increased the colloidal stability decreases, as shown by a decrease in the value of  $W$  until a minimum is reached that corresponds to the ccc.

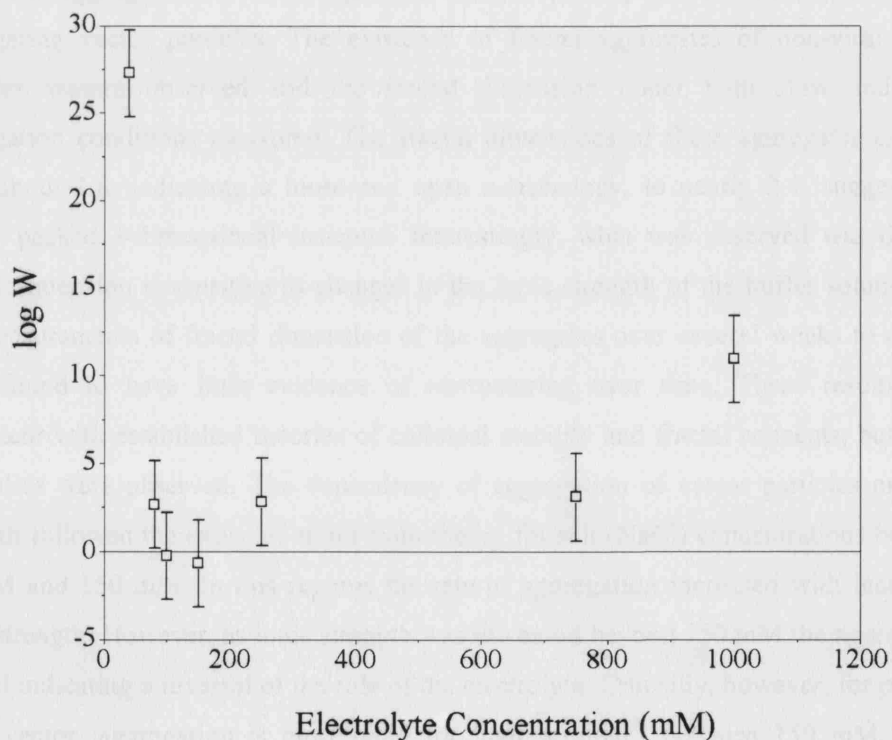


Figure 5.8: Experimental dependence of stability ratio ( $W$ ) on electrolyte concentration. Stability values were determined from the Reerink and Overbeek approximation.

According to data in Figure 5.4, beyond the ccc value (80-150 mM), the stability ratio increases with further increase in the electrolyte concentration. This type of behaviour is contrary to what may be expected from the DLVO theory but has been reported previously for proteins and other systems.

The theoretical understanding of the impact of key controlling factors on the strength of these hydration forces is limited, particularly for practical systems such as the non-viral gene delivery particles of interest in this study. In the absence of this information it is recommended that the stability profiles shown in Figure 5.8 are determined experimentally as described in this study.

### 5.3 Conclusion

New measurements are reported in this chapter on the aggregation processes that cause instability of colloidal non-viral vector particles in suspension. The vector particles were prepared by charge neutralisation of plasmid DNA using a patented Lipofectin/Integrin-Targetting peptide mixture. Dynamic light scattering was employed to measure the kinetics of aggregation and static light scattering to quantify the internal structure of the aggregating vector particles. The existence of fractal aggregates of non-viral vector particles was observed and the fractal dimension under both slow and rapid aggregation conditions measured. The fractal dimensions of these aggregates changed from about 1.8, indicating a loose and open morphology, to nearly 2.4, suggesting a tightly packed 3-dimensional structure. Interestingly, what was observed was that the fractal dimension is sensitive to changes in the ionic strength of the buffer solution and the measurements of fractal dimension of the aggregates over several weeks to months were found to have little evidence of restructuring over time. These results were consistent with established theories of colloidal stability and fractal concepts, but a few anomalies were observed. The dependency of aggregation of vector particles on ionic strength followed the expected trend from theory for salt (NaCl) concentrations between 40 mM and 150 mM. In this regime, the rate of aggregation increased with increasing ionic strength. However, as ionic strength was increased beyond 150 mM the aggregation slowed indicating a reversal of the role of the electrolyte. Crucially, however, for plasmid DNA vector, aggregation is most rapid for ionic strengths between 150 mM, which represents physiological conditions.

## Chapter 6 : Aggregation Profiles

### 6.1 Introduction

The drive for delivery vectors that have the transfection capacity of viral vectors and the safety aspects of non-viral systems has focussed on understanding the mechanisms of cellular barriers to transport of vectors and establishing the relationships between the molecular structure of vectors and their function (Duguid *et al.*, 1998; Smith *et al.*, 1997; Hart *et al.*, 1997; Pouton *et al.*, 1998; Kwoh *et al.*, 1999). These studies are leading to the rational design of a new generation of non-viral vectors with highly complex molecular architecture involving different domains and moieties. These formulations have been shown to improve cell-culture and *in-vitro* animal-cell transfection, but in many cases they create new problems including the loss of physical stability of the vector particles, which is currently a major challenge to vector development (Anchordoquy *et al.*, 1999).

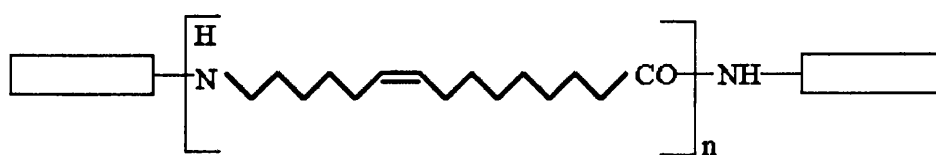
Chapter 4 reported a “proof of concept” data on an integrin targeting lipid-peptide-DNA (LPD) vector delivery system using *in-vivo* cell-culture tests and *in-vitro* animal models (Lee *et al.*, 2003). The rationale for the design of the LPD vector has been fully described elsewhere (Hart *et al.*, 1997). Briefly, the original vector consisted of four basic domains (modules). These included a lipid domain (LD) consisting of (1:1 (w/w)) a cationic lipid N-[1-(2,3-dioleoyloxy) propyl]-n-n-n-trimethyl ammonium chloride (DOTMA) and the co-lipid, DOPE. The peptide domain (PD) consisted of a short-chain (16-lysine repeats), DNA-binding, cationic peptide. The PD domain was linked to a cyclic RGD (RRETAWA) integrin cell-receptor targeting head domain (TD) and the targeting and peptide domains were separated by a –Gly-Ala- moiety acting as the spacer domain (SD), as shown in schematic 4.1.

*In vitro* animal tests with the original LPD vector demonstrated cell transfection efficiencies comparable with adenovirus (Ayazi Shamlou *et al.*, 2003) vectors, but the

vector particles were physically unstable under most conditions of ionic strength and pH including physiological conditions (Lee *et al.*, 2001, Sarkar *et al.*, 2003). Condensation of plasmid DNA molecules by charged neutralisation resulted in vector particles with weak repulsive double later interaction force making them susceptible to aggregation. Size measurements indicated that vector size increased from about 150 nm immediately after preparation to well over 1000 nm in around ten minutes. Formation of macroaggregates caused precipitation of the vector particles out of solution. Optimal *in vitro* cell transfection is thought to occur when vector particles are below about 200 nm. Additionally, aggregation reduces the shelf-life of the vector particles and will cause serious problems with regulatory agencies. Similar observations have been reported for other vector systems (Rolland *et al.*, 1998; Zelphati *et al.*, 1998; Allison *et al.*, 2000).

A major advantage of the LPD vector is its flexible modular structure allowing independent design and optimisation of each of the four domains in its architecture (chapter 7). This approach has motivated our long term research strategy the ultimate aim of which is to establish structure-function relationship for different vector delivery systems. Mathematical modelling of the kinetics of particle aggregation is an important aspect of this approach. In the work described here we propose the use of Monte-Carlo simulation techniques to predict the dynamics of aggregating vector particles. The technique is demonstrated by providing simulations for two variants of the vector architecture, which have shown to be highly aggregating under most conditions of pH and ionic strength. The two variants include the original “proof of concept” vector (SD)<sub>GA</sub> and one in which the original spacer domain (SD) was synthesised to include a 16-carbon hydrophobic linker (SD)<sub>HYD</sub> with the general formula given by schematic 6.1.

The rational for optimisation of the SD domain is based on the hypothesis that an optimal spacer domain would assist the orientation of the peptide in the complex facilitating the presentation and accessibility of the targeting domain in the vector (Further details of the hydrophobic spacer are outlined in section 7.2.3).



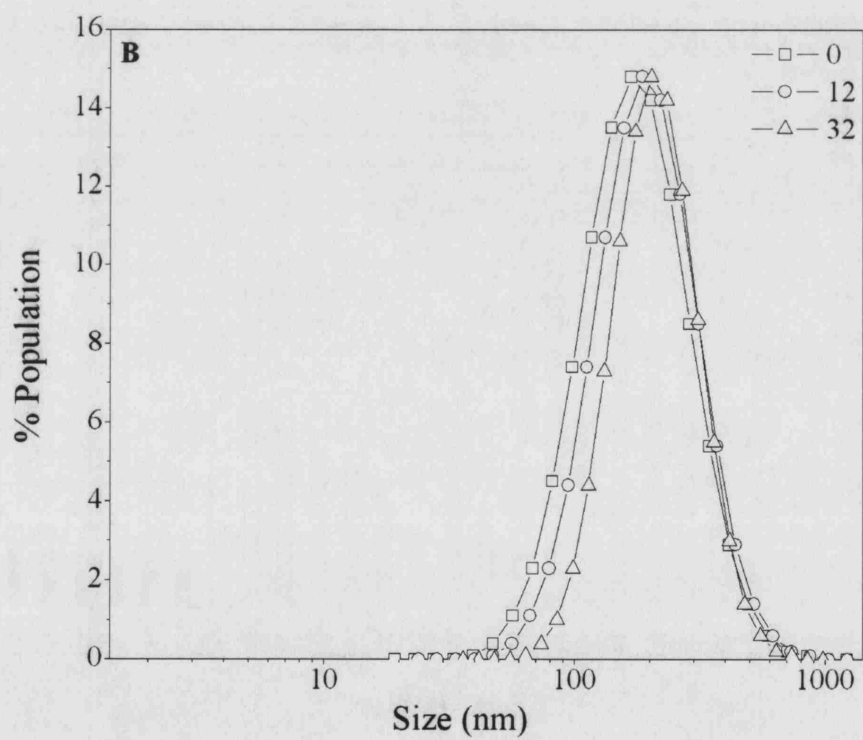
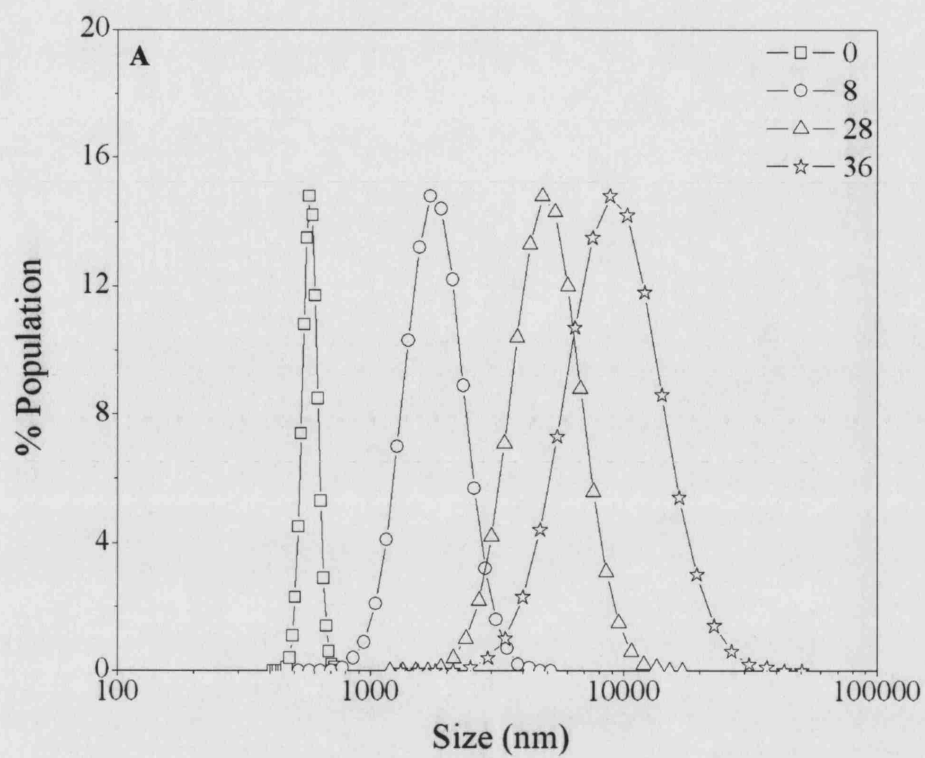
Schematic 6.1: Hydrophobic linker space domain

## 6.2 Results and Discussion

Figure 6.1 shows the change in size distribution of the LPD particles in three different buffers. The profiles refer to the vector containing the hydrophobic spacer domain. Based on these results it can be speculated (see section 4.3.1) that all vector particles start from an initial mean size of approximately 150 nm as shown by the non-aggregating particles prepared in water [Figure 6.1(C)]. The Monte Carlo program chose an average particle size of 150 nm as one of the input parameters, a sensitivity analysis was conducted to assess the influence of the initial complex size on the final aggregate size; the initial LPD size was found not to have a significant affect on the predicted aggregate size, within the range  $150 \text{ nm} \pm 50 \text{ nm}$  (data not shown). The large initial size distribution observed in Figure 6.1(A) for particles prepared in PBS is caused by the highly dynamic nature of this system and the relatively slow response of the optical size measuring technique.

In the PCS technique, particle size distribution is measured continuously over a five minutes time-span, the data are pooled, analysed and displayed as a single average distribution for that time-span. The shift in the size distribution towards larger particles in PBS and HEPES buffers as a function of time is indicative of condensation-induced aggregation, and it is noticeable that vector particles aggregation rate in PBS is significantly more rapid than those prepared in HEPES buffer. The rapidly changing size distribution of particles in PBS during the measurements time-span introduces large errors in the results. A measure of the accuracy of particle size measurements is given the polydispersity (broadness) of the distribution.

Typical polydispersities are shown for different vector-systems in Figure 6.2. Size data having a polydispersity above about 0.7 are normally discounted because of calculation errors. Examining the data in Figure 6.2 demonstrates the difficulty in measuring particles size distributions for rapidly aggregating systems like those in PBS and 150 ml NaCl solutions. Another limitation of the optical PCS technique is that it has an upper particle size limit of about 3000 nm. For that reason, particle size measurements that fall above 3000 nm are either not shown, or where there are given (in dotted line) the data are not included in any of the analysis.





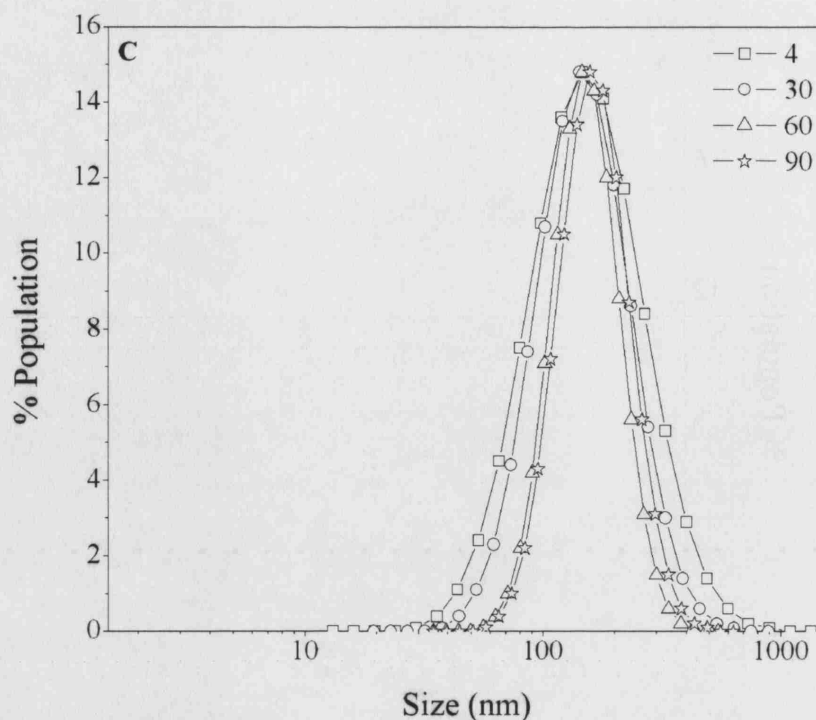


Figure 6.1: Size distributions of: Lipid/Peptide/DNA (LPD) complexes as a function of time. Data are for different buffers (A) Phosphate Buffer Saline pH 7.4 (B) 20 mM HEPES pH 7.2. (C) Distilled water pH 7.0. All measurements were taken using PCS techniques. The LPD system contained the  $(SD)_{HYD}$

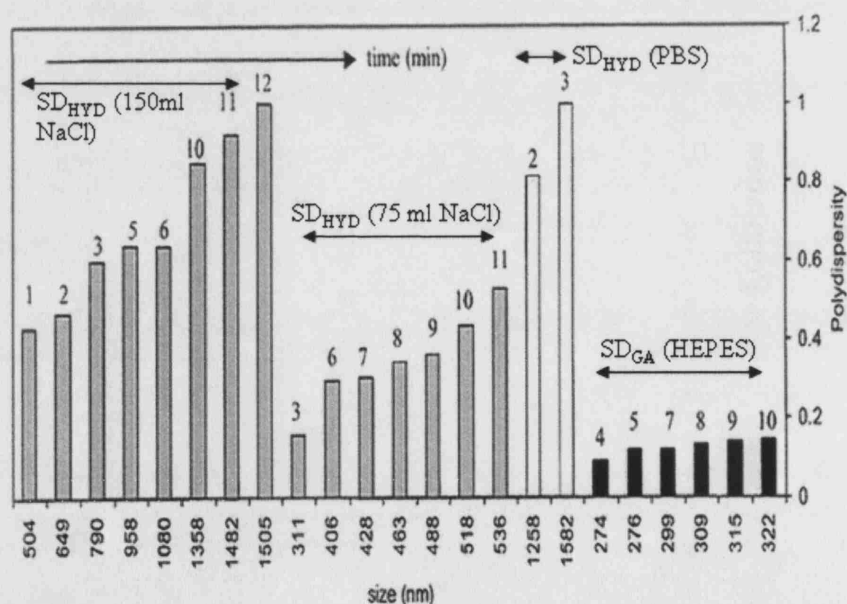


Figure 6.2: Polydispersity of LPD complexes in different buffers. Data refer to the  $(SD)_{HYD}$  in 150Mm NaCl pH 7.5 (grey bars),  $(SD)_{HYD}$  in 75 mM NaCl, pH 7.5 (grey bars),  $(SD)_{HYD}$  in PBS (pale bars), and  $(SD)_{GA}$  in HEPES pH 7.2 (black bars) The data shows the dependence of polydispersity on the buffer conditions which in turn controls the rate of aggregation.

Aggregation of vector particles may be predicted by using the DLVO theory of colloidal interactions. Under purely Brownian motion, and in the absence of any steric interaction forces the theory predicts that the potential for aggregation of a system may be obtained by the balance between the long-range repulsive electrical double layer force and the short-range Van-der-Waals force of attraction between the colliding particles (Popescu *et al.*, 1996; Elimelech *et al.*, 1995). The key physico-chemical parameters of the system including zeta potential, ionic strength and temperature of the buffer and the initial size of the particles are taken into calculations and the results are normally presented in the form of energy interaction plots shown in Figure 6.3.

The profiles in Figure 6.3 represent the potential energy of interaction for the vector particles shown in Figure 6.1. Peak interaction energy values greater than about 10-15 KT results in stable colloids. The low interaction energy profile for vector particles in PBS buffer is caused the low zeta potential of the system.

In comparison, vector particles prepared in water had a zeta potential of 30mv resulting in peak interaction energy profile of over 40kT. It is noted that while the DLVO theory gives a good indication of whether or not a vector particle-buffer system is likely to be aggregating, it does not allow prediction of the size distribution of the aggregating particles.

Peptide Component	$\xi$ (mV)	pH	Ionic Strength	$\epsilon$ (F/m)	$k$ ( $m^{-1}$ )	$A(J)$ (E-21)	$K_b$ (J/K)	$\gamma_1 \gamma_2$
SD <sub>HYD</sub>	32.0	7.0	-	6.95E-10	1.27E+09	5.00E-21	1.38E-23	2.85E-01
SD <sub>GA</sub>	30.4	7.4	-	6.95E-10	1.27E+09	5.00E-21	1.38E-23	2.87E-01
SD <sub>HYD</sub>	19.8	7.5	75mM NaCl	6.95E-10	1.27E+09	5.00E-21	1.38E-23	1.9E-01
SD <sub>HYD</sub>	13.0	7.5	150mM NaCl	6.95E-10	1.27E+09	5.00E-21	1.38E-23	1.26E-01
SD <sub>GA</sub>	11.0	7.2	20mM Hepes	6.95E-10	1.27E+09	5.00E-21	1.38E-23	1.07E-01
SD <sub>HYD</sub>	8.0	7.2	150mM NaCl, 150mM Na <sub>2</sub> HPO <sub>4</sub>	6.95E-10	1.27E+09	5.00E-21	1.38E-23	7.96E-02

Table 6.1: The total interaction,  $V_T$ , between the particles obtained by summing the van der Waals attractive potential,  $V_A$ , and the repulsive double layer electrostatic potential,  $V_R$ , as outlined in (5.6) (5.7) and (5.8). The components used to calculate  $V_T$  are shown.

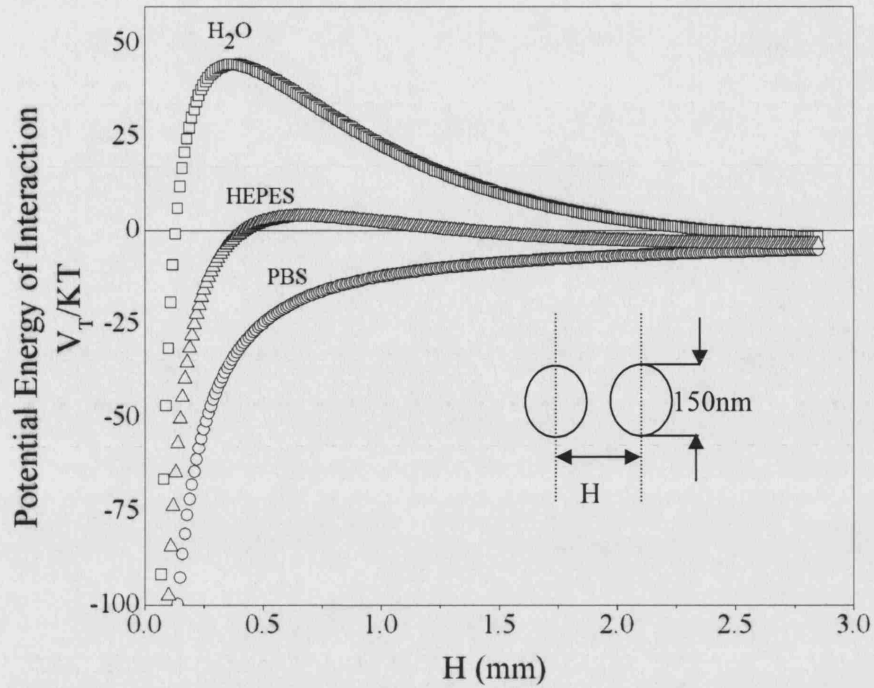


Figure 6.3: Influence of buffer conditions on the dimensionless total energy of interaction between two spherical particles of 150 nm in size as a function of distance  $H$ , between their surfaces.

Modelling of the kinetics of particle aggregation may be achieved by numerical solution of population balance equations (Nicmanis *et al.*, 1996; Elimelech *et al.*, 1995; Ramkrishna *et al.*, 2003). Traditional approaches are based on the solution of a set of differential equations, which requires discretization of the size distributions (Kumar *et al.*, 1997; Hounslow *et al.*, 1990). Monte Carlo simulation techniques provide an alternative means of simulating population balances without the need for discretization and have been applied in the past to growth processes including coagulation of colloidal particles (Laurenzi *et al.*, 1999). In the present study a constant-number Monte Carlo technique recently proposed by Smith and Matsoukas is used (Smith *et al.*, 1998) to simulate the evolution of size distribution of the condensed LPD particles.

A full description of Monte Carlo simulation techniques and the solution algorithm are presented in the original paper (Smith *et al.*, 1998) and only the main points are given below (Smith *et al.*, 1998). Two particles of mass  $M_i$  and  $M_j$  combine to form a particle of mass  $M_i + M_j$  with rate constant  $K_{ij}$ , which is defined by the coagulation kernel  $K_{ij} = K(M_i, M_j)$  for the coagulation of two particles  $i$  and  $j$ . The rate constant  $K_{ij}$  can be rewritten in the form:

$$K_{ij} = K_c k_{ij} \quad 6.1$$

For perikinetic coagulation due to Brownian motion, the rate constant  $K_{ij}$  is given by (Atteia, 1998):

$$K_{ij} = \alpha \frac{2k_B T}{3\eta} \left( 2 + \left( \frac{M_i}{M_j} \right)^{\frac{1}{3}} + \left( \frac{M_j}{M_i} \right)^{\frac{1}{3}} \right) \quad 6.2$$

The coagulation rate,  $K_c$ , is related to the mean mass size at  $t=0$  and defined as:

$$K_c = \alpha \frac{8k_B T}{3\eta} \quad 6.3$$

$K_c$  is related to the characteristic coagulation time,  $\tau_c$  by the following equation:

$$\tau_c = \frac{1}{K_c C_0} = \frac{3\eta}{8\alpha k_B T C_0} \quad 6.4$$

where  $\eta$  is the viscosity and  $T$  is the temperature of the buffer and  $k_B$  is the Boltzmann's constant.  $C_0$  is the initial total number concentration ( $t=0$ ).

The definition of  $\tau_c$  given by Equation 6.4 is different by a factor of  $1/4$  from what is often used in the literature (Atteia *et al.*, 1998). An adjustable parameter  $\alpha$  is included in Equation 6.4 to account for the effects of hydrodynamics and colloidal interaction forces. In the present study the former was absent so that  $\alpha$  accounts for the impact buffer conditions (pH and ionic strength).

In Equation 6.1,  $k_{ij}$ , is the Brownian coagulation kernel, defined as:

$$k_{ij} = \frac{1}{4} \left[ 2 + \left( \frac{M_i}{M_j} \right)^{\frac{1}{3}} + \left( \frac{M_j}{M_i} \right)^{\frac{1}{3}} \right] \quad 6.5$$

where  $M_i$  and  $M_j$  are the mass of two colliding particles  $i$  and  $j$ , respectively.

At each time step, two particles are randomly selected and a coagulation event occurs according to the following definition:

$$R < p_{ij} = \frac{k_{ij}}{k_{\max}} \quad 6.6$$

$p_{ij}$  is the coagulation probability,  $k_{\max}$  is the maximum value of the coagulation kernel among all particles and  $R$  is a random number drawn from a uniform distribution. If two

particles are rejected, two new particles are picked and the above steps repeated until the coagulation condition is met.

The relation between the expected mean size of aggregate,  $M_k$ , after  $k$  coagulation events, the number of particles,  $N$ , in the Monte Carlo simulation and time interval,  $\Delta t_k$ , and cumulative time for  $k$  coagulation events are as follows (Smith *et al.*, 1998):

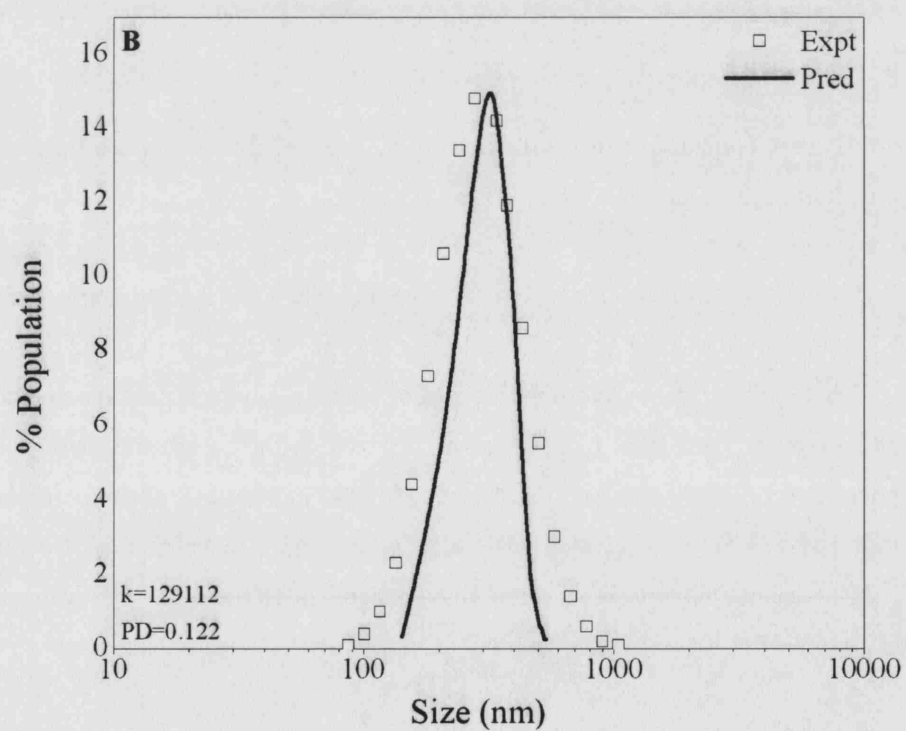
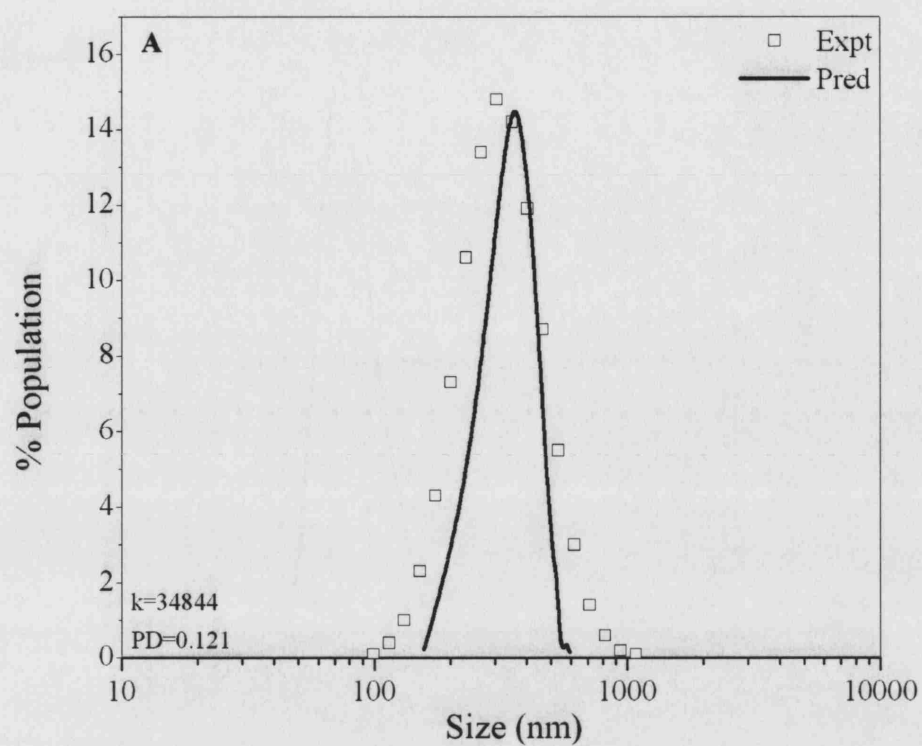
$$\frac{M_k}{M_{Av(0)}} = \left( \frac{N}{N-1} \right)^k \quad 6.7$$

$$\Delta t_k = \frac{2\tau_c}{\langle k_{ij} \rangle} \frac{1}{N} \left( \frac{N}{N-1} \right)^k \quad 6.8$$

$$t_k = \sum_{k=1}^k \Delta t_k \quad 6.9$$

Here  $\langle k_{ij} \rangle$  is the ensemble average kernel, which is estimated as the average of those particle pairs that are picked (but are rejected). The above algorithm was applied to simulate the evolution of the size distribution of the condensed LPD particles. The distributions were calculated using 20 size bins exponentially spaced between the largest and smallest mass in the simulations. The results that follow were obtained from a single simulation run with  $N=50,000$  using an in-house code. The simulations in Figure 6.4 are shown for a total of 34844 events ( $k$ ) obtained for a fixed cumulative time,  $t_k$ , of 1200 seconds corresponding to the experimental time over which particle size measurements were obtained. Figure 6.4 shows the Monte Carlo simulations and experimental data for the LPD particles prepared in PBS buffer and HEPES buffer.

Each simulation required two input parameters including an initial size distribution and a value for  $\alpha$  in Equation 6.4. In the absence of any prior information on  $\alpha$ ,  $\alpha$  was initially treated as a fitting parameter. Figure 6.5 shows the size distribution over time of LPD complexes in water (A), Hepes (B) and PBS (C) as predicted using Monte Carlo simulations, experimental data is also plotted to compare the two sets of data.



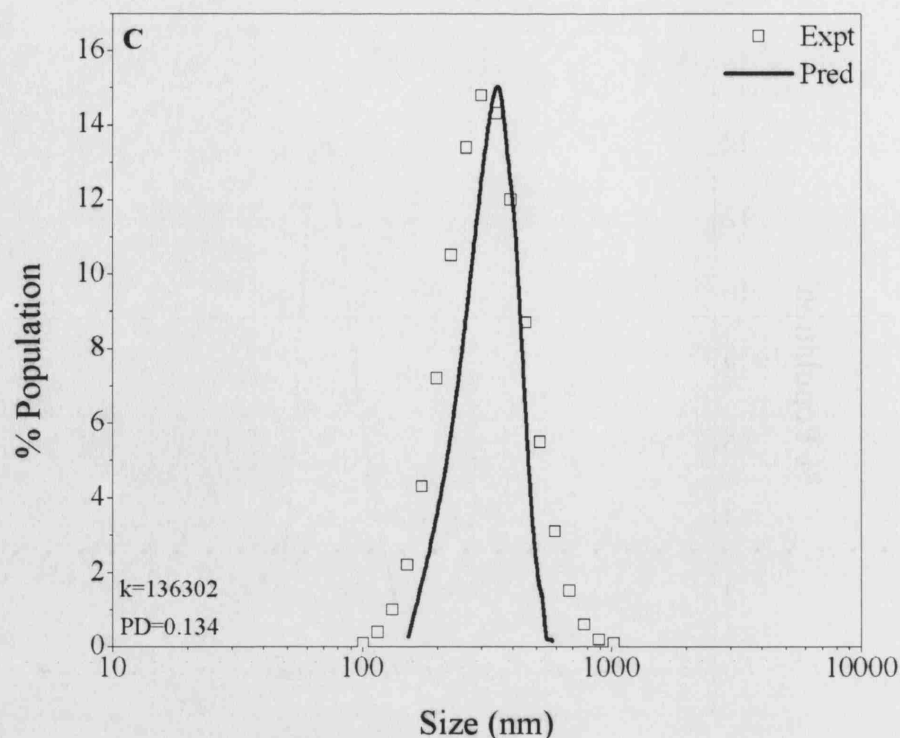


Figure 6.4: Comparison of Monte Carlo simulated data (-) of particle size distributions, with experimentally determined values ( $\nabla$ ), when placed in HEPES buffer pH 7.2, (A) 920 sec, (B) 1200 sec (C) 1680 sec. The total number of events ( $k$ ) for a fixed cumulative time,  $t_k$  is stated for each time period.

Subsequent comparison of results (Figure 6.6) revealed that  $\alpha$  was a function of the zeta potential of the vector particles.

Figure 6.4 shows typical simulations obtained using the Monte Carlo techniques. The simulations refer to the original “proof-of-concept” vector [6.4(A)] and the variant vector [6.4(B)] containing the hydrophobic spacer domain. In each case the symbols show the experimental data, the total number of events for each time period ( $k$ ) and the polydispersity (P.D.) of the distribution are also included. From the simulations it was also possible to plot average particle sizes over time this was possible for a range of buffers, each with varying levels of  $\alpha$  dependent on the differing levels of aggregation (Figure 6.6).

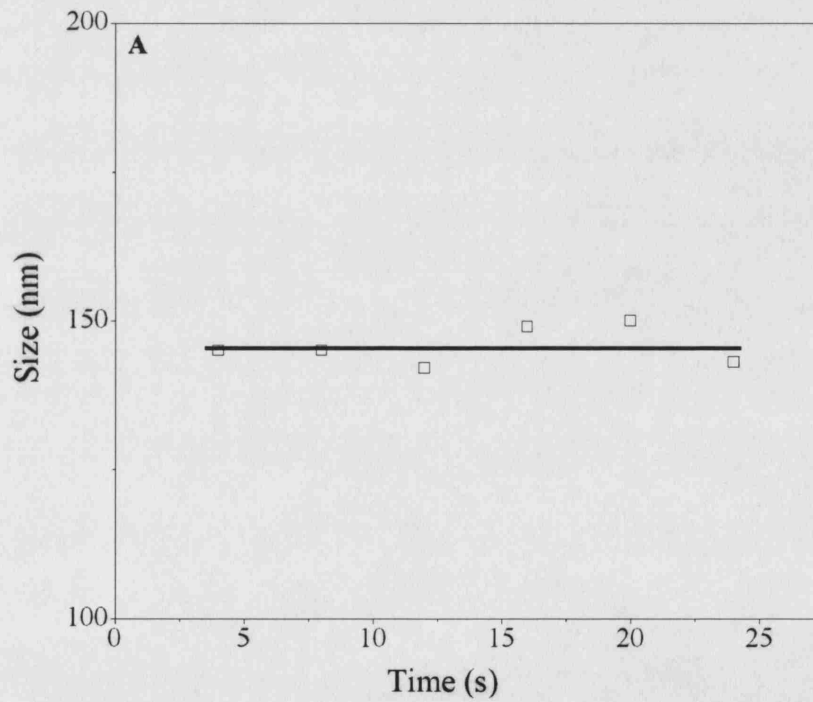
Comparison with experimental data over many different buffer conditions led to the conclusion that accurate simulation was obtained provided polydispersity of the initial size distribution of the vector particles was below about 0.7.

Figure 6.7 shows the average size of the vector particles, after 30 minutes obtained from the simulation distributions as a function of zeta potential.

Friedlander and Wang (Jenkins *et al.*, 2003) recommend the following analytical equation for the calculation of the average mass,  $M_{Av}$ , of the particles as a function of time:

$$\frac{M_{av}}{M_{Av(0)}} = \left( 1 + a \frac{t}{2\tau_c} \right) \quad 6.10$$

where 'a' is only weakly time-dependent and has an asymptotic value 1.075 (Gregory *et al.*, 1993). Predictions from Equation 6.10 were indistinguishable from those obtained from the Monte Carlo simulations. In equation 10,  $M_{Av(0)}$  was obtained by assuming an average initial ( $t=0$ ) size of 150 nm for the vector particles and a density equal to that of water.





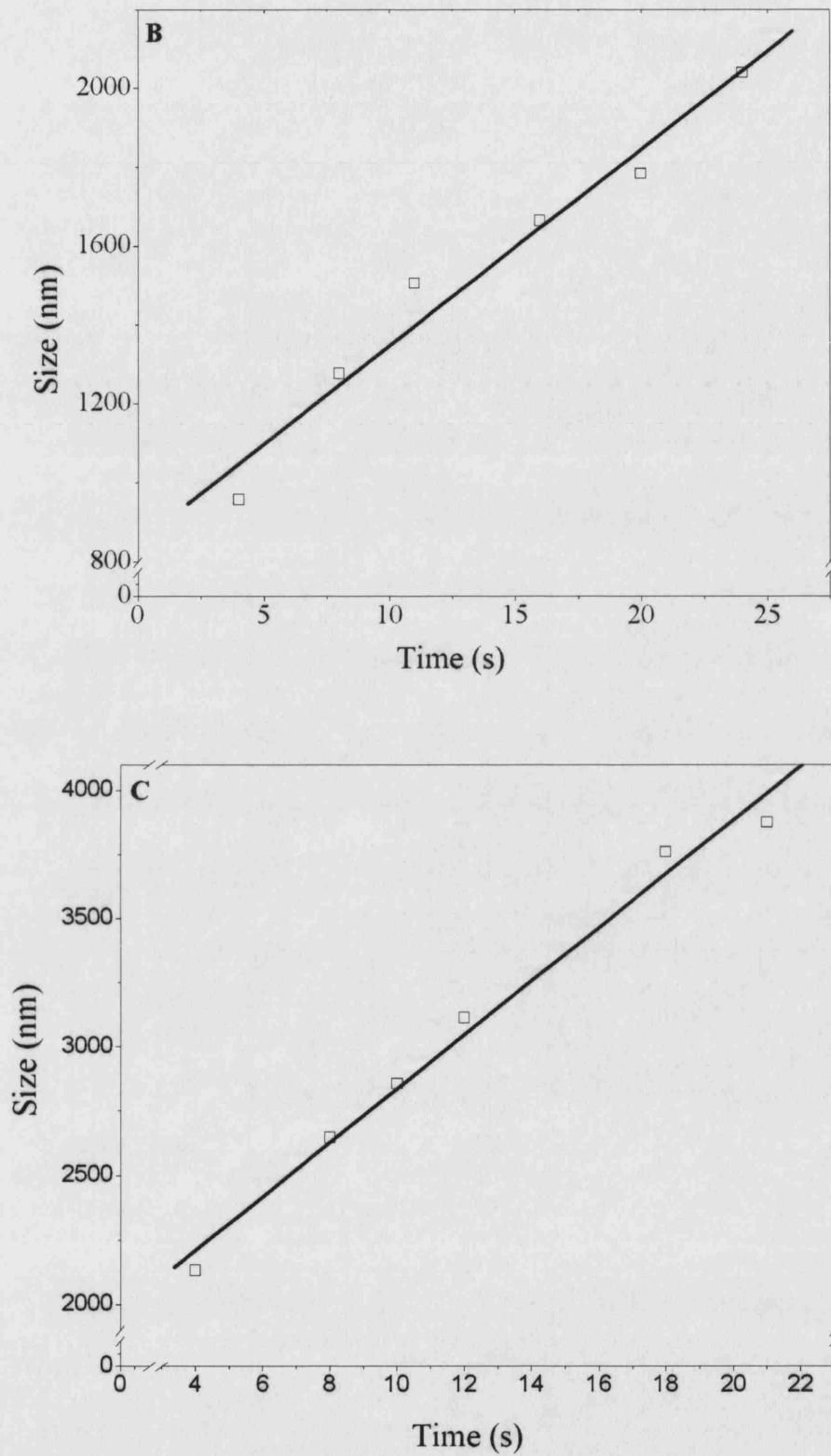


Figure 6.5: Data shows predicted size measurements using Monte Carlo Simulations (—) and actual experimental data ( $\square$ ). Systems shown are for (A) distilled water, (B) Hepes Buffer and (C) Phosphate Buffer Saline.

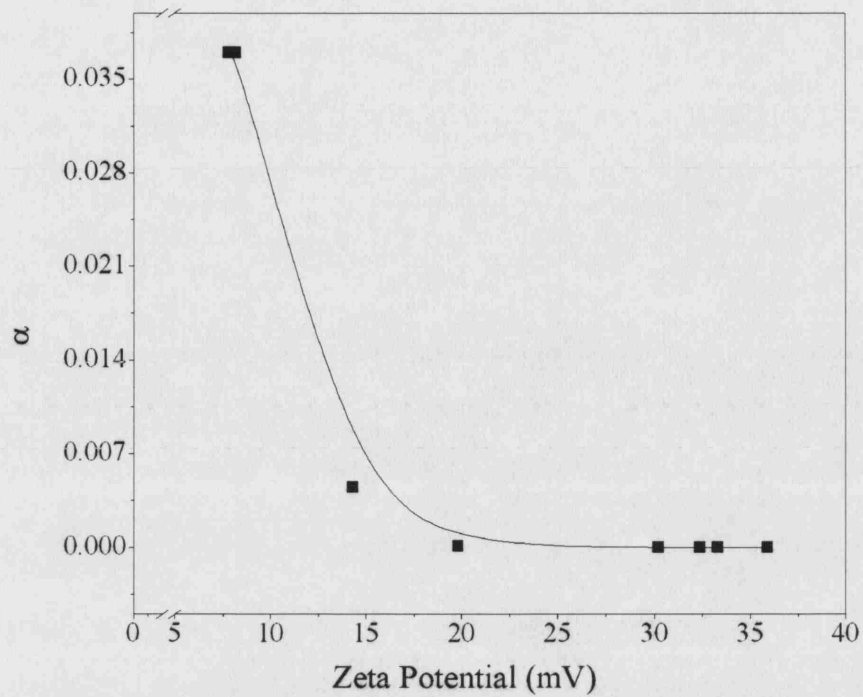


Figure 6.6: The fitting parameter ( $\alpha$ ) used in particle size simulations shows a strong dependency on zeta potential.

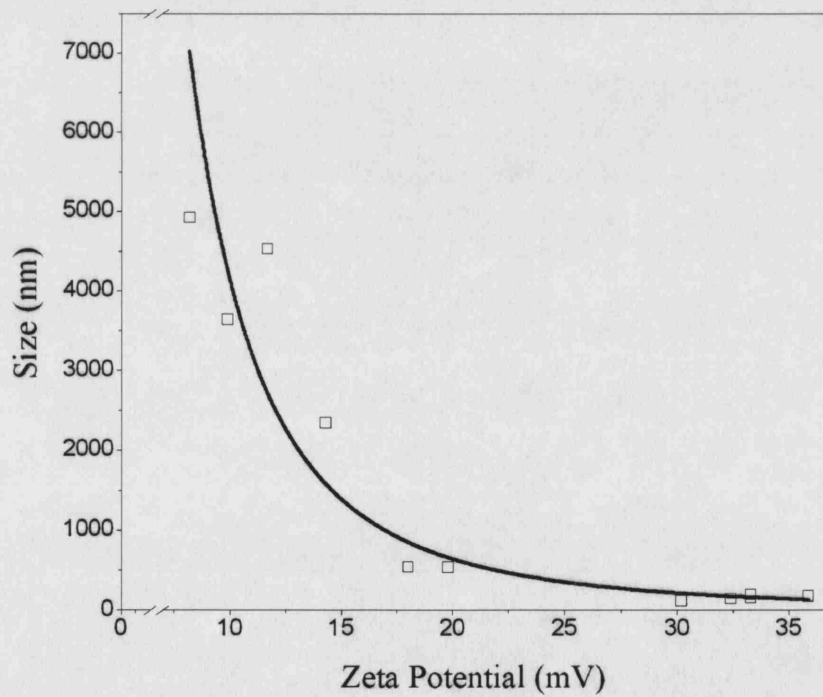


Figure 6.7: The average size of the vector particles obtained from Monte Carlo simulations (-), after a period of 30 minutes. Symbols refer to experimental data obtained from experiment under different conditions.

The goodness of fit between experimental data and predictions support the view that all vector particles started with an initial size distribution with a mean of approximately 150 nm, regardless of buffer conditions. It is noted that sensitivity analysis (simulations not shown) revealed that predictions were more sensitive to changes in the value of  $\alpha$  (via  $\tau_c$  – Equation 6.4) than the mean average aggregate size.

Taken together, these observations make it possible to predict a priori the aggregation kinetics of the LPD vector particles in a given buffer.

Using Equation 6.10, a value of  $\alpha$  obtained from Figure 6.6 and assuming the initial mean size of the vector particles to be 150 nm, the average size of the vector particles may be predicted as a function of time as shown Figure 6.8, where the symbols represent experimental data.

The slope of each curve at  $t=0$  gives an estimate of the severity of aggregation, as shown in Figure 6.9.

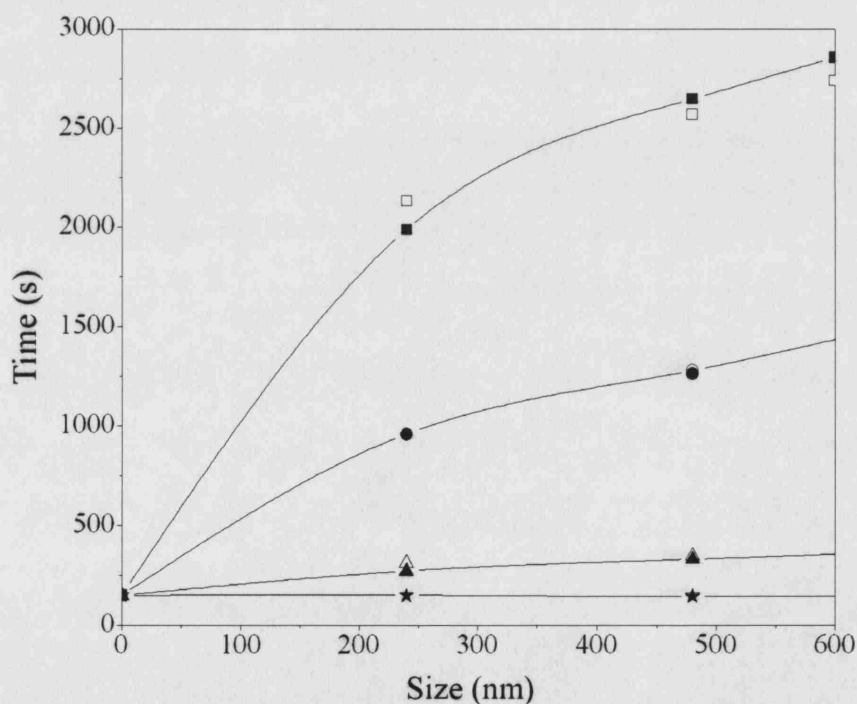


Figure 6.8: Evolution of average particle size simulated by Monte Carlo techniques (- solid) and experimental data (clear symbols), data refer to  $(SD)_{HYD}$ . PBS pH 7.4 ( $\nabla$ ), 150 mM NaCl, pH 7.5 (-), 75mM NaCl pH 7.5 (8),  $H_2O$  ( $\psi$ ). The Initial gradient of each system gives the severity of aggregation.

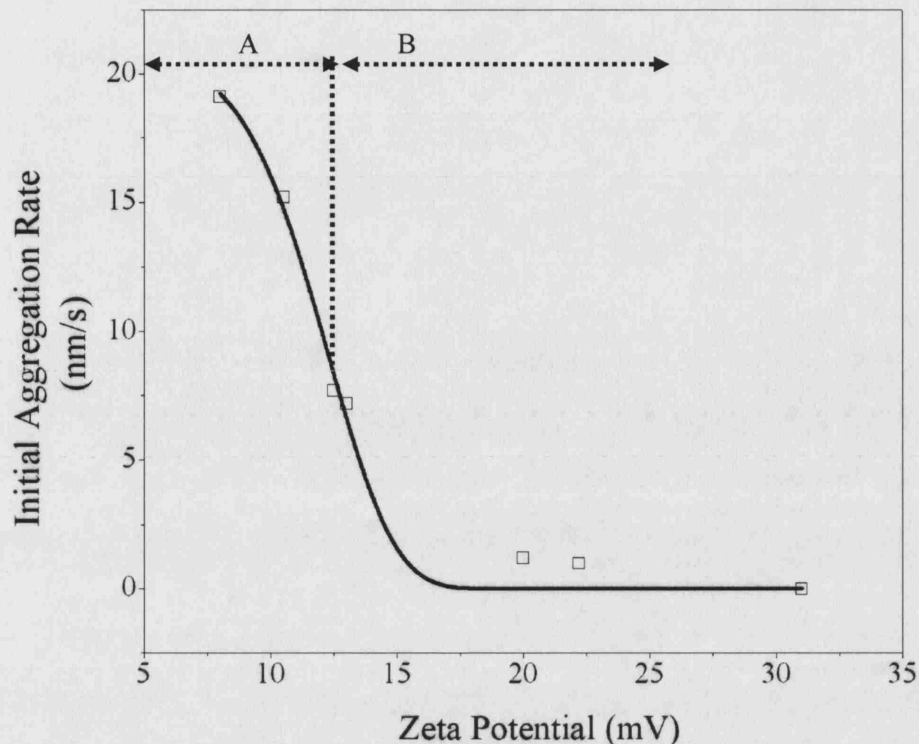


Figure 6.9: The initial rate of aggregation of LPD particles is strongly dependent on zeta potential, and provides a powerful means of assessing the potential aggregation of a vector buffer system. (A): High-Moderate Aggregation. (B): Slow-No Aggregation.

The plot indicates the shows the strong dependency of the initial rate of aggregation on the zeta potential of the system, particularly for values less than 15 mv. It appears that a vector buffer system with a buffer zeta potential less than 15 mv will exhibit significant aggregation.

### 6.3 Conclusion

A major challenge currently limiting the development of non-viral vector delivery systems is the tendency of the vector particles to aggregate. The ability of Monte-Carlo simulation techniques to describe the dynamics of aggregation of lipid-peptide-DNA (LPD) vector particles is demonstrated. Simulations are reported for vector particles under Brownian aggregation in buffers of different pH and ionic strength and results compared with experimental data. The analysis indicates that the zeta potential of vector particles has a vital role in determining whether, and if so to what extent, aggregation is likely to be a problem. The mathematical tools presented in this chapter allow quantification of the dynamics of aggregation as a function of zeta potential of the buffer

solution and the initial size of the particles. The approach may be applicable to other vector particle delivery systems.

## Chapter 7 : Rationale Vector Design

### 7.1 Introduction

Gene therapy has the potential to revolutionise treatment strategies for diseases. Synthetic vectors for gene transfer have many advantages over viral vector systems in terms of increased packaging capacity, low immunogenicity, safety and the ease of manufacture. However, the advantages of non-viral delivery systems will only be realised if gene transfer efficiencies can be improved to levels comparable with viral vectors. Section 4.1 introduced the LPD vector, a synthetic gene delivery system comprised of a lipid mixture Lipofectin (L), an integrin-targeting peptide (P) and DNA (D) (Hart *et al.*, 1997). Successful gene therapy requires not only the identification of an appropriate therapeutic gene for treatment of the disease, but also a delivery system by which the gene can be delivered to the desired cells to ensure effective and efficient transgene expression (Miller *et al.*, 1995). Recent concerns about the use of viral vectors (Mountain, 1997), including insertional mutagenic events, adverse immunological reactions in the host and antibody formation against the injected DNA resulting in adverse immunological reactions in the host (Marquet *et al.*, 1997) have motivated research into non-viral gene therapy strategies. Non-viral vectors are safer than viral systems and are simpler to manufacture (Lotfian *et al.*, 2003). However the comparatively low transfection efficiency of non-viral complexes (Spack *et al.*, 2001) is problematic. Significant research efforts are currently being developed to finding a delivery vector that combines the safety parameters of non-viral vectors with the transfection efficiency of viral vectors (Jenkins *et al.*, 2000).

The LPD vector moieties combine electrostatically to form the LPD vector complex (Hart *et al.*, 1998). This system aims to incorporate the targeting elements that bind efficiently to cell surface receptors including integrins (Cheng *et al.*, 1996; Schaffer *et al.*, 1998). *In vitro* animal tests with the LPD vector demonstrated cell transfection efficiencies comparable with adenovirus (Jenkins *et al.*, 2000). However, biophysical characterisation

of the system has shown it to be highly unstable and undergo rapid aggregation in physiological conditions (Rolland *et al.*, 1998; Zelphati *et al.*, 1998; Allison, 2000; Lee *et al.*, 2001; Mount *et al.*, 2003; Sarkar *et al.*, 2003). This presents additional challenges when faced with long term storage of the formulation and safety concerns associated with the formation of large aggregates in a physiological environment (Hart *et al.*, 1998; Maguire *et al.*, 2003; Ayazi Shamlou *et al.*, 2003).

## 7.2 Modular Structure of LPD

The flexible modular structure of the LPD vector allows independent design and optimisation of the different moieties in its architecture (Sarkar *et al.*, 2003). The first generation vector was comprised of a lipid component (L) in the form of commercially available Lipofectin, a 1:1 formulation of DOTMA and DOPE, the peptide component contained the targeting domain (TD), an CRETAWACG domain and a 16 lysine chain (PD) to bind to the DNA. The targeting domain is connected to the lysine chain by a spacer domain (SD) GA, as shown in Schematic 4.1

Previous work by Lee *et al.*, (2001) and Mount *et al.*, (2003) among others have identified the issues associated with aggregation of vector complexes. These studies have highlighted the importance of size and zeta potential as a guide to determining the stability of a system, and their impact on transfection (Jenkins *et al.*, 2000). The effects of altering the composition and length of the spacer domain; the length of the lysine chain may provide information into possible mechanisms involved during the delivery process and a means to control the properties of the complex aggregates to improve cell transfection. Furthermore, it has been reported that the chain length and unsaturation of the lipid component in Lipid-DNA (LD) formulations can influence transfection efficiency (Felgner *et al.*, 1994; Balasubramanian *et al.*, 1996; Hurley *et al.*, *In press*). Thus information on the size of the particle using different lipids may enhance our understanding of the vector formulation and stability. Physiochemical properties such as hydrodynamic size, size distribution, zeta potential, rate of aggregation, aggregate fractal dimension offer information that allow different delivery systems to be characterised and provide a base to identify the factors that affect the transfection efficiency of differing complex architectures. These provided the motivation for the present study, the aim of which is to assess the impact of changes in the base chemistry of the LPD vector on its physical stability.

Peptides and lipids are convenient vector components that are readily synthesised and purified allowing the production of a well-defined vector formulation. The optimal lipid component in the first generation 3 component system was Lipofectin, a 1:1 formulation of 2,3-dioleoyloxypropyl-1-trimethyl ammonium bromide (DOTMA) and the neutral phospholipid dioleoyl L- $\alpha$ -phosphatidylethanolamine (DOPE) (Felgner *et al.*, 1987). Other commercially available lipids assessed, including Lipofectamine, resulted in low transfection efficiency (Jenkins *et al.*, 2003).

### 7.2.1 Lipid Optimisation

Liposomes of various compositions can extensively bind to cell surfaces. For gene transfer, it was established that that dioleoylphosphatidylethanolamine (DOPE) is by far the most efficient lipid for *in vitro* gene transfection for pH-sensitive liposomes or as lipid helper in cationic liposomes (Bergstrand *et al.*, 2003). It has been assumed that the function of phosphatidylethanolamine (PE) is that of a membrane fusion promoter, since in fact this lipid undergoes changes upon acidification. The composition of liposomes may play an important role in their interactions with cells. The size of liposomes and the type of cells are fundamental for an efficient capture by cells. After binding to the cell surface, liposomes are internalised into endosomes where they encounter a more acidic pH than in the external medium. Early endosomes generally have a pH of 6.50. Their contents are then transferred to a more acidic environment by maturation or vesicular fusion. The last endosome environment with an internal pH of 5.5-6.0, is reached 10-15 min after uptake. The last endocytotic compartment, the lysosome, is further acidified to pH values of 5.0 or lower and is reached 20 min or more after uptake. The lysosomes are the main degrading compartment. pH sensitive liposomes were designed based on the concept of viruses that fuse with the endosomal membrane by means of a protein at pH 5-6 delivering their genetic material to the cytosol before reaching the lysosomes. Generally, the lipid used to design pH sensitive liposomes is PE. PE represents a class of lipids which, when dispersed in pure form, assemble into nonbilayer structures in an inverted hexagonal phase. To stabilise PE in the lamellar phase in liposomes a series of stabilisers possessing titratable acid headgroups such as oleic acid (OA), palmitoylhomocysteine (PHC) and cholesterolhemisuccinate (CHEMS) were used.

Structure-activity studies have been performed on several lipid/DNA (LD) systems to gain insights into parameters governing gene transfection (Felgner *et al.*, 1994; Balasubramanian *et al.*, 1996; Rosenzweig *et al.*, 2000; Heyes *et al.*, 2002). For example,



several DOTMA analogues have been synthesised, such as 1,2-dioleoyloxypropyl-3-dimethylhydroxyethyl ammonium bromide (DORIE) and 1,2-dimyristyloxypropyl-3-dimethylhydroxyethyl ammonium bromide (DIMRIE), possessing a hydroxy ethanol and tetradecanyl chains respectively, leading to higher *in vitro* activities in COS.7 cells when formulated with DOPE (Felgner *et al.*, 2000). For DIMRIE it was rationalised that the higher potency may have been due to a shorter aliphatic chain, facilitating endosomal escape. Thus, such studies have indicated that the efficiency of transfection depends on the application, the cytofectin and co-lipid combination and structure of the lipid: notably the head group, aliphatic chain, functional group present and the carbon skeleton. Indeed, the factors governing gene delivery are highly complex and also include the physical structure of the lipopolyplex as well as how it interacts with the biological system.

The creation of liposomes which become unstable in response to changes in their environment has been the objective of longstanding interest in connection with applications in gene therapy. After binding to the cell surface liposomes are internalised into endosomes where they encounter a more acidic pH than in the external medium. pH-sensitive liposomes were designed based on the concept of viruses that fuse with the endosomal membrane by means of a protein at pH 5-6, delivering their genetic material to the cytosol before reaching the lysosome. However, for much of the recent development on cationic formulations, the approach has been empirical rather than a systematic investigation into structure-activity relationships. In this chapter the effect of lipid chain type on release of calcein, and complex size and zeta with a view to understanding the interactions between the peptide, lipid and DNA components is looked at, with the aim of identifying and improving transfection systems.

The calcein release experiments were designed as a model system to mimic the affect of a change in pH experienced by LPD delivery vector during its path through to the endosome. The level of calcein release from the lipid is indicative of DNA release. These experiments form the first step in assessing the affect that different lipid chain length, level of saturation and addition of DOPE potentially play in the transfection efficiency of LD and LPD complexes. The experiments look at the release profiles of calcein from lipid only and not in a formulation with DNA or peptide which may affect the formation of the final structure and hence the system's release properties, none the less the biophysical properties of the lipids form an important guide as to the biological efficiency of the complexes.

The molecular mechanisms by which pH-sensitive liposomes surpass the cytoplasmic and endosomal membranes to deliver the contents into the cytoplasm are still not fully understood (Bhattacharaya *et al.*, 1999). We have investigated the influence of lipid chain length, saturation and presence of DOPE on the dynamics of calcein leakage from the lipids over a pH range. The development of an efficient liposome system requires low leakage of the encapsulated molecules in order to minimise unwanted side effects while the liposomes are in circulation (Balasubramaniam *et al.*, 1996). The need for rapid release arises from the fact that the active substance is normally prevented from exercising its therapeutic effect while still being enclosed in the lipid carrier; the liposomes internalised via the endocytotic pathway often end up in lysosomes where the action of degrading enzymes may decrease or destroy the biological activity of the delivered substance (Balasubramaniam *et al.*, 1996).

The calcein release experiments were designed as a model system to mimic the effect of a change in pH experienced by LPD delivery vector during its path through to the endosome. The level of calcein release from the lipid is indicative of DNA release. These experiments form the first step in assessing the affect that different lipid chain length, level of saturation and addition of DOPE potentially play in the transfection efficiency of LD and LPD complexes. The experiments look at the release profiles of calcein from lipid only and not in a formulation with DNA or peptide which may affect the formation of the final structure and hence the system's release properties, none the less the biophysical properties of the lipids form an important guide as to the biological efficiency of the complexes.

### 7.2.2 Peptide Optimisation

Among non-viral gene delivery methods, receptor mediated delivery is particularly attractive for gene therapy applications, since it permits targeting of therapeutic DNA to a desired cell population by an appropriate receptor ligand. The vectors for targeted gene delivery are assembled in a modular manner from a minimal number of simple components (Plank *et al.*, 1999). It is reasonable to assume that the interaction of microparticles such as polycation-DNA complexes with the biological mileu and its macromolecular solutes are governed by the physiochemical characteristics of the interacting molecules. Although one cannot easily alter the characteristics of blood components, the properties of the DNA complexes can be modified to be compatible with the envisioned application. In this respect important parameters include size and surface

characteristics of DNA complexes that are directly influenced by the nature of the cationic component and the mixing procedure. The binding affinity and the DNA-compacting capacity of the cationic component govern the stability of the complex toward dissociation, while the surface characteristics of the particles have a direct impact on their solubility and their stability *in vivo* during the delivery phase (Felgner *et al.*, 1996).

Cationic macromolecules linked with cell targeting ligands are being extensively investigated as targetable carriers of genes. In these approaches, the ligands will transport genes to cells having the corresponding receptors. Evidence has suggested that cell transfection is linked to particle size; some vector particles are susceptible to significant aggregation under most conditions of pH and ionic strength, including physiological conditions. These studies include investigations into the influence of the lipid component on the aggregation of the complexes in physiological conditions. Systems in distilled water have previously been shown to be stable (Bergstrand *et al.*, 2003; Pouton, *et al.*, 1998), an important consideration when looking at storage and transportation of the vector system. It has been shown in chapter 4 that the peptide component is predominantly responsible for the compaction of the plasmid DNA, in addition to providing a targeting moiety. The peptide has also been shown (Pouton *et al.*, 1998; Tsai *et al.*, 1999) to be responsible for aggregation of the complexes in physiological conditions. Although there is a balance between the level of DNA compaction and extent of charge ratio, at a charge ratio much greater than +7 complexes would be unsuitable for biological testing. Current LPD complexes are prepared at this charge ratio. The investigation into studying the affect of peptide chain length on LPD complexes aims to assess the ability of different length peptide residues to condense the plasmid DNA (6.9 kb). Different charge ratios are also employed to see if and the extent to which this parameter influences plasmid condensation and physical stability. Three alternative peptides were also studied MPM 108, MPM 109 and MPM 110, in these cases the spacer domain of the peptide was modified to incorporate hydrophilic and hydrophobic regions (Schematic 7.1).

### 7.2.3 Plasmid DNA Optimisation

The size of the genomic locus for most genes is between 20 and 200 kb, beyond the capacity of most viral vectors. In contrast, nonviral gene delivery vectors have in theory

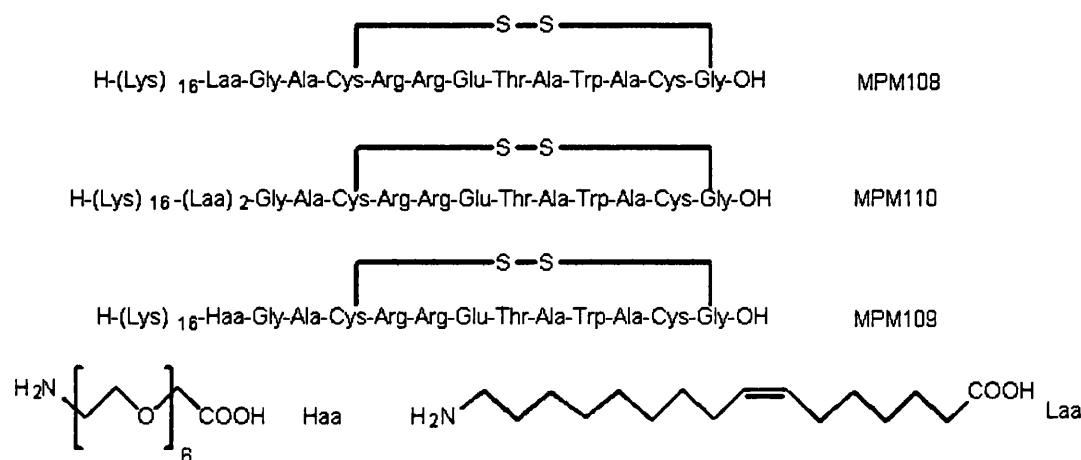
unlimited capacity for DNA, in addition to their simplicity and reduced immunogenicity. Previous work by White *et al.*, 2003, has shown that constructs of up to 242 kb can be delivered to cultured cells with relatively high efficiency by a nonviral gene therapy vector. The aim of these experiments was to look at the difference in aggregation properties of gWiz (5.7 kb), psv $\beta$  (6.9 kb), pQR150 (20kb) and p5180 (72 kb), while assessing the level of condensation achieved by peptide 6.

## 7.3 Results and Discussion

### 7.3.1 Lipids

The structure of lipids C12-C18, saturated and unsaturated; with and without DOPE are shown in Table 7.1 Results indicated the biophysical properties of the lipids in the LPD complexes to be relatively independent of structure changes in the lipid chain length; although C16:0 was the most unstable, it was influenced by the addition of DOPE (Figure 7.1). Lipids in the presence of DOPE were shown to be more stable than those without, independently of chain length.

The calcein release experiments were designed as a model system to investigate the implications of lipid chain length and level of saturation on the ability and the rate of release of calcein by mimicking the affect of a change in pH experienced by the delivery vector.



Schematic 7.1: Peptides MPM 108, MPM 109 and MPM 110. Peptides were synthesised using standard solid phase synthesis methods.

Compound	R	Length: Unsaturatoin
1	(CH <sub>2</sub> ) <sub>8</sub> (Z)CH=CH (CH <sub>2</sub> ) <sub>7</sub> CH <sub>3</sub>	C18:1
2	(CH <sub>2</sub> ) <sub>10</sub> (Z)CH=CH (CH <sub>2</sub> ) <sub>3</sub> CH <sub>3</sub>	C16:1
3	(CH <sub>2</sub> ) <sub>10</sub> (Z)CH=CHCH <sub>2</sub> CH <sub>3</sub>	C14:1
4	(CH <sub>2</sub> ) <sub>6</sub> (Z)CH=CH (CH <sub>2</sub> ) <sub>3</sub> CH <sub>3</sub>	C12:1
5	(CH <sub>2</sub> ) <sub>17</sub> CH <sub>3</sub>	C18:0
6	(CH <sub>2</sub> ) <sub>15</sub> CH <sub>3</sub>	C16:0
7	(CH <sub>2</sub> ) <sub>13</sub> CH <sub>3</sub>	C14:0
8	(CH <sub>2</sub> ) <sub>11</sub> CH <sub>3</sub>	C12:0

Table 7.1: Structure of C12-C18 saturated (0) and unsaturated lipids (1).

These initial experiments assess the pH release profiles of calcein from liposomes only. Without the addition of DNA and peptide, the true release properties of LPD complexes cannot be elucidated. The level of calcein release from the lipid was indicative of DNA release.

Calcein experiments focussed on lipids: C18:1, C16:1, C14:1 and C12:O, since these lipids had the greatest transfection efficiencies (Hurley *et al.*, 2005). Greater levels of transfection with shorter chain length lipids can rationalised by consideration of the phase transition temperatures and greater fluidity of the shorter chain lipids leading to enhanced membrane fusion. DOPE is known to induce the lamellar ( $L_\alpha^C$ ) to two-dimensional hexagonal lattice  $H_{II}^C$  structural transition by controlling the spontaneous curvature  $C_0 = 1/R_0$  of the lipid monolayer, where  $R_0$  is the natural radius of curvature (Koltover *et al.*, 1998).

Although greater calcein release was observed with C14:1 + DOPE than with C14:1 outlined in Figure 7.2 (A), this was not the case in the case of C16:1 where there was a greater level of fluorescence from the non DOPE containing lipid as shown in (B).

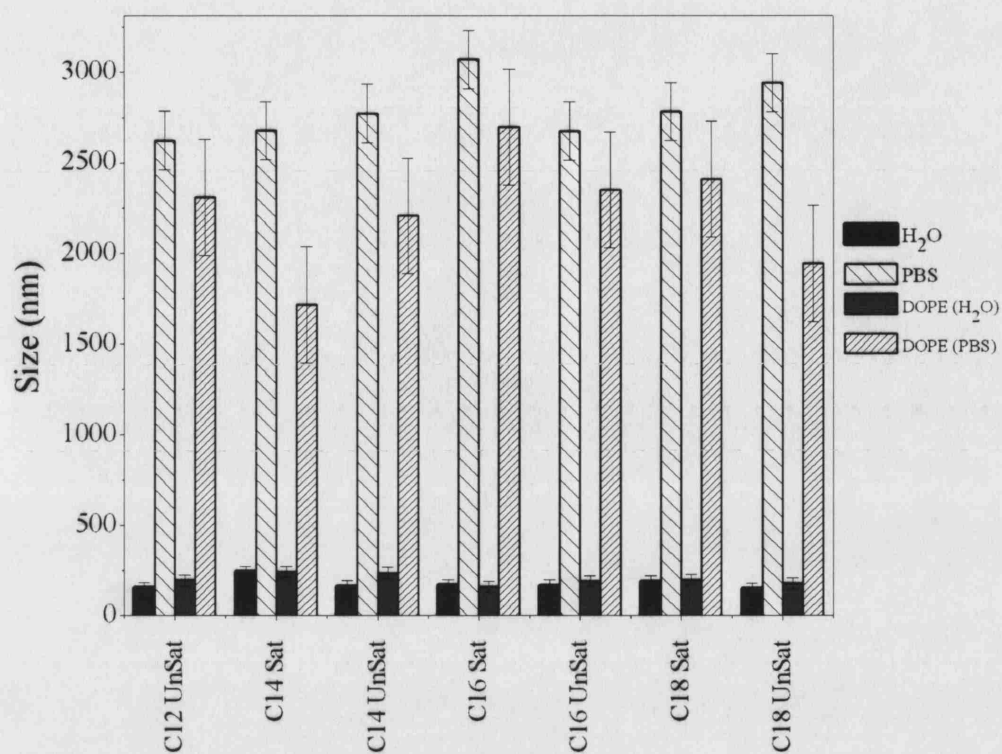
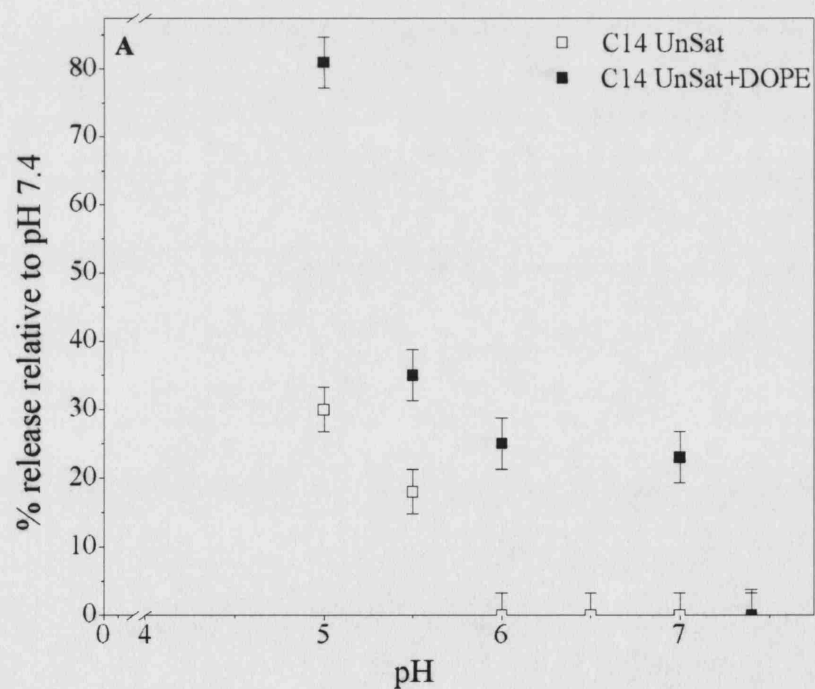


Figure 7.1: Size of aggregates 20 minutes after mixing. Data is given for saturated and unsaturated lipids, C14-C18 (C12 unsaturated only) in water and PBS in and not in the presence of DOPE.



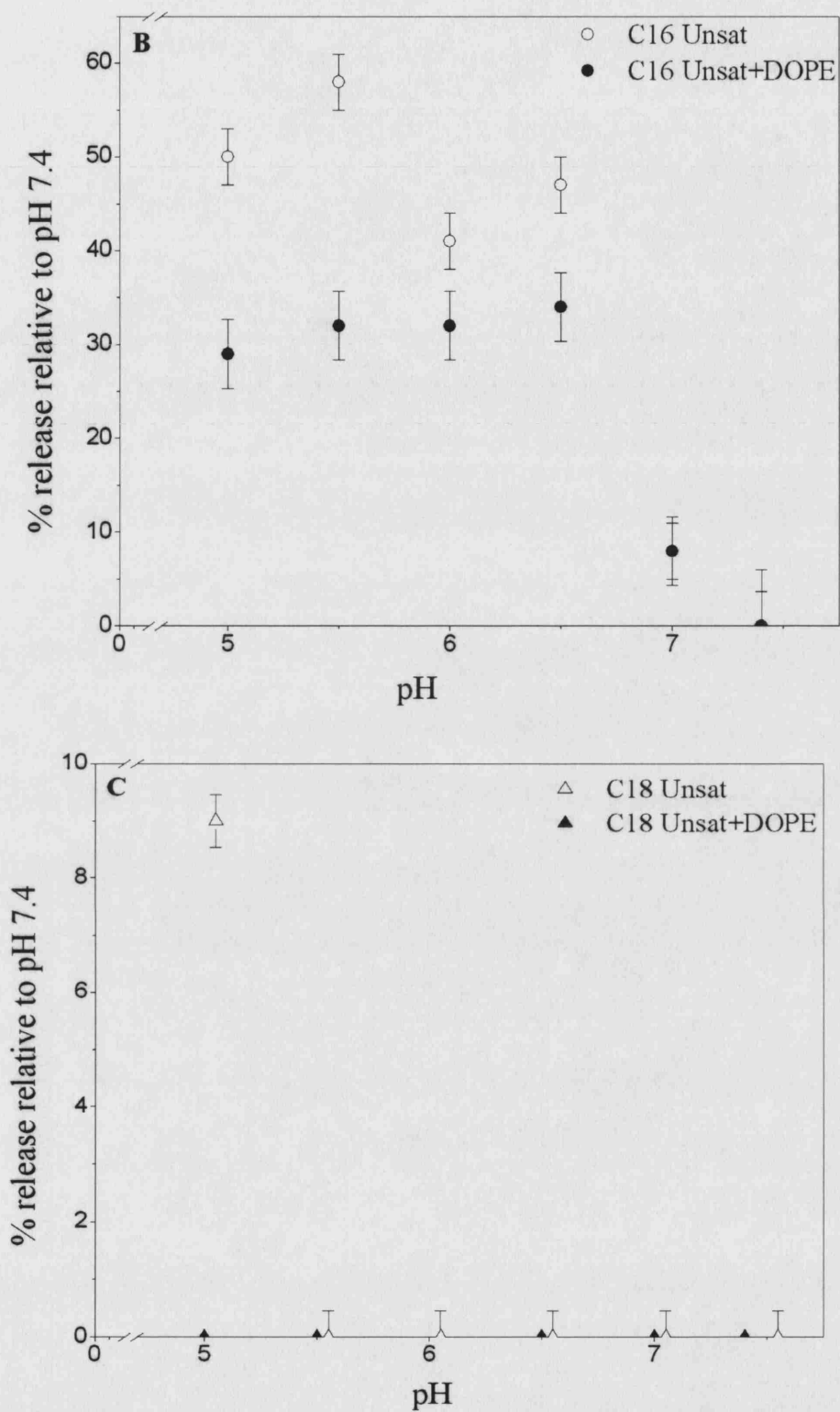


Figure 7.2: Percentage release of calcein from lipids across pH range 5.0-7.4, 100% release was obtained from sonication of the sample. Vertical bars indicate standard deviation, based on a set of three measurements.

Very little calcein release was observed with the C18 Unsaturated lipid (C). Under all the measured cases, the most acidic levels of pH induced the greatest levels of release of calcein. At pH 5.5 the following trend was observed

$$\text{C14:1} + \text{DOPE} \approx \text{C16:1} + \text{DOPE} \gg \text{C18:1} + \text{DOPE}$$

$$\text{C14:1} \succ \text{C16:1} \gg \text{C18:1}$$

Lipids with and without DOPE followed the same trend, this could be due to the greater fluidity and increased curvature demonstrated by the shorter chain length lipids as described by Koltover for higher levels of transfection among shorter chain lipids, this may be responsible for the greater rate of calcein release in C14 lipids.

### 7.3.2 Peptide

Figure 7.3 shows the change in size distribution over time of LPD complexes in phosphate buffer saline (PBS); a system representative of physiological conditions. It has previously been shown in chapter 4 that the size distribution plots are dependent on physico-chemical conditions such as pH and ionic strength. The first parameter investigated was the design of the spacer domains (SD) in the peptide by looking at the MPM 108-110 series (Schematic 7.1).

The rationale behind the design of the SD was to provide better accessibility of the targeting domain to cell surface integrins by being able to span a lipid bilayer. MPM 108 and MPM 110 contained hydrophobic spacers, thought to interact with the hydrophobic tails of lipid molecules. MPM 109 contained hydrophilic domains thought to allow the peptides to project beyond the complex and into the aqueous environment surrounding the complex. MPM 108 contained a single hydrophobic spacer and MPM 110 double spacers. Transfection data (private communication Hart, S.L. Institute of Child Health, UCL) showed there to be poor transfection with the incorporation of all three peptides especially so of MPM 108 and MPM 110, the transfection efficiency was better with MPM 109. Nevertheless all three complexes were less successful compared to the original spacer domain. Biophysical data showed that all systems were stable in distilled water (not shown), but aggregated rapidly in PBS (Figure 7.3).

Interestingly MPM 109 aggregated the least rapidly compared to the other complexes; the original peptide 6 was the least stable in PBS. For K16, 24 and 32 the alteration in chain



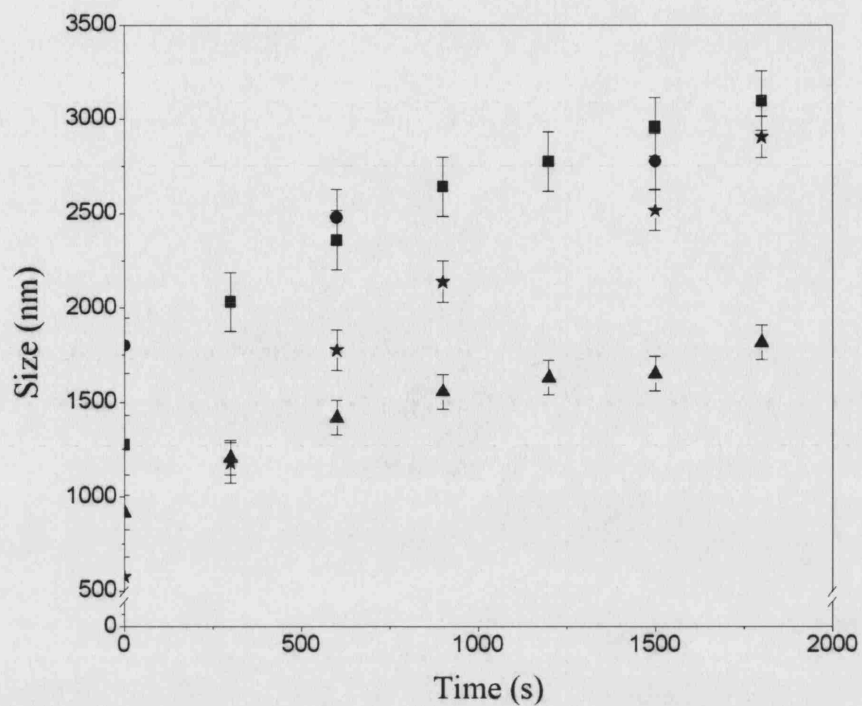
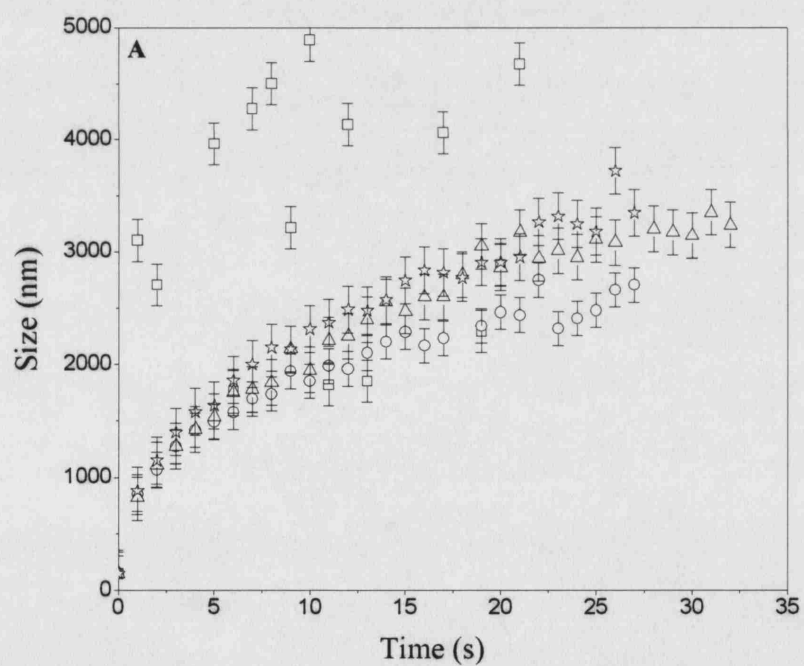


Figure 7.3: Average aggregate sizes in PBS, pH 7.4 as a function of time. Data refers to Peptide 6(■), MPM 108 (●), MPM 109 (▲) and MPM 110 (★).



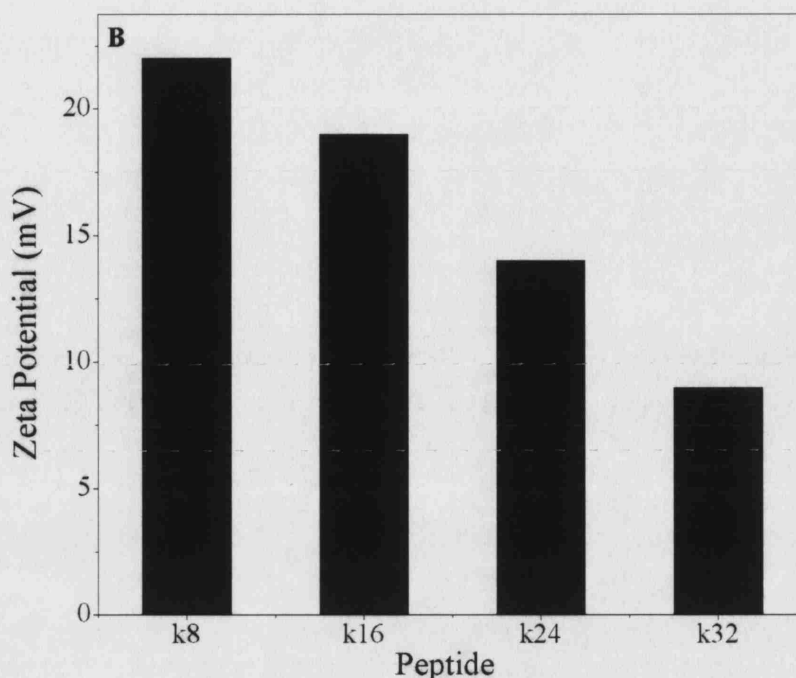


Figure 7.4: (A) Average aggregate size as a function of time for different lysine chain length LPD complexes in PBS, pH 7.4. Data refers to K8 ( $\nabla$ ), K16 ( $-$ ), K24 ( $\delta$ ) and K32 ( $\psi$ ). (B) Zeta potential of K8, K16, K24 and K32. All measurements were conducted at a charge ratio of +7.

length of the lysine residues of the peptides had little effect on the aggregation profiles Figure 7.4 (A). The K8 chain did not bind well to the complex and hence formed a very polydisperse system; this was supported by Atomic Force Microscopy data (private communication Hart, S.L. Institute of Child Health, UCL). The zeta potential data Figure 7.4 (B) supported the sizing measurements for the K16-24 range so it is unclear as to why the K8 system was less stable, it may be that the DNA had not been fully condensed by K8.

Figure 7.5 suggests that at all charge ratios for the lysine series follow a similar pattern with the LPD particles incorporating the K8 peptide demonstrating the highest zeta potential value, and hence forming the most stable system. This effect seems to become less pronounced as the charge ratio decreases. At a charge ratio of +4 there is very little difference between K8 and K32. These measurements must however be compared with the aggregation profiles of the complex as highlighted in Figure 7.4 (A) where there is an increase in stability (based on the rates of aggregation) from K32-K16, although K8 is unable to condense the DNA sufficiently as so does not form a condensed complex as seen in other cases.

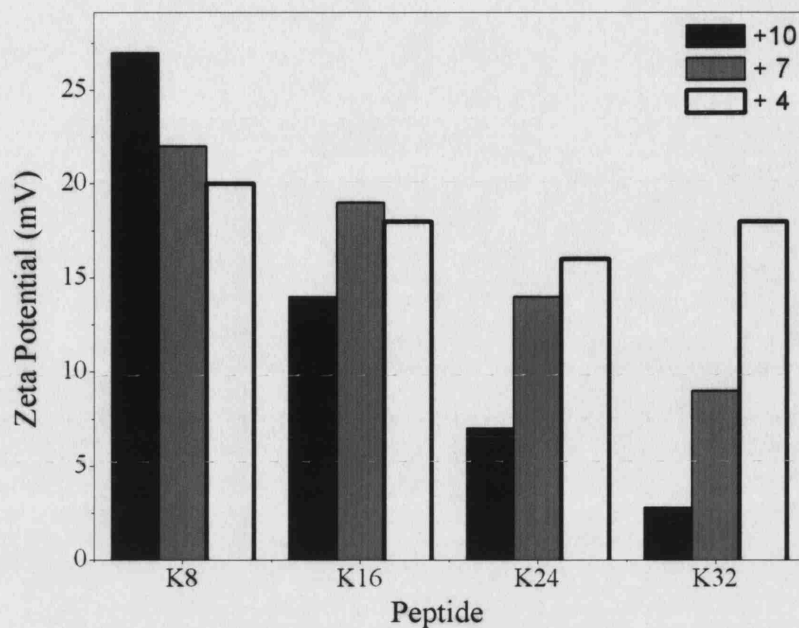


Figure 7.5: Zeta potential measurements of LPD complexes with peptide component comprising of lysine series K8, K16, K24, K32. Measurements are shown for charge ratios +4, +7 and +10.

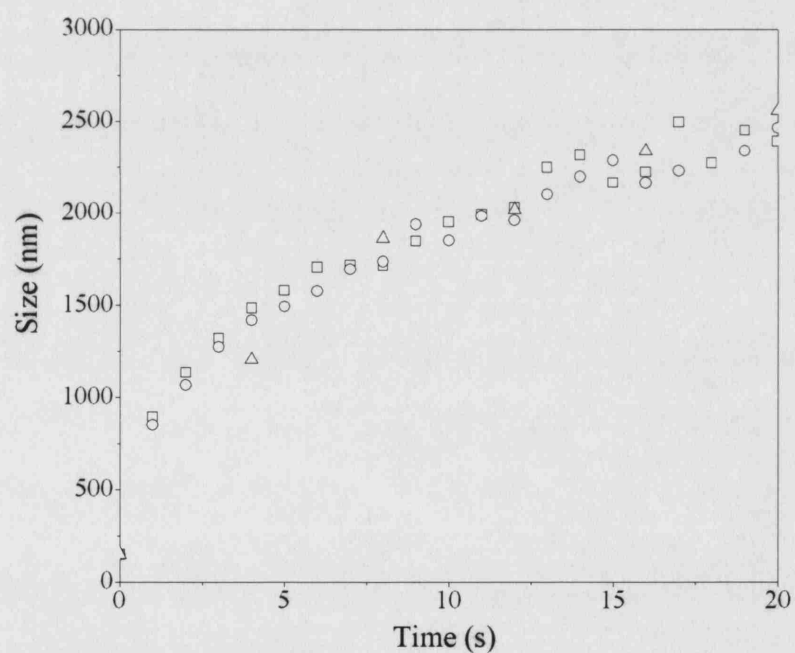
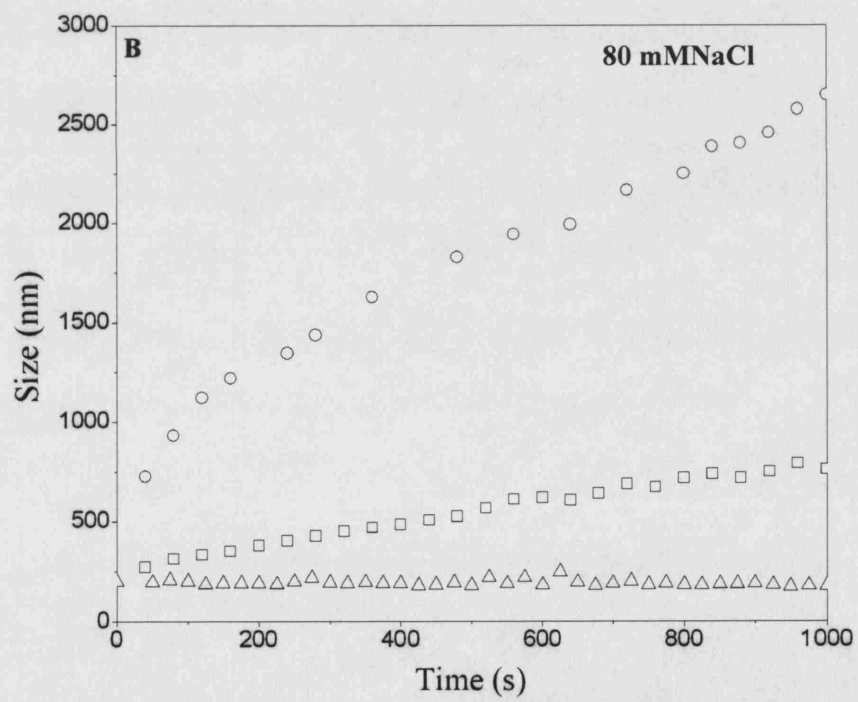
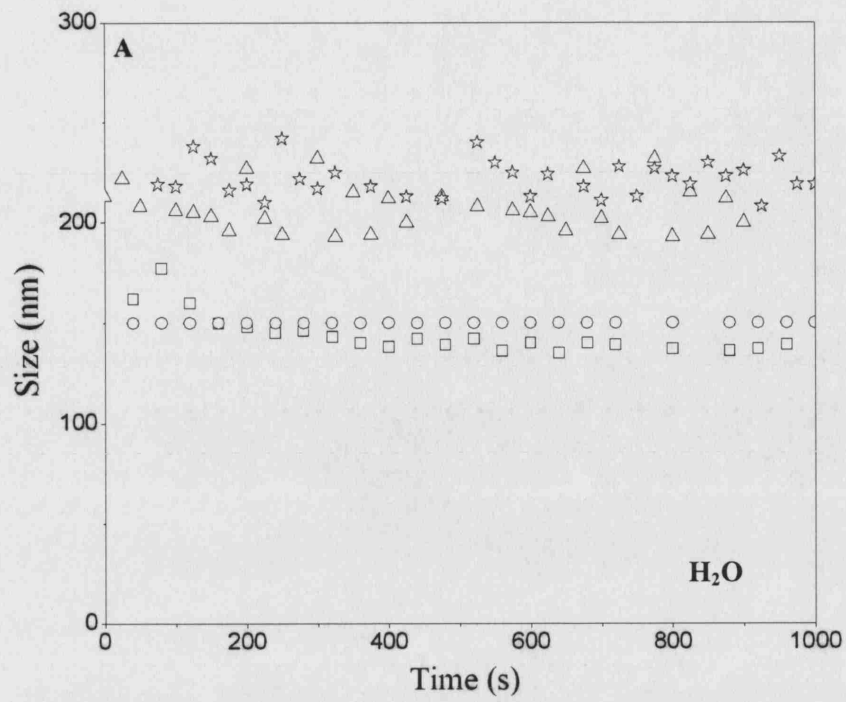


Figure 7.6: Data shows LPD complexes (containing K16) at charge ratio +4 (□), +7 (○) and +10 (△).



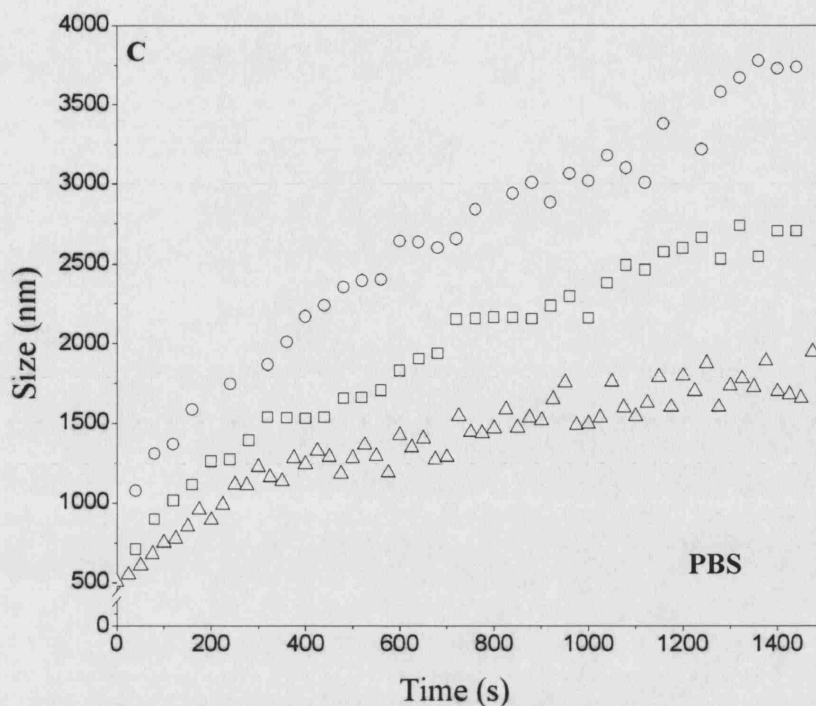


Figure 7.7: Particle size distribution of LPD complexes in (A) distilled water, (B) 80 mM NaCl and (C) PBS. All complexes contain peptide 6 and lipofectin, with differing size plasmids, gWiz ( $\nabla$ ), psv $\beta$  ( $\square$ ), pQR150 ( $\Delta$ ), p5180 ( $\psi$ ). All complexes were prepared at a charge ratio of +7.

### 7.3.3 Plasmid DNA

Figure 7.6 suggests that for LPD complexes containing lipofectin (1 mg/ml), psv $\beta$  (1.5 mg/ml) and peptide 6 (4 mg/ml) there is no greater observed compaction on increasing the charge ratio from +4 to +7 to +10, this has also been shown for the 72 kb plasmid.

Figure 7.7 shows the difference in initial size of the complexes for the plasmid sizes 5.7 kb, 6.9 kb, 20 kb and 72 kb at a charge ratio of +7. All the complexes in water were stable as observed for the original vector complex containing psv $\beta$ , peptide 6 and lipofectin.

Plasmid	Molecular weight (kb)	Average size (nm)
gWiz	5.7	141
Psv $\beta$	6.9	150
pQR150	20.0	219
p5180	72.0	275

Table 7.2: Average LPD complex size in distilled water, all experiments were conducted at 25 °C.

The differing average sizes of the complexes can be attributed to their initial size before compaction. Based on studies at higher charge ratio with LPD, higher levels of compaction cannot be achieved by increasing the charge ratio. Table 7.2 shows the average size of the particles in water.

Figure 7.8 shows the aggregation profiles of all of the plasmid complexes. The LPD complex containing psV $\beta$  is shown to exhibit the two highest levels of aggregation PBS and 80mM NaCl respectively. LPD complexes containing gWiz and pQR150 also had high levels of aggregation in PBS. In contrast pQR150 (20 kb) complexes showed no aggregation in 80mM NaCl. Due to lack of materials, measurements of LPD containing p5180 could not be conducted. It is possible that this too does not undergo aggregation in salt conditions, but remains to be investigated.

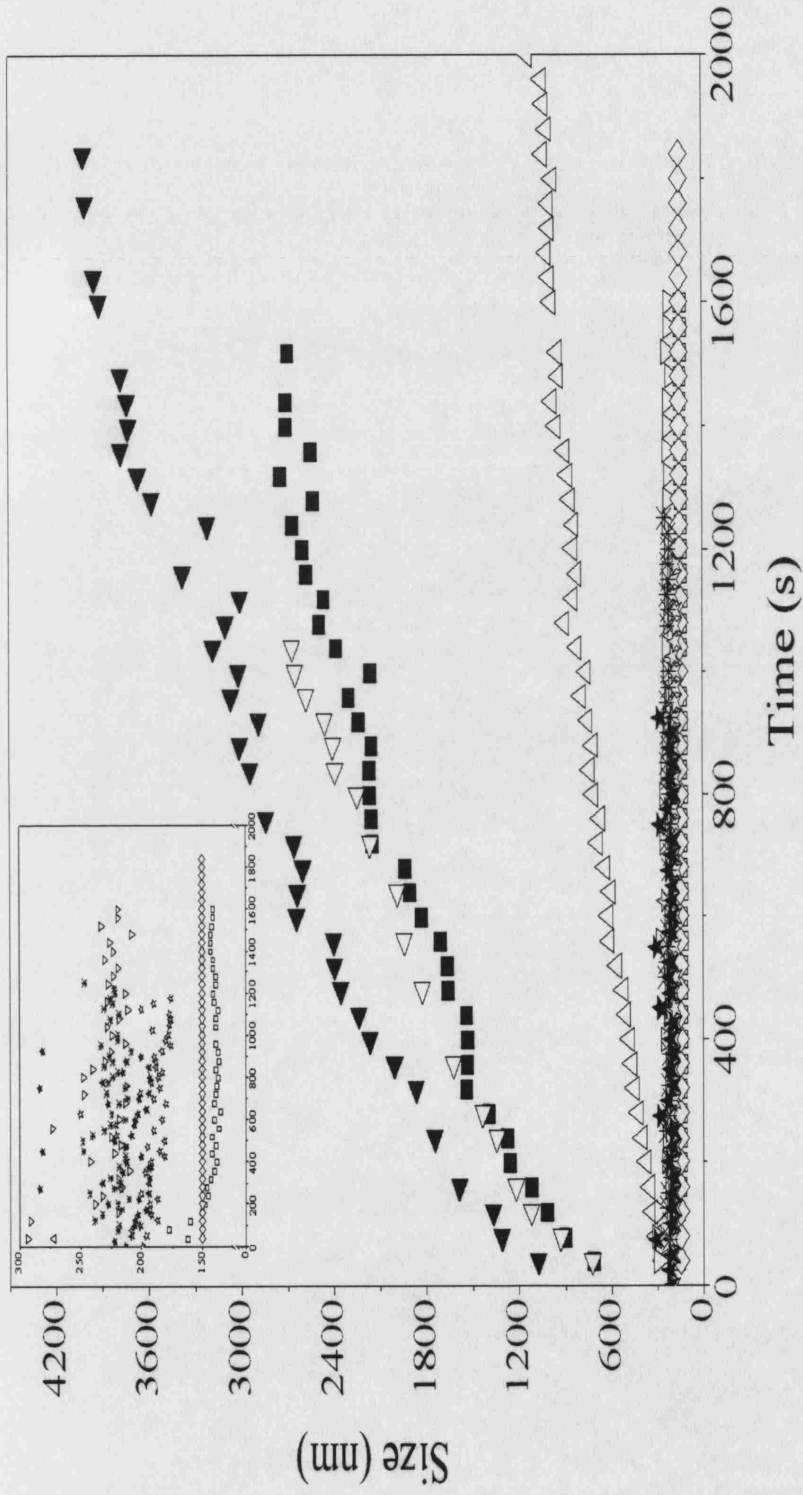


Figure 7.8: Data shows plasmids: gWiz + H<sub>2</sub>O (▽), gWiz + PBS (!), gWiz 80mM NaCl (\*), psvβ + H<sub>2</sub>O (M), psvβ + PBS (Ω), psvβ + 80 mM NaCl (Ξ), (v), pQR 150 + H<sub>2</sub>O (ξ), pQR150 + PBS (v), pQR150 + 80 mM NaCl (ψ), p5180 + H<sub>2</sub>O (□). All systems contain lipofectin and peptide 6 at a +7 charge ratio.

## 7.4 Conclusion

There has been a lot of work in the development of synthetic vectors for gene therapy applications, and while Lipid/Peptide/DNA complexes have shown high levels of transfection compared to other non-viral vector (Hart *et al.*, 1998), it still remains a first generation vector. The rationale design of the LPD vector allows the flexible modular structure to be investigated component by component. Assessing the feasibility of varying the physical and chemical nature of the components and relating it to size, zeta potential and fluorescence measurements.

What is most evident is that there is not a logical pattern in determining an optimal complex for a both storage and physiological conditions. Lipid size showed smaller aggregate formation in the presence of DOPE after a period of 20 min, this was most evident with C14 Saturated + DOPE. C14 Unsaturated + DOPE, had the highest level of calcein release at pH 5.5, pH conditions observed in the endosome. The hydrophilic spacer MPM 109 aggregated the least in physiological conditions, it could be hypothesised that the addition of a hydrophilic component can reduce aggregation, although this has not yet been investigated further; in all cases the level of aggregation in physiological conditions render the complexes inapplicable for medical applications from a biophysical perspective. Transfection data (private communication Dr Stephen Hart) showed all the systems to exhibit poorer levels of transfection compared to the unaltered spacer domain, peptide 6. The MPM 109 peptide at a +7 charge ratio showed the most promise, while pQR150 was the only plasmid that did not aggregate in salt conditions. What is vital is the need to optimise each component, bearing in mind its physical stability in addition to its transfection properties, a physiologically stable complex may not be the best transfecting agent. A delivery vector that provides high levels of transfection efficiency in addition to forming a stable system during storage, transport and most importantly delivery to the target is desirable.



## Chapter 8 : Conclusions

### 8.1 Introduction

This work presents a comprehensive experimental and theoretical investigation of the effects of various physiochemical parameters on the biophysical properties of DNA complexes. New methods of using modelling techniques to aid this process are described. The modification of such complexes is also investigated through rationale component design.

Different techniques were used to measure the properties of these self assembling particles. When developing novel delivery systems, particle properties such as size, rate of aggregation, zeta potential and fractal dimension can be used to evaluate new complexes. Some of the important issues encountered in this study were:

1. Under physiological condition all LPD particles investigated experienced aggregation.
2. Fast growing aggregates produced open structures, slow forming aggregates formed compact structures.
3. Monte Carlo simulations can be used as a tool to predict rates of aggregation.
4. Increasing the charge ratio of positive to negative equivalents of the LPD vector did not affect the extent of complex compaction.
5. Lipids with shorter chain length had better release properties than those with longer chains.
6. Lipids containing DOPE experienced lower levels of aggregation compared to systems lacking DOPE.

## 8.2 Fractals

The fractal dimension of LPD complexes have been observed for the first time and provide evidence that they form fractal aggregates of both loose and compact nature. The structure formed is essentially determined by the mode of aggregation, which in turn is primarily determined by the rate of aggregation. This is the first time that lipopolyplexes have been quantified using fractals, and is a way of distinguishing differing systems based on this parameter. Size measurements provide a very important indicator of aggregation but had previously not provided a structural guide to the aggregates. Fractal measurements of 1.6 were observed under physiological conditions, a relatively loose structure that may provide information as to how the aggregates can be best treated, loose aggregates are somewhat easier to dissociate than those that form a compact structure and so fractal dimension may pave the way for research into dealing with the aggregates once formed, in addition to current work which aims to prevent them forming in the first place. The former may prove to be critical to the development of non-viral vector treatment. The fractal dimensions determined here for a range of salt conditions also enable simulations, most notably Monte Carlo which have been discussed in Chapter 6 to form more accurate predictions based on the coalesced fractal sphere model discussed in Section 2.8.

## 8.3 Monte Carlo Simulations

The use of Monte Carlo simulations has been a successful tool in predicting the aggregation of LPD complexes by relating it to the zeta potential of the system. There is much scope based on recent calls by the Food and Drug Administration to develop process analytical technologies (PAT) that allow real time measurement of a system that give complete information about a process and allows the manufacturer to be confident that all final products are of a designated quality without the assumed assurance provided by the testing of random samples and batches. Monte Carlo simulations developed and tested here have allowed for the first time a means of simulating and understanding the growth of aggregating DNA complexes. The theoretical predictions were in excellent agreement with the experimental results.

## 8.4 Rationale Design

‘One factor at a time’ (OFAT) testing offers a basis for determining the properties of each component, which in turn can lead to an improvement in the LPD vector. C14

Unsaturated + DOPE had the greatest level of calcein release at pH 5.5 (although this may change when the lipid is in a complex with peptide and DNA). MPM 109 aggregated the least of all the peptides tested while the larger plasmids showed greater stability although this is not conclusive from the experiments conducted.

## 8.5 Recommendations

There are important issues that require further investigation but at present are beyond the scope of this thesis:

1. Shearing may provide a means of dissociating aggregates, such that they do not reform. The looser structures formed in physiological conditions are more susceptible to this and may be broken into smaller particles if exposed to low levels of shear. The delivery method of choice, for example a nebuliser may be able to provide such conditions.
2. MC simulations should be modified to take into consideration the CS model based on fractal dimensions determined from PCS measurements.
3. The hydrophilic spacer MPM 109 has the lowest rate of aggregation of those studied; comparison of other hydrophilic and hydrophobic spacers may show this to be true of simply MPM 109 or may be a property of hydrophilic spacers that enhance the stability of LPD complexes.
4. pQR150 showed the formation of a stable complex in 80 mM NaCl, further investigation into the relationship between plasmid size and aggregation should be conducted to determine whether larger complexes are indeed more stable.
5. Factorial design should be employed to study potential interactions between parameters and to test a larger number of variables based on the major factors determined in this work.

Much work remains to be done before the reality of a safe, physically stable and effective gene therapy vehicle is achieved. The need to develop stable vectors under physiological conditions remains a true challenge, the stability demonstrated during the storage and transportation conditions needs to be seen under physiological conditions to provide the efficacy and efficiency needed for successful levels of transfections, and allow non-viral gene therapy to be a realistic alternative to viral vector delivery systems.

## Chapter 9 : Application to Industry

### 9.1 Introduction

In the final year of my PhD, I spent three months at the London Business School, studying the MBA module: *Technology and Competition*. I was sponsored by the *Centre for Scientific Excellence* (UCL) to learn about the transfer of research into a commercial reality. This chapter focuses predominantly on the comparison between *First* and *Second Mover* advantages. First mover advantage is a concept that gained popularity in the 1980s, but since then there has been evidence of practical benefits to being second; a belief currently held in all sectors but the pharmaceutical industry, where the importance of patent protection and brand loyalty outweigh those factors that makes second mover advantages more significant in other industries.

### 9.2 Current Commercialisation for Gene Therapy

Gene therapy aims to be one of the most important developments in medicine over the next 20 years. However, in the short-term and possibly longer, it is likely to be limited to the treatment of a relatively small number of diseases, including cystic fibrosis, Gaucher's disease, differing forms of cancer and HIV/AIDS. Of these, the treatment of cancer is the most promising.

Gene therapy is increasingly viewed as a novel form of drug therapy and a source of new therapeutic products for the pharmaceutical industry. As a consequence, gene therapy firms are rapidly being integrated into the pharmaceutical industry. By the early part of the century, gene therapy is likely to influence the types of therapies developed by the European pharmaceutical industry (Martin *et al.*, 1998). In order for a company to capitalise on this new market, it must be first to market with the product. The introduction

of this 'novel drug' follows the same rules as those of traditional products in the marketplace today.

First mover advantage is seen by most today as a risky venture that can ultimately result in a futile effort to capture a large market share in the face of fierce second movers who do not bear the sunk costs of development faced by the first entrant. Second mover can be either differentiated or imitative; the former is essentially offering the consumer a different version of the same product, and if it is quick enough it can even become the standard to which future products have to comply with. An imitator, on the other hand, offers the same product but at a cheaper price to the consumer. So what do these second mover, also more commonly known as *free riders*, gain from being entering the market at a later date than the pioneers, is it a strategic move or simply that they have not been quick enough to enter the race? A first mover often bears substantial pioneering costs, such as gaining regulatory approval, achieving code compliance, educating buyers, developing infrastructure in areas such as service facilities and training. Development requires inputs such as raw material sources and new types of machinery and investment in the development of complementary products. There is also a high cost of early inputs because of scarcity of supply or small scale needs. Many new products, especially radically new products, fail to generate much interest among buyers. Expectations for demand typically turn out to be much higher than actual sales. For every mobile phone there is a picture phone, for every Polaroid camera there is a 'Nimslo', a three dimensional camera. The fact is that, many pioneers introduce new products for which there is no demand. This means they spend time, effort, and money on opportunities that do not exist.

### 9.2.1 Demand Uncertainty

A first mover bears the risk of uncertainty over future demand. It must first put capacity in place first, while later movers can base their decisions on more current competition. Though committing before competitors has some advantages, it also has some betting on an early takeoff of the new technology. Later movers learned from Radio Corporation of America's (RCA) experience that demand for colour television sets some years away and avoided a period of losses. The strategy employed by many free-riders is to sit back and watch. Only when the market potential becomes clearly favourable do they move in and gain viable and often commanding lead. This reduces their risks and lowers their costs

considerably, although they may have to spend heavily during the later stages of market development to overcome their later start.

### **9.2.2 Changes in Buyer Needs**

A first mover is vulnerable if buyer needs change and its technology is no longer valued. A first mover's reputation and advantage may also be eliminated if buyers' need change and the first mover is identified with the old generation of technology. Unless buyer needs shift radically, then substantial changes in the technology is required to serve them; however a first mover can maintain its lead by modifying technology over time.

### **9.2.3 Investment Specificity**

A first mover may be at a disadvantage if early investments are specific to the current technology and cannot be easily modified for later generations. In semiconductors, for example, Philco moved early for leadership with a large automated plant. It enjoyed a period of success but later development of a different manufacturing process for semiconductor chips made its earlier investments obsolete. Similarly the early movers will be disadvantaged if its product or process reflected factor costs or factor quality that have changed.

### **9.2.4 Technological Discontinuities**

Technological Discontinuities work against the first mover by making obsolete its investments in the established technology. Technological discontinuities are the major shifts in technology that a first mover may be ill prepared to respond to given its investment in the old technology. Discontinuity favours the first follower who does bear the high cost of pioneering. Where technology evolves along a relatively continuous path, then a first mover's head start is an advantage. It can transfer learning from the old technology to the new and stay ahead on the learning curve.

### **9.2.5 Low Cost Imitation**

A first mover exposes itself to followers who may be able to imitate the innovation at lower cost than the cost of innovating. Followers often have to bear some costs of imitation and adaptation, which work to the benefit of the first mover.

The majority of new product ideas are killed before ever being sold to actual customer; once the product is brought to market it can either be rejected or accepted by customers.



Schematic 9.1: Generic Product Path.

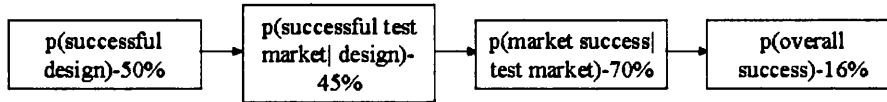
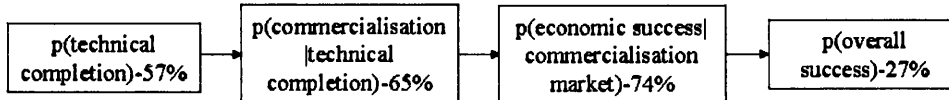
The highest rate of product failure occurs during the first stage, the time between an idea's conception and its introduction into the market. Although precise estimates vary greatly, there is general agreement that the majority of new product ideas never make it to market. They are terminated at some stage of the development process. Between 70-90% of all new products that make it onto the market place fail in the market place. The overall probability of success falls in the region of 16-27% (Schnaar, 1995) depending on whether it is a consumer good or industrial product.

There is a tremendous amount of financial risk in new product development. The chances of failure are especially high for radically new technological products and products that establish entirely new categories. Generally, the higher a project's financial return, the higher the risk of failure associated with it. The fruits of the financial reward are dependent on the extent to which a company can hold on to its product development. Otherwise, a later entrant is able to partake in the rewards without having to partake in the risks, which are borne solely by the pioneer. The risks fall solely to the pioneer, while the rewards are spread to the others.

### 9.3 Second Mover Benefits

Imitation is less expensive than innovation. It avoids many of the costs that must be borne solely by the first entrant. The innovator for example, is forced to spend heavily on research and development and educating wary customers as to the desirable benefits of the new product. The question is not whether imitation is less expensive than innovation it clearly is, but whether substantial benefits accrue to the pioneer who take on those enormous expenses.

An empirical study by Edwin Mansfield found that imitation occurs quickly and that innovators are not able to get a long lead on imitators. New product R&D projects typically found their way into the hands of competitors within twelve to eighteen months. In 20% of the cases, competitors knew of new product development project within six months of their inception. Since it takes about three years for a new product to make its

**Consumer Goods****Industrial Goods**

Schematic 9.2: Success probability comparison between consumer and industrial goods.

way from an idea to a marketplace, there is a better than even chance that the decision will leak out before the innovation is half completed. Companies learn about each other's patent applications, which require going public with the firm's innovative ideas. Knowledge spreads through papers and presentations at professional and academic conferences attended by scientists and engineers and also when technical and marketing personnel switch jobs; taking with them inside information (unintentional or intentional).

#### 9.4 First Mover Advantage: When Does It Really Exist?

As a concept, first mover advantage is a very well known and frequently used term. In recent years many people have questioned the true benefits of being a pioneer. However, in certain sectors first movers can reap large benefits when favourable conditions are created and capitalised on (Porter, 2004). Essentially first mover advantages exist when an environment is such that the benefits from being first into market exceed the costs of having to be the first to explore the risks. This advantage is greater in some industries than others (Boulding *et al.*, 2001). In all cases what is required for the first mover is to create conditions such that the competition can be pre-empted. By being the first to put together the precise combination of features, value, and sound business economics allows a firm to unlock a profitable new market. This can be achieved by erecting resource barriers and economies of time. Resource barriers concern reputation, brand name, particular relationships with suppliers and experience, and every factor enabling the first mover to build a resource barrier preventing competitors from effectively imitating or substituting the pioneer's bundle of resources (Wernerfelt, 1984).



### 9.4.1 Market Change

The time at which a first mover enters is crucial. In cases of technological change, if the first mover has technological advantage and enough commercial resources, business overturn is possible during the change. A change in technology can be a key determinant to whether a mover should enter the market first. Two categories exist; changes that are *discontinuous* or *incremental*.

Discontinuous changes occur when there happens to be major innovations in technological or economical areas that overturn the nature of the whole industry field or create a completely new market area. Incremental development is less radical and often based on development of production processes and distribution (Tushman *et al.*, 1987). If a firm can enter at the critical phase of an overturn, it can benefit from change since the incumbents are unlikely to adopt the new technology and market factors rapidly enough. Successful innovators tend to enter at this point; examples include Pilkington (Float Glass), Searle (Nutra-sweet) and DuPont (Teflon) (Johansson *et al.*, 2002).

### 9.4.2 Learning Curve

First moving companies will receive real life feedback earlier than competitors. This information is essential and it is from the feedback that the learning curve can begin. Companies that employ high numbers of workers benefit more from first mover advantages than those that are highly automated processes, where productivity improvements are far smaller. It was found in the 1930s that the man hours required to put a plane together decreased as production increased, i.e. the fourth plane took 80% of the time of the second plane and the eighth 80% of the fourth plane. Productivity improved by a steady 20% each time and the cumulative output doubled. The learning curve benefits expansion and economies of scale not available to later entrants.

### 9.4.3 Switching Costs

The first mover has the opportunity to create large switching ones, once critical mass is achieved, and have the effect of excluding competitors. Early entrants may gain advantages in loyal customers who are unlikely to try competing following products. If switching costs are involved in the use of a new technology, the first entrant to a market benefits because consumers who adopt the product would have to incur a cost to use a competing product. In hospital management contracts for example, the pioneer that signed up hospitals first gained a significant edge in contract renewals because of the

substantial costs to the hospital of changing management firms; switching would result in disruption caused by a new administrator, a new computer system etc (Porter *et al.*, 2004). The entrant's profits are eroded by the difference between what the customers would be willing to pay and switching costs to induce the change (Schnaar, 1995).

#### **9.4.4 Distribution Channels**

The first mover can also lock in the most attractive supplier relationships, distribution channels, and market segments. One of the reasons why it is difficult for any cereal producer to gain entry into the market is that the incumbents control shelf space in the supermarkets. The control of this distribution channel is a key barrier hindering later entrants from gaining access to this market. In cases where there can only be a limited number of brands in distribution channels, by virtue of being first, pioneers can ensure that their products have access to preferential distribution (Schnaar, 1995). This point may only be seen as a temporary advantage in most industries, however having access to scarce resources, natural resources and land is a source of sustainable first mover advantage in such industries such as De Beers' diamonds.

#### **9.4.5 Brand Reputation**

When a firm can get customers to identify it with creative ideas rather than a 'copycat' image, it can reap the benefits of a strong reputation. Leadership places a company, at least temporarily, in the position of being unique which can produce a long-term image benefit (Porter, 2004). This advantage is best capitalised on by companies that have the resources to publicise their lead.

#### **9.4.6 Patent Protection**

Patents granted on innovative products can be used to lock out later entrants, it is most useful in cases where a product is very distinctive and can be specifically defined such as a molecule. No where are the benefits of first mover advantage greater than in the Pharmaceutical Industry (Kotler, 2000).

### **9.5 Pharmaceuticals**

The pharmaceutical industry is the most research intensive U.S. manufacturing industry not dependent on direct government contract support for its innovative activities. It has consistently been one of the most profitable industries. Most pharmaceutical products are available in the U.S. only under a physician's prescription. In such cases a consumer does

not choose what he or she will consume; a third party does. The industry therefore can be divided into two broad groups: *prescription* (or ethical drugs), and *proprietary* (or over the counter drugs). In the 1970s, prescription drugs accounted for over three quarters of the total U.S. pharmaceutical product sales. Individuals suffering from some acute illness will commonly be willing to pay a very considerable sum for relief. This means that over a wide range of prices, the demand for an appropriate medicine tends to be quite price elastic. In addition when the number of relevant suppliers is small, the suppliers may possess considerable monopoly power.

## 9.6 Case Study: Clamoxyl Antibiotic (GSK-France)

Clamoxyl<sup>®</sup> was launched in 1974 by Beecham (SB) laboratories in France (Chandon, 2004). It was the first amoxycillin available in France, and was a rare breakthrough that enjoyed immense success. Clamoxyl<sup>®</sup>, a patented antibiotic for respiratory infections, enjoyed an exclusive monopoly on a fast growing market, before a new entrant was allowed to enter. It was able to acquire immense brand loyalty through strong relations with doctors and strong scientific support for its benefits, strengthened by the lack of side effects. SmithKline Beecham provided excellent services for doctors, ranging from a 24 hour hotline, to jars of sweets for children during medical visits. It had a dedicated sales force and distinctive advertisements emphasising the uniqueness of Clamoxyl<sup>®</sup> and its red colour, thus making switching conditions for the doctor unfavourable. SB was able to get feedback from its customer base early on and move down the learning curve, making the antibiotic adaptable to all situations and suitable for adults and children alike. SB continued its process development to allow the productions of the two forms of drug in both oral and injectable forms by investing in new technologies. They continued to communicate on the therapeutic benefits of these improvements, by publicising their strong reputation, thereby cementing their innovative reputation further in the minds of physicians and patients alike.

After the expiry of Clamoxyl<sup>®</sup>'s patent in 1980, generics and branded copies entered, selling for at least 30% less than Clamoxyl<sup>®</sup>, although they were not available in as many forms. The generics however were not able to break even since they didn't have the economies of scale enjoyed by SB. SB invested by developing new forms and dosages, i.e. allowing one dose per day rather than multiple administrations, and creating a sugar free version for children. SB continued with its aggressive advertising, aware that the new

entrants would be unable to compete on the same scale. Doctors who did not share in the cost of the prescriptions given had no incentive to consider the price of different products in making a prescription decision, and so continued to prescribe Clamoxyl® through brand loyalty and the fear of switching costs to themselves and patients that would result from moving away from the tried and tested methods of Clamoxyl®. Additionally, many consumers (85%-French) have some type of insurance that weakens incentives based on price. Up until 1999, pharmacists were also not allowed to substitute the prescribed drug with its generic counterpart. Long after the patent protection had gone, awareness and image of the brand was so strong in the mind of patients and doctors that it retained most of its equity after the loss of patent protection.

These factors all allowed Clamoxyl® to maintain its lead for another 10 years, before regulatory laws were introduced to force physicians to prescribe cheaper generic drugs, to reduce the states growing health costs. Although this initially resulted in the loss of market share for SB, ironically doctors were once again encouraged to prescribe Clamoxyl® (by the social security agency responsible for the reimbursement of costs: CNAM) after it slashed its prices by 30%, making it a more competitive alternative to the new more potent and costlier *macrolides* and *sephalosporins* that had entered the market. This allowed SB to benefit from a discontinuous technical change that under normal circumstances would have forced them out of the market.

Clamoxyl® is a strong example of how a first mover benefited from efficient patent protection. It allowed SmithKline Beecham to take advantage of a lead-time, in which it was able to create strong brand loyalty and create switching costs early on in the product life cycle. SB benefited from the learning curve, creating newer and more diverse products that strengthened the company image as an innovator as well as creating economies of scale. After patent expiration, SB continued to enjoy success, since physicians and customers were more influenced by SB's strong brand name and motivated sales force than by the cheaper generics. Even during a period of discontinuous technological change brought about by the introduction of *macrolides* and *sepharosporins*, SB was able to take advantage of French legislation by reducing Clamoxyl®'s price by 30%, a profit margin it was able to bear due to economies of scale fuelled by continued brand loyalty.

## 9.7 Gene Therapy and LPD Commercialisation

The key to patenting LPD lies in the biophysical properties of the vector itself. LPD is made up of three parts, lipid, peptide and DNA. The modularity of each component can be optimised individually, and as a complex. Each component can be patented individually which includes the chemistry and physical dimensions of the peptides, and the chain length of the lipids with all their levels of saturation. The DNA plasmid can range from psv $\beta$  (6.9kb), gwiz (5kb) and pQR150 (20kb), but essentially is not a component that will be patented. What is more important is collectively how the components come together to form a complex, and this is dependent on what weight ratios the complexes are most effective at, the concentration at which DNA, peptide and lipid should be incorporated in and the system in which it can be best stored and transported at before administration. Physiological conditions, of course, cannot be altered and so an effective vector is one which is optimal in a physiological environment. From a physical perspective it may be necessary to patent the exact conditions under which the system is stable and also administered, if shearing of the complexes can reduce aggregation, a device unique to LPD may have to be designed such that the vector in addition to the transportation vehicle used will have to be patented. The exact design of the delivery device and the levels of shear subjected to the complexes may form part of this patent. The patent will have to be such that it covers the full breadth of all the possible medical application the system may have, and not just the condition it is geared towards i.e. cystic fibrosis. The benefits of the product must be capitalised on within the time of the 20 year monopoly, with the initial financial rewards being re-invested into continued research and development. The learning curve begins early in the product life cycle and is initially generated from access to the customer information base.

### 9.7.1 Learning Curve

The sooner LID is able to capture a sizeable proportion of the market, the sooner the learning curve can begin, like SmithKline, if the market is customer driven then new forms of the medication should be developed to provide the customer with convenient methods of administration that are different for adults and children and can be adapted to different situations and environments. The learning curve should also bring technological advances to the process at hand, creating newer and more efficient yields, continued information and investment should allow research and the development of new processes such that a discontinuous change in the market brought about by a competitor does not allow perhaps a more inferior product to benefit since it can charge a lesser price for a

product due to a more efficient administration method brought about by a technological change and thus setting a new standard. The aim of LPD should be to create economies of scale, once a large customer base has been established. This should include diversifying the product range, i.e. methods of administrations and differing options for children and adults. The need to create complimentary products is also important. If specific needles and nebulisers are also made by the same company, these are then also likely to be used.

### **9.7.2 Switching Costs**

If the vehicle which is used for the administration is specific to the drug itself, then the company can benefit in a number of ways. Firstly, all the physician or patient is unlikely to move away from the product because of the problems associated with a) moving away from the drug itself and b) the implications of using a new drug with the already established delivery method. What can ideally happen is in the establishment of an industry standard, such that a new entrant will have to use the established method to administer their drug or face the repercussions of competing with an industry standards. If LPD was to be signed up to hospitals through management contracts, it will gain a significant advantage through contract renewals, because of the unwillingness of the hospital to pay the subsequent switching costs.

### **9.7.3 Brand Reputation**

If LID is identified as an innovative company, it will serve well in the minds of physicians and consumers. A company that can successfully promote and supply gene therapy solutions to establish conditions in addition to diseases where no current treatment exists is likely to benefit generously from a pioneering status. This should be capitalised on by the constant improvement of the product through the learning curve.

### **9.7.4 Brand Loyalty**

Like with SmithKline and Clamoxyl®, it is important to 'sell' the benefits of LPD, this can be through sending representatives to doctors, organising seminars, distribution of leaflets to inform doctors of the benefits of LPD. If prior to market launch the benefits of the product can be published in medical journals or literature, the time taken to educate consumers post market introduction can be saved. Once the brand is established, help-lines and continued contact with the physicians must be maintained, this is especially necessary to easily introduce them to any new/modified products brought out by the company.

## **9.8 Research and Development and Current Legislation**

Theoretically one can see how a product such as LPD will benefit from its application to cystic fibrosis applications during its 20 year monopoly (although this is the total number of years from filing a patent and not from product launch). However, unless it can introduce multiple applications for the use of LPD as well as its delivery vehicle it runs the high chance of falling foul to imitating strategies once patent protection has ceased. If one assumes that the delivery vehicle has become an industry standard, it can act as a cash cow to further research into modification of LPD to treat other genetic diseases. Without heavy emphasis on research and development a new entrant can essentially imitate the LPD vector and modify it to treat other diseases, this becomes more acute when the patent expires.

As healthcare costs around the world continue to rise, governments faced with the challenge of managing and financing their healthcare provision, are increasingly devising cost saving measures. One such measure involves encouraging the development of the market for generic products. This is being achieved through administrative initiatives designed to increase the market penetration of generics. In addition, legislative initiatives and court decisions are eroding the ability of innovators to protect research data submitted to regulatory authorities to support incremental improvements to existing products.

Biological products are as susceptible to this interest in generic copying as other types of conventional pharmaceutical products containing chemically synthesised drug substances. A number of first generation biotechnology products will come off patent or lose marketing exclusivity or data protection in the next five to ten years. The market value of such products is estimated in the region of US\$1.7 billion dollars, presenting an attractive business opportunity for those looking to develop generic products.

However, there are high costs associated with developing a biological product. In addition to high research and development costs, there are significant additional costs in the routine production of biological products. These costs are the result of both the complexity of the manufacturing process for these products and the increasing regulatory demand for tighter control over the manufacturing process to ensure continued product safety. As a result, generic manufacturers have been exploring various ways to maximise reliance on an innovator manufacturer's non-clinical (animal) and clinical data or that

published in the literature (including information derived from public assessment reports and pharmacopoeia monographs) to support, at least in part, regulatory filings for biogeneric product authorisations.

European pharmaceutical law requires an applicant for a marketing authorisation to submit an extensive data package, including results of non-clinical toxicological studies in animals and clinical trials in humans in order to demonstrate safety and efficacy of the product under normal conditions of use. However, exemptions do exist from the requirement to submit results of the applicant's own non-clinical and clinical studies under Article 10, Directive 2001/83/EC.

In comparison with other types of pharmaceutical products, biological products are structurally more complex and involve manufacturing processes that require tight control in order to ensure their safety, quality and efficacy.

Biological products, because of their sheer size are orders of magnitude more complicated than small molecule drugs. This can be seen by a comparison of molecular weight, which can be used as a measure of the size of a given product. For example while aspirin (a well characterised chemical drug) has a molecular weight of 180.2, factor VIII, a coagulation factor for treating haemophiliacs, has a molecular weight in the region of 300,000.

In addition, biological products possess a complex structure that is more susceptible to the conditions of manufacturing. An apparently innocuous change to the process or a formulation for one product may have a detrimental consequence. The product arising from the manufacturing process is often not pure, homogenous mixture. Rather, various forms of these molecules are usually present in the final product. In the absence of supporting data, one cannot predict whether a newly identified product change will be important or not to the safety and biological activity of a biological product. As a result, the conventional approach to testing the finished product in terms of its pharmaceutical and pharmacokinetic characteristics may not be sufficient to assess fully the clinical safety and efficacy of a biogeneric product.

The judgement in the Generic UK case (C-368/96) sets out the criteria for assessing similarity between the originator's product and the generic product. The European Court



of Justice (ECJ) held that two products, when compared, are essentially similar if they satisfy three criteria, namely that they:

- Have the same qualitative and quantitative composition with respect to the active drug substance.
- Have the same pharmaceutical form.
- Are bioequivalent.

However, the ECJ indicated that satisfying the three criteria is not sufficient if the relevant medicinal product differs significantly from the original product in relation to safety and efficacy, for example as a result of the inclusion of a novel excipient or because of different impurity levels.

As a result of *Generics UK*, it appeared that a generic manufacturer could rely on an originator's non-clinical (animal) and clinical data only if both products were essentially similar and the data protection period had expired. This seemed to indicate that data for a related product which was essentially similar; could be protected from cross-referral. However, this apparent protection has been eroded significantly by *Novartis*. In this case the ECJ determined that related products, regardless of whether or not they are essentially similar, are not protected from cross-referral, even if the relevant data protection period has not expired.

As a result of *Novartis*, incremental research using the same active substance is not generally protected, and resulting products can immediately be copied without the consent of the innovator.

EC pharmaceutical legislation has been under review in recent years, culminating in the adoption of Directive 2004/27/EC (amending Directive), which amends Directive 2001/83/EC. Member states must implement the amendments by October 2005. In addition, a new regulation, a new regulation, Regulation 726/2004/EC, replaces the existing regulation governing the centralised procedure for marketing authorisations (Regulation 2309/93/EC).

The legislation replaces the concept of 'essential similarity' with that of a 'generic medicinal product'. The latter term is defined using the first criteria set out in the

*Generics UK* case. A special provision is added relating to biological medicinal products. Where a biological medicinal product claims to be similar to a reference product, but ‘does not meet the conditions in the definition of generic medicinal, owing to, in particular, differences relating to raw materials or differences in manufacturing processes of the biological medicinal product, the results of appropriate pre-clinical tests or clinical trials relating to these conditions must be proved’ (Article 10(4), amending Directive).

The language of the amending Directive makes clear that an assessment of quality and bio-equivalence may not be sufficient to assure the clinical safety and efficacy of a ‘similar biological medicinal product’. Such clinical parameters can only be established by appropriately designed clinical and non-clinical tests.

Annex 1 to Directive 2001/83/EC also appears to recognise the limitation of in vitro testing of the end product, and of conventional bio-equivalence studies in the case of biological medicinal products. It states that the particulars supplied to register a copy biological product are not limited to the data package normally required for the approval of conventional pharmaceutical generic products. However, the amending Directive leaves a sufficiently wide margin of discretion to the regulatory authorities to determine the extent of the non-clinical and clinical testing required for follow-on biological products, taking into account the characteristics of each individual medicinal product (Tsang *et al.*, 2005).

## 9.9 Conclusion

SmithKline was a good example of how generics are not necessarily as great a threat to an incumbent as initially envisaged. In the majority of other industries generics reduce price and by doing so entice customers to buy their product. In the pharmaceutical industry this is less influential since the brunt of the cost of a drug is bared by the NHS in the UK. The main problem lies in not being able to modify or alter the structure of LPD so that it can be used to target other conditions. This is an evolution process that requires heavy emphasis on R&D. When assessing competition, it is important to assess future market potential as well as current. Even if LPD is able to capture a good market share of the CF market, if it cannot evolve to treat other conditions such as HIV/cancer it will not be a major player in the gene therapy market.

New legislation put in place will make it harder for generics to come to market by having to show more than bio-equivalence to the original drug, the more complex the molecule the more difficult this process will prove to be. Despite the difficulties, the demand for an easier route to market has intensified as biological products have reached or neared patent expiry.

## Chapter 10 : References

Adami, R., C., Collard, Wendy, T., Gupta, Shamita, A., Kwok, Kai, Y., Bonadio, Jeffrey., Rice, Kevin, G., (1998). "Stability of Peptide condensed Plasmid formulations." Journal of Chemical Technology, Biotechnology **87**(6): 678-682.

Akhtar, S., Hughes, M., Khan, A., Bibby, M., Hussain, M., Nawaz, Q., Double, J., Sayyed, P. (2000). "The delivery of antisense therapeutics". Advanced Drug Delivery Reviews **44** 3-21.

Allison, S., Anchordoquy, T. (2000) "Mechanisms of Protection of Cationic Lipid-DNA Complexes during Lyophilization". Journal of Pharmaceutical Science **89**: 682-691.

Almgren, M., Edwards, K., Karlsson, G. (2000). "Cryo transmission electron microscopy of liposomes and related structured". Colloids and Surfaces A: Physiochemical and Engineering Aspects **174**: 3-21.

Almofti, M., Harashima, H., Shinohara, Y., Almofti, A., Baba, Y., Kiwada, H. (2003) "Cationic liposome-mediated gene delivery: Biophysical study and mechanism of internalization". Archives of Biochemistry and Biophysics **410**: 246-253.

Anchordoquy, T., J., Allison, S, Dean., Molina, Marion, D, C., Girouard, Lorinda, G., Carson, Taylor, K., (2001). "Physical stabilization of DNA-based therapeutics." Drug Discovery Today **6**(9): 463-470.

Atteia, O. (1998). "Evolution of size distribution of natural particles during aggregation: modelling versus field results." Colloids and Surfaces A: Physiochemical and Engineering Aspects **139**: 171-188.

Atkinson, E., Kum, Wolfgang., (2001). "Innovation in formulation." www.currentdrugdiscovery.com: 39-40.

Avnir, David., (1990). "The fractal approach to heterogeneous chemistry". Surfaces, Colloids, Polymers. :13

Ayazi Shamlou, P. (2003). "Scaleable processes for the manufacture of therapeutic quantities of plasmid DNA" Biotechnology and Applied Biochemistry 37:207-218.

Bailey, A., Sullivan, S. (2000) "Efficient encapsulation of DNA plasmids in small neutral liposomes induced by ethanol and calcium". Biochimica et Biophysica Acta 1468:239-252.

Baldwin, J., L., Dempsey, Brian, A., (2001). "Effects of Brownian motion and structured water on aggregation of charged particles." Colloids and Surfaces A: Physicochemical and Engineering Aspects 177: 111-122.

Baru, M., Nahum, O., Jaaro, H., Sha'anani, J., Nur, I. (1998). "Lysosome-disrupting Peptide increases the Efficiency of *In-vivo* Gen Transfer by Liposome-encapsulated DNA". Journal of Drug Targeting 6: 191-199.

Bedu-Addo, F., K., Huang, Leaf (1995). "Interaction of PEG-phospholipid conjugates with phospholipid:implications in liposomal drug delivery." Advanced Drug Delivery Reviews 16: 235-247.

Biggs, C., A., Lant, P,A., (2002). "Modelling activated sludge flocculation using population balances." Powder Technology 124: 201-211.

Birchall, J., Kellaway, I., Gumbleton, M. (2000). " Physical stability and in-vitro gene expression efficiency of nebulised lipid-peptide-DNA complexes". International Journal of Pharmaceutics 197:221-231.

Birchall, J., Kellaway, I., Gumbleton, M., Mills, S. (1999) "Physico-chemical characterization and transfection efficiency of lipid-based gene delivery complexes". International Journal of Pharmaceutics 183:195-207.

Blessing, T., Remy,J., Behr, J. (1998). "Monomolecular collapse of plasmid DNA into stable virus-like particles". Proceedings of the National Academy of Science, USA 95: 1427-1431.

Bloomfield, V. (1996) "DNA Condensation". Current Opinion in Structural Biology 6; 334-341.

Bradley, D. (1999). "Cystic Fibrosis treatment: a new era?" Pharmaceutical Science and Technology Today 2(7): 267.

- Bryman, A. (1997) "Animating the pioneer versus late entrant debate: An historical case study ". Journal of management studies **34**: 415-433.
- Bonner, G., Kilbanov, A. (1999). "Structural Satbility of DNA in Nonaqueous Solvents". Biotechnology and Bioengineering **68**:339-344.
- Boulding, W., Christen, M. (2001). "First Mover disadvantage". Harvard Business Review **79**: 12-14.
- Boyce, N. (1999). "Cure that killed". New Scientist **9**: 1-2.
- Bushnell, G., Yan, Y., Woodfield, D., Raper, J., Amal, R. (2002). "On techniques for the measurement of the mass fractal dimension of aggregates". Advances in Colloid and Interface Science **95**: 1-50.
- Bushell, G. (1998). "Primary particle polydispersity in fractal aggregates". Ph.D Thesis.
- Carrion, F., De La Maza, A., Parra, J. (1994) "The influence of ionic strength and lipid bilayer charge on the stability of liposomes". Journal of Colloid and Interface Science **164**: 78-87.
- Chakraborti, R., Gardner, K., Atkinson, J., Van Benschoten, J. (2003). "Changes in fractal dimension during aggregation". Water Research **37**: 873-883.
- Chandon, P. (2003). "Innovative marketing strategies after patent expiry: The case of GSK's antibiotic Calmoxyl in France". International Journal of Medical Marketing **4**: 65-73.
- Chiron Vaccines (2005). "Research". [www.chironvaccines.com](http://www.chironvaccines.com)
- Connor, J., Yatvin, M, Huang, L. (1984). " pH sensitive liposomes: Acid-induced liposome fusion". Proceedings of the National Academy of Science USA **91**: 1715-1718.
- Cristiano, R., J., (1998). "Targeted Non-viral gene delivery for cancer gene therapy." Frontiers in Biosciences **3**: 1161-1170
- Crystal, R. (1995) "Transfer of Genes to Humans: Early Lessons and Obstacles to Success". Science **270**:404-409.
- Darquenne, C. (2001). "A realistic two-dimensional model of aerosol transport and deposition in the alveolar zone of the human lung". Journal of Aerosol Science **32**: 1161-1174.

- Davies, J., Geddes, D., Alton, E. (2001). "Prospects for gene therapy in lung disease". Current opinion in Pharmacology **1**: 272-277.
- Davis, H. (1997). "Plasmid DNA expression systems for the purpose of immunization". Current Opinion in Biotechnology **8**:636-640.
- Dean, S., Molina, M., Anchordoquy, T (2000). "Stabilization of lipid/DNA complexes during the freezing step of the lyophilization process: the particle isolation hypothesis". Biochimica et Biophysica **1468**: 127-138.
- Deeds, D., Hill, C. "Strategic Alliances and the rate of new product development: An empirical study of entrepreneurial biotechnology firms". Journal of Business Venturing **11**: 41-55.
- Dennis, J., (1999). "Stabilization of poly-L-lysine/DNA polyplexes for in vivo gene delivery to the liver." Biochimica et Biophysica Acta **1444**: 171-190.
- Delteil, C., Teissié, J., Rols M. (2000) "Effect of serum in vitro electrically mediated gene delivery and expression in mammalian cells". Biochimica et Biophysica Acta **1467**: 362-368.
- Deshmukh, H., Huang, L. (1997). "Liposome and polylysine mediated gene transfer". New Journal of Chemistry **21**: 113-124.
- Durland, R., Eastman, E. (1998) "Manufacturing and quality control of plasmid-based gene expression systems". Advanced Drug Delivery Review **30**: 33-48.
- Duzgunes, N., Straubinger, R.M., Baldwin, P.A., Friend,D.S., Paphadjopoulos, D. (1985) "Proton-Induced Fusion of Oleic Acid- Phospatidylethanolamine Liposomes" Biochemistry **24**: 3091-3098.
- Eastman, S., Tousignant, J., Smith, A., Cheng, S., Scheule, R. (1997). "Biophysical characterization of cationic lipid:DNA complexes". Biochimica et Biophysica Acta **1325**: 41-62.
- Elimelech, M., Gregory, J., Jia, X., Williams, R., (1995). Particle Deposition and Aggregation-Measurement, Modelling and Simulation-Colloids and Surface Engineering Series.: 180-186
- El Ouahabi, A., Thiry, M., Pector, V., Fuks, R., Ruyschaert, J, M., Vandenbranden, M., (1997). "The role of endosome destabilizing activity in the gene transfer process mediated by cationic lipids." Federation of European Biochemical Societies **414**(2): 187-192.

Even-Chen, S., Barenholz, Y. (2000) "DOTAP cationic liposomes prefer relaxed over supercoiled plasmids". Biochimica et Biophysica **1509**: 176-188.

Felgner, P., L., (1997). "Nonviral strategies for Gene Therapy." Scientific American **276**(6): 102-106.

Ferrari, M., Nguyen, C., Zelphati, O., Tsai, Y., Felgner, P. (1998). "Analytical Methods for the Characterisation of Cationic Lipid-Nucleic Acid Complexes". Human Gene Therapy **9**: 341-351.

Ferrari, M., Rusalov, D., Enas, J., Wheeler, C. (2001). "Trends in lipoplex physical properties dependent on cationic lipid structure, vehicle and complexation procedure do not correlate with biological activity". Nucleic Acids Research **29**: 1539-1548.

Finsinger, D., Remy, J., Koch, C., Plamk, C. (2000). "Protective copolymers for nonviral gene vectors: synthesis, vector characterization and application in gene delivery". Gene Therapy **7**: 1183-1192.

Fischer, D., Bieber, T., Brüsselbach, S., Elasässer, H., Kissel, T. (2000). "Cationized human serum albumin as a non-viral system for gene delivery? Characterization of complex formation with plasmid DNA and transfection efficiency". International Journal of Pharmaceutics **225**: 97-111.

Frederiksen, K., Petri, N., Abrahamsen, N., Poulsen, H. (1999). "Gene therapy for lung cancer". Lung Cancer **23**: 191-207.

Frederiksen, S., Kalus., Petri, Andreas., Abrahamsen, Niels., Poulsen, Hans, Skovgaard (1999). "Gene therapy for lung cancer." Lung Cancer **23**: 191-207.

Galanis, E., Vile, R., Russell, S. (2001) "Delivery systems intended for in vivo gene therapy of cancer: targeting and replication competent viral vectors". Critical Reviews in Oncology/Hematology **38**; 177-192.

Girão da Cruz, M., Simões, S., Pires, P., Nir, S., Pedroso de Lima, M. (2001). "Kinetic analysis of the initial steps involved in lipoplex-cell interactions: effect of various factors that influence transfection activity". Biochimica et Biophysica Acta **1510**: 136-151.

Godbey, W., T., Mikos, A.G., (2001). "Recent progress in gene delivery using non-viral transfer complexes." Journal of Controlled Release **72**: 115-125.



- Godbey, W., Wu, K., Mikos, A. (1999) "Tracking the intracellular path of poly(ethylenimine)/DNA complexes for gene therapy". Proceedings of the National Academy **96**: 5177-5181.
- Goldman, C., Soroceanu, L., Smith, N., Gillespie, Y., Shaw, W., Burgess, S., Bilbao, G, Curiel, D. (1997) "In vitro and in vivo delivery mediated by a synthetic polycationic amino polymer". Nature Biotechnology **15**:462-466.
- Gorecki, P. (1986). "The importance of being first". International Journal of Industrial Organization **41**: 371-395.
- Gregoriadis, G., Bacon, A., Caparros-Wanderley, W., McCormack, B. (2002). "A role for liposomes in genetic vaccination". Vaccine **20** B1-B9.
- Hambleton, P. (1996). "Extended Summaries: SCI Biotechnology Group Meeting Gene Therapy: Are there prospects for Industry?" Journal of Chemical Technology, Biotechnology **66**: 95-104.
- Hara, M., Miyake, J., (2001). " Calcium alginate gel-entrapped liposomes" Materials Science and Engineering **17**: 101-105
- Hart, S., L., Harbottle, R.P., Cooper, R., Miller, A., Williamson, R., Coutelle, C., (1995). "Gene delivery and expression mediated by an integrin binding peptide." Gene Therapy: 552-554.
- Hart, S., L., (1999). "Integrin-mediated vectors for gene transfer and therapy." Current Opinion in Molecular Therapeutics **1(2)**: 197-203.
- He, S., Arscott, P., Bloomfield, V. (2000). "Condensation of DNA by Multivalent Cations: Experimental Studies of Condensation Kinetics". Biopolymers **53**: 329-341.
- Hellweg, T., Henry-Toulmé, Chambon, M., Roux, D. (2000). "Intercation of short DNA fragments with the cationic polyelectrolyte poly(ethylene imine): a dynamic light scattering study". Colloids and Surfaces: Physicochemical and Engineering Aspects **163**: 71-80.
- Helt, N., Gauger, M., Zhao, J., Slack, G., Pietryka, J., I, Y. (2001). "Characterization of a polymer-stabilized liposome system". Reactive and Functional Polymers **48**: 181-191.
- Ho, M. (2003). "Horizontal Gene Transfer-The hurdle hazards of Genetic Engineering". Institute of Science in Society. Websource: <<http://www.i-sis.org>>

Hong, K., Zheng, W., Baker, A., Papahadjopoulos, D. (1997). "Stabilisation of cationic liposome-plasmid DNA complexes by polyamines and poly(ethylene glycol)-phospholipid conjugates for efficient *in vivo* gene delivery". FEBS Letters **400**: 233-237.

Hounslow, M., J., Mumtaz, H, S., Collier, A, P., Barrick, J,P., Bramley, A,S., (2001). "A micro-mechanical model for the rate of aggregation during precipitation from solution." Chemical Engineering Science **56**: 2543-2552.

Jenkins, R., Meng, Q., Hodges, R., Lee, L., Bottoms, S., Laurent, G., Willis, D, Ayazi Shamlou, P., McAnulty, R., Hart, S. (2003) "Formation of LID vector complexes in water alters physiochemical properties and enhances pulmonary gene expression in vivo". Gene Therapy **10**: 1026-1034.

Jenkins, R., G., Herrick, S.E., Meng, Q-H., Kinnon, C., Laurent G,J., McAnulty, R.J., Hart, S, L., (2000). "An integrin-targeted non-viral vector for pulmonary gene therapy." Gene Therapy **7**: 393-400.

Kay, M., Liu, D., Hoogerbrugge, P. (1997). "Gene Therapy". Proceedings of the National Academy **94**: 12744-12746.

Kennedy, M., T., Pozharski, Edwin, V., Rakhmanova, Vera, A., MacDonald, Robert, C., (2000). "Factors Governing the Assembly of Cationic Scherman, D., Bessodes, Michael., Cameron, Beatrice., Herscovici., Hofland Hans., Pitard, Bruno., Soubrier, Fabienne., Wils, Pierre., Crouzet, Joel., (1998). "Application of lipids and plasmid design for gene delivery to mamalian cells." Current Opinion in Biotechnology **9**: 480-485.

Kirjavainen, M., Urtti, A., Jaaskelainen, Marjukka Suhonen, T., Paronrn, P., Valjakka-Koskela, R., Kiesvaara, J., Monkkonen, J., (1996) " Interaction of liposomes with human skin in-vitro – the influence lipid composition and structure", Biochimica et Biophysica **1304**: 179-189

Kreiss, P. C., Beatrice., Rangara, Ravi., Mailhe, Philip., Aguerre-Charriol, Oliver., Airiau, Marc., Scherman, Daniel., Crouzet, Joel., Pitard, Bruno (1999). "Plasmid DNA size does not affect phsiochemcial properties of lipoplexes but modulates gene transfer efficiency." Nucleic Acids Research **27(19)**: 3792-3798.

Kumar, N., Scheer, L., Kotler, P. (2000) "From Market Driven to Market Driving". European Management Journal, **18**: 129-142.

Kwoh, D., Y., Coffin, Christopher, C., Lollo, Charles, P., Jovenal, Jocelyn, Banaszczyk, Mariusz, G., Mullen, Patricia., Philips, Alison., Amini Arjang., Fabrycki, Joanne., Bartholomew, Richard, M., Brostoff, Steve, W., Carlo, Dennis, J., (1999). "Stabilization of poly-L-lysine/DNA polyplexes for in vivo gene delivery to the liver." Biochimica et Biophysica Acta **1444**: 171-190.

Lai, E., Van Zanten, J. (2001). "Monitoring DNA/Poly-L-Lysine Polyplex Formation with Time-Resolved Multiangle Laser Light Scattering". Biophysical Journal **80**: 864-873.

Lambert, G., Fattal, E., Couvreur, P. (2001). "Nanoparticulate systems for the delivery of antisense oligonucleotides". Advanced Drug Delivery Reviews **47**: 99-112.

Le Berre, F., Chauveteau, G., Pefferkorn, E. (1998). "Shear Induced Aggregation/Fragmentation of Hydrated Colloids". Journal of Colloid and Interface Science **199**: 13-21.

Le Brun, P., de Boer, A., Gjaltema, D., Hagedoorn, P., Heijerman, H., Frijlink, H. (1999). "Inhalation of tobramycin in cystic fibrosis Part 1: The choice of nebulizer". International Journal of Pharmaceutics **189**: 205-214.

Lee, D., Bonner, J., Garton, L., Ernest, A., Autenreith, R. (2002). "Modelling coagulation kinetics incorporating fractal theories comparison with observed data". Water Research **36**: 1056-1066.

Lee, L., Siapati, E., Jenkins, R., McAnulty, R., Hart, S., Ayazi Shamlou, P. (2003) "Biophysical characterization of an integrin-targeted non-viral vector". Medical Science Monitor **9**; 54-61.

Lee, D., Gon., Bonner, James, S., Garton, Laurie, S., Ernest, Andrew, N.S., Autenreith, Robin, L., (2002). "Modelling coagulation kinetics incorporating fractal theories: comparison with observed data." Water Research **36**: 1056-1066.

Lee, L. K., Mount, C.N., Ayazi Shamlou, P. (2001). "Characterisation of the physical stability of colloidal polycation-DNA complexes for gene therapy for gene therapy and DNA vaccines." Chemical Engineering Science **56**: 1-10.

Ledley, F., D., (1996). "Pharmaceutical Approach to Somatic Gene Therapy." Gene Therapy **13**(11): 1595-1614.

Levy, M., Susana., O'Kennedy, Ronan, D., Ayazi-Shamlou, P., Dunnill, Peter., (2000). "Biochemical engineering approaches to the challenges of producing pure plasmid DNA." Trends in Biotechnology **18**: 296-304.

Levy, M., Ciccolini, L., Yim, S., Tsai, J., Titchner-Hooker, N., Ayazi-Shamlou, P., Dunnill, P. "The effects of material properties and fluid flow intensity on plasmid DNA recovery during cell lysis". Chemical Engineering Science **54**: 3171-3178.

Levy, M., Collins, I., Yim, S., Ward, J., Titchener-Hooker, N., Ayazi Shmalou, P., Dunnill, P. (1999). "Effect of shear plasmid DNA solution." Bioprocess Engineering **20**:7-13.

Li, S., Tseng, W., Beer Stolz, D., Wu, S., Watkins, S., Humag, L. (1999) "Dynamic changes in the characteristics of cationic lipidic vectors after exposure to mouse serum: implications for intravenous lipofectin". Gene Therapy **6**:585-594.

Liang, K., W., Hoffman, Eric, P., Huang, Leaf., (2000). "Targeted delivery of plasmid DNA to Myogenic cells via Transferin-Conjugated Peptide Nucleic Acid." Molecular Therapy **1**(3): 236-243.

Luo, D., Saltzman, W, Mark., (2000). "Synthetic DNA delivery systems." Nature Biotechnology **18**: 33-37.

Maa, Y-M., Pretrelski, S. (2000). "Biopharmaceutical Powder: Particle Formation and Formulation Considerations." Current Pharmaceutical Biotechnology **1**: 283-302.

Marquet, M., Horn, Nancy, A., Meek, Jennifer, A. (1997). "Characterization of Plasmid DNA Vectors for Use in Human Gene Therapy, Part 2". BioPharm: 40-45.

Marquet, M., Horn, Nancy, A., Meek, Jennifer, A (1997). "Characterization of Plasmid DNA Vectors for Use in Human Gene Therapy, Part 1". BioPharm: 42-48.

Marquet, M., Horn, Nancy, A., Meek, Jennifer, A. (1995). "Process Development for the Manufacture of Plasmid DNA Vectors for use in Gene Therapy." BioPharm: 26-37.

Martin, P., Thomas, S. (1998) " The Commercial Development of Gene Therapy in Europe and the USA". Human Gene Therapy **9**:87-114.

Miller, N., Vile, R. (1995). " Targeted vectors for gene therapy". The FASEB Journal: **9** 190-199.

Mok, K., W,C., Lam, Angela, M,I., Cullis, Pieter, R., (1999). "Stabilized plamsid-lipid particles: factors influencing plasmid entrapment and transfection properties." Biochimica et Biophysica Acta **1419**: 137-150.

- Molina-Bolívar, J., Galisteo-González, F., Hidalgo-Álvarez. (1998). "Cluster Morphology of Protein-Coated Polymer Colloids". Journal of Colloid and Interface Science **208**: 445-454.
- Moret, I., Peris, J., Guillem, V., Benet, M., Revert, F., Dasi, F., Crespo, A., Alimo, S. (2001). "Stability of PEI-DNA and DOTAP-DNA complexes: effect of alkaine pH, heparin and serum". Journal of Controlled Release **76**: 169-181.
- Morris, M.C., Chaolin, L., Méry, J., Heitz, F., Divita, G. (1999). "A novel potent strategy for gene delivery using a single peptide vector as a carrier". *Nucleic Acids Research* **27**: 3510-3517.
- Morton, F. (2000) "Barriers to entry, brand advertising, and genetic entry in the US pharmaceutical industry". International Journal of Industrial Organization **18**: 1085-1104.
- Mount, C., Lee, L., Yasnin, A., Scott, A., Fearn, T., Ayazi Shamlou, P. (2003). "The influence of physio-chemical and process conditions on the physical stability of plasmid DNA complexes using response surface methodology". Biotechnology and Applied Biochemistry **37**: 225-234.
- Mountain, A. (2000). "Gene therapy: the first decade." Trends in Biotechnology **18**: 119-128.
- Mui, B., Ahkong, L., Chow, L., Hope, M. (2000). "Membrane perturbation and mechanisms of lipid-mediated transfer of DNA into cells". Biochimica et Biophysica Acta **1467**: 281-292.
- Napper, D.H. (1989) Polymeric stabilization of colloidal dispersions, Academic Press Limited, London.
- Nishikawa, M., Huang, L (2001). "Nonviral Vectors in the New Millennium: Delivery Barriers in Gene Therapy." Human Gene Therapy **12**: 861-870.
- Nishikawa, M., Yamauchi, K., Morimoto, K., Ishida, E., Takakura, Y., Hshida, M. (2001). "Hepatocyte-targeted in vivo gene expression by intravenous injection of plasmid DNA complexed with synthetic multi-functional gene delivery system". *Gene Therapy* **7**: 548-555.
- Olesik, J., Bates, L. (1995). "Characterisation of aerosols produced by pneumatic nebulizers for inductively coupled plasma sample introduction: effect of liquid and gas flow rates on volume based drop size distributions". Spectrochimica Acta **50B** 285-303.
- Quemada, D., Berli, Claudio (2001). "Energy of interaction in colloids and its implications in rheological modelling." Advances in Colloid and Interface Science.

Ogris, M., Wagner, E. (2002) "Targeting tumors with non-viral gene delivery systems". Drug Discovery Today **8**: 479-485.

Ogris, M., Brunner, S., Schüller, S., Kirches, R., Wagner, E. (1999). "PEGylated DNA/transferring-PEI complexes: reduced interaction with blood components, extended circulation in blood and potential for systemic gene delivery". *Gene Therapy* **6**: 595-605.

Pedroso de Lima, M., C., Simoes, Sergio., Pired Pedro., Faneca, Henrique, Duzgunes, Nejat., (2001). "Cationic lipid-DNA complexes in gene delivery: from biophysics to biological applications." Advanced Drug Delivery Reviews **47**: 277-294.

Plank, C., Tang, M., Wolfe, A., Szoka, F. (1999) "Branched Cationic Peptides for Gene Delivery: Role of Type and Number of Cationic Residues in Formation and in Vitro Activity of DNA Polyplexes".

P.-Miksa, Michael.,(2001). "The synthesis of modified integrin-binding peptides." First Year Report. University College London : 1-97

Popescu, A., I., (1996). "Cell-cell interactions." Bioelectrochemistry and Bioenergetics **40**: 153-157.

Porter, M.E., (2004) *Competitive Advantage, Creating and Sustaining Superior Performance*, Free press, New York.

Pouton, C., W., Seymour, Leonard, W. (1998). "Key issues in non-viral gene delivery." Advanced Drug Delivery Reviews **34**: 3-19.

Prazeres, D., Ferreira, G., Monteiro, G., Cooney., C. Cabral, J. (1999) " Large scale production of pharmaceutical-grade plasmid DNA for gene therapy: problems and bottlenecks". *TIBTECH* **17**:169174.

Ramsay, E., Hadgraft, Jon., Birchall James., Gumbleton, Mark., (2000). "Examination of the biophysical interaction between plasmid DNA and the polycations, polylysine and polyornithine, as a basis for their differential gene transfection in-vitro." International Journal of Pharmaceutics **210**: 97-107.

Raper, A., Amal, R. (1993). "Measurement of Aggregate Fractal Dimensions Using Static Light Scattering". Part. Part. Syst. Charact. **10**: 239-245.

- Reddy, J., Low, P. (2000). "Enhanced folate receptor mediated gene therapy using a novel pH-sensitive lipid formulation". Journal of Controlled Release **6**: 27-37.
- Robinson, H., Ginsberg, H., Davis, H., Johnston, S., Liu, M. (1996) "The scientific future of immunization". The American Academy of Microbiology 7-21.
- Safinya, C., R., (2001). "Structures of lipid-DNA complexes: supramolecular assembly and gene delivery." Current Opinion in Structural Biology **11**: 440-448.
- Sakurai, F., Nishioka, Tsuyoshi., Yamashita, Fumiyo., Takakura, Yoshinobu., Hashida., Mitsuru., (2001). "Effects of erythrocytes and serum proteins on lung accumulation of lipoplexes containing cholesterol or DOPE as a helper lipid in the single-pass rat lung perfusion system." European Journal of Pharmaceutics and Biopharmaceutics **52**: 165-172.
- Sakurai, F., Inoue, R., Nishino, Y., Okuda, A., Matsumoto, O., Taga, T., Yamashita, F., Takakura, Y., Hashida, M. (2000). "Effect of DNA/liposome mixing ratio on the physicochemical characteristics, cellular uptake and intracellular trafficking of plasmid DNA/ cationic liposome complexes and subsequent gene expression". Journal of Controlled Release **66**: 255-269.
- Salman, H., Zbaida., Rabin, Y., Chatenay, D., Elbaum, M. (2001). "Kinetics and mechanisms of DNA uptake into the cell nucleus". Biophysics **98**:7247-7752.
- Sarkar, S., Levy, M.S., Hart, S.L., Hailes, H.C., Tabor, A.B., Ayazi Shamlou, P. (2004). "The fractal structure of polycation-DNA complexes". Biotechnology and Applied Biochemistry ,**40**: 1-10.
- Sarkar, S., Levy, M.S., Hart, S.L., Wong, J.C., Hurley, C.A., Pilkington-Miksa, M., Hailes, H.C., Tabor, A.B., Ayazi Shamlou, P. (2003). "Impact of biophysical and chemical properties of non-viral formulation on cell transfection". AIChE Annual Conference Proceedings **2003**.
- Sarkar, S., Zhang, H., Levy, M.S., Hart, S.L., Hailes, H.C., Tabor, A.B., Ayazi Shamlou, P. (2003). "Prediction of size distribution of lipid-peptide-DNA vector particles using Monte Carlo simulation technique". Biotechnology and Applied Biochemistry **38**: 95-102.
- Schaffer, D., Fidelman, N., Dan, N., Lauffenburger, D. (1999). "Vector Unpacking as a Potential Barrier for Receptor-Mediated Polyplex Gene Delivery". Biotechnology and Bioengineering, **67**:598-606.

Schmutz, M., Durand, D., Debin, A., Palvadeau, Y., Etienne, A., Thierry, A. (1999). "DNA packing in stable lipid complexes designed for gene transfer imitates DNA compaction in bacteriophage". Biophysics 96: 12293-12298.

Scherman, D., Bessodes, M., Cameron, B., Herscovici, J., Hofland, H., Pitard, B., Soubrier, F., Wils, P., Crouzet, J. (1998). "Application of lipids and plasmid design for gene delivery to mammalian cells". Current Opinion in Biotechnology 9: 480-485.

Schnaar, S. (1995). "Managing Imitation Strategy: How later entrants seize markets from pioneers". New York: Free Press.

Schreier, H., Gagne, Lucie., Bock, Thomas., Erdos, E, Gregory., Druzgala, Pascal., Conary, Jon, T., Muller, Bernd, W., (1997). "Phsiochemical properties and in vitro toxicity of cationic liposome cDNA complexes." Pharmaceutica Acta Helvetiae: 215-223.

Simons, J. (2003) "Taking on Viagra". Fortune 147: 10-15.

Simones, S., Slepishkin, V., Gaspar, R., Pedroso de Lima., Düzgüneş. (1998) "Gene delivery by negatively charged ternary complexes of DNA cationic lipospmes and transferring or fusigenic peptides". Gene Therapy 5 955-964.

Smisterova, J., Wagenaar, Anno., Stuart, Marc, C,A., Polushkin, Evgeny., Brinke, Gerrit ten., Hulst, Ron., Engberts, Jan, B, F, N., Hoekstra, Dick., (2001). "Molecular Shape of Cationic Lipid Controls the Structure of Cationic Lipid/ Diolephosphatidy lethanolamine-DNA Complexes and the Efficiency of Gene Delivery." The Journal of Biological Chemistry 276(50): 47615-47622.

Smith, J., Zhang, Yilin., Niven, Ralph., (1997). "Toward development of a non-viral gene therapeutic." Advanced Drug Delivery Reviews 26: 135-150.

Smith, M., Matsoukas, Themis., (1998). "Constant-number Monte Carlo simulation of population balances." Chemical Engineering Science 53(9): 1777-1786.

Smoluchowski, M. (1917). "Versuch einer mathematischen Theorie der Koagukationskinetic kolloider Lsungen." Z. Physik Chem 92: 129-168.

Son, K., K., Tkach, Diane., Hall, Kevin, J., (2000). "Efficient in vivo gene delivery by the negatively caherged complexes of cationic liposomes and plasmid DNA." Biochimica et Biophysica Acta 1468: 6-10.



- Subramanian, M., Holpainen, J., Paukku, T., Eriksson, O., Huhtaniemi, I., Kinnunen, P. (2000). "Characterisation of three novel cationic lipids as liposomal complexes with DNA". *Biochimica et Biophysica Acta* **1466**: 289-305.
- Sudimack, J., B.A., LEE, Robert, J., (2000). "Targeted drug delivery via the folate receptor." *Advanced Drug Delivery Reviews* **42**: 147-162.
- Szoka, J., Francis, C., Xu, Yuhong, Zelphati, Oliver., (1997). "How are nucleic acids released in cells from cationic lipid-nucleic acid complexes." *Advanced Drug Delivery Reviews* **24**: 291.
- Tam, P., Monck, M., Lee, D., Ludkovski, O., Leng, E., Clow, K., Stark, H., Scherrer. (2000) "Stabilized plasmid-lipid particles for synthetic gene therapy" *Gene Therapy* **7**: 1867-1874.
- Tang, S., Preece, J.M., McFarlane, C.M., Zhang, Z., (2000) "Fractal Morphology and Breakage of DLCA and RLCA Aggregates" *Journal of Colloid and Interface Science* **221**: 114-123.
- Tang, S. (1999) "Prediction of fractal properties of polystyrene aggregates". *Colloids and Surfaces A: Physicochemical and Engineering Aspects* **157**: 185-192.
- Tang, F., Wang, W., Hughes, J. (1999). "Cationic liposomes containing disulphide bonds in delivery of plasmid DNA". *Journal of Liposome Research* **9**: 331-347.
- Templeton, S., Nancy., Lasic, D. Danilo. (1999). "New Directions in Liposome Gene Delivery." *Molecular Biotechnology* **11**: 175-180.
- Thomas, C., Ehrhardt, A., Kay, M. (2003). "Progress and problems with the use of viral vectors for gene therapy". *Nature* **4**: 346:359
- Thomas, D., N., Judd, S.J., Fawcett, N., (1999). "Flocculation Modelling: A Review." *Water Research* **33**(7): 1579-1592.
- Tirasdo-Mirando, M., Schmitt, A., Callejas-Fernández., Fernández-Barbero. (2000). "Dynamic scaling and fractal structure of small colloidal clusters". *Colloids and Surfaces A: Physicochemical and Engineering Aspects* **162**: 67-73.
- Tros de Ilarduya., Düzgüneş, N. (2000). "Efficient gene transfer by transferrin lipoplexes in the presence of serum". *Biochimica et Biophysica Acta* **1463**: 333-342.

Trubetskoy, V., Loomis, A., Hagstrom, J., Budker, V., Wolff, J. (1999). "Layer by layer deposition of oppositely charged polyelectrolytes on the surface of condensed DNA particles". Nucleic Acids Research **27**: 3090-3095.

Trubetskoy, V., Loomis, A., Slattum, P., Hagstrom, J. (1999). "Caged DNA does not aggregate in high ionic strength solutions". Bioconjugate Chemistry **10** : 624-628.

Tureck, J., Bubertret, C., Jaslim, G., Antonakis, K., Scherman, D, Pitard, B. (2000). "Formulations which increase the size of lipoplexes prevent serum-associated inhibition of transfection". The Journal of Gene Medicine **2**: 32-30.

Tushman, M., Anderson, P (1986). "Technological discontinuities and organizational environments." Administrative Science Quarterly **31**: 439-465.

Tsang, L., Beers, D., (2005) "Follow-on biological products: the regulatory minefield". Life Sciences: 105-110.

Udeuehi, A., N., Stammberger, U., Frese, S, Schmid, R,A., (2001). "Efficiency of non-viral gene delivery systems to rat lungs." European Journal of Cardio-thoracic Surgery: 159-163.

Uike, H., Sakakibara, R., Iwanaga, K., Ide, M. (1998) "Efficiency of targeted gene delivery of Ligand-Poly-Lysine Hybrids with different cross links". Bioscience, Biotechnology, Biochemistry **62**: 1247-1248.

Varga, C., M., Wickham, Thomas, J., Lauffenburger, Douglas, A., (1999). "Receptor-Mediated Targeting of Gene Delivery Vectors: Insights from Molecular Mechanisms for Improved Vehicle Design." Biotechnology Bioengineering **70**: 593-605.

Verbaan, F., J., Oussoren, C., van Dam, I,M., Takakura, Y., Hashida, M., Crommelin, D,J,A., Hennink, W,E., Storm, G., (2001). "The fate of poly(2-dimethyl amino ethyl)methacrylate-based polyplexes after intravenous administration." International Journal of Pharmaceutics **214**: 99-101.

Walde, P., Ichikawa, S. (2001). "Enzymes inside lipids vesicles: preparation, reactivity and applications". Biomolecular Engineering **18**: 143-177.

Wade-Martins, R., Frampton, J., James, M. (1999). "Long-term stability of large insert genomic DNA episomal shuttle vectors in human cells". Nucleic Acids Research. **27**:1674-1682.

Wattiaux, R., Laurent, Nathanael., Wattiaux-De Coninck, Simone., Jadot, Michel., (2000). "Endosomes, lysosomes: their implications in gene transfer." Advanced Drug Delivery Reviews **41**: 201-208.

Welsh, M., Smith, A, (1995) "Cystic Fibrosis". Scientific American **December** 1-8.

Wernerfelt, B. (1984) "A resource-based view of the firm." Strategic Management Journal. **5** (April-June):171-180.

Wheeler, C., J., Felgner, Philip, L., Tsai, Yali, J., Marshall, John., Sukhu, Loretta., Doh, Soeun, G., Hartikka, Jukka., Nietupski, Jennifer., Manthorpe, Marston., Nichols, Margaret., Plewe, Michael., Liang, Xiaowu., Norman, Jon., Smith, Alan., Cheng, H, Seng., (1996). "A novel cationic lipid greatly enhances plasmid DNA delivery and expression in mouse lung." Proc. National Academy of Science, USA **93**: 11454-11459.

Whitmore, M., Li, S., Huang, L. (1999) "LPD lipopolyplex initiates a potent cytokine response and inhibits tumour growth". Gene therapy **6**: 1867-1875.

Wilson, J.M. (1999) "Human Gene Therapy: Present and Future". Human Genome News **10** 1-3.

Xu, Y., Hui, S., Frederik, P., Szoka, C. (1999). "Physiochemical Characterisation and Purification of Cationic Lipopolyplexes". Biophysical Journal **77**: 341-353.

Yan, Y.D., Burns, J.L., Jameson, G.J., Biggs, S., (2002) "The fractal properties of latex particle aggregates formed in the presence of salt and non-adsorbing polymer" In print.

Yan, C., Chaudhari, A., Lee, S. (2002). "Dynamic scaling of diffusion limited reactions over fractal surfaces: computer simulation". Applied Surface Science **7856**: 1-8.

Yates, P., Yan, Y., Jameson, G., Biggs, S. (2001). "Heterocoagulation of Particle systems: Aggregation and aggregate structure determination". 6<sup>th</sup> World Congress of Chemical Engineering, Melbourne Australia 2001 1-11.

Yokoyami, M. (2002) "Gene delivery using temperature responsive polymeric carriers". Drug Discovery Today **7**:426-431.

Zauner, W., Brunner, S., Buschle, M., Ogris, M., Wagner, E. (1999). "Differential behaviour of lipid based and polycation based gene transfer systems in transfecting primary human fibroblasts: a potential role of polylysine in nuclear transport". Biochimica et Biophysica Acta **1428**: 57-67.

Zelphati, O., Uyechi, Lisa, S., Barron, Lee, G., Szoka Jr, Francis, C., (1998). "Effect of serum components on the physio-chemical properties of cationic lipid/ oligonucleotides complexes and on their interaction with cells." Biochimica et Biophysica Acta **1390**: 119-113.

Zhang, P., Reimer, D., Zhang, G., Lee, P., Bally, M. (1997). "Self-Assembling DNA-Lipid Particles for Gene Transfer". Pharmaceutical Research **14**: 190-196.

# Appendices

## INTENSITY SCANS (STATIC LIGHT SCATTERING) ON PCS 4800

### Pre-experiment

Allow laser to warm up.

Run pump to clean vat water. Change membrane frequently.

### Performing angular scans on sample

File-New-Intensity Window

Enter parameters in Measure- Document

Temperature 25 C

Refractive index 1.330

Wavelength 633 nm

Setup- Intensity v. Angle graph should be on PC screen

Setup: Measurement sequence for angular scan

### Example:

No. of angles 23

Start angle 12 degrees

End angle 100 degrees

Subscans/angle 10

Duration/angle 10 seconds

Inspect - yes

Manually rotate aperture for PM to appropriate width, e.g. 100  $\mu\text{m}$

Measure-Start sequence-Angle scan

Goniometer should swing round to 12 degrees and begin collecting intensity data at rate of 10 seconds per angle. Number of scanned angles = 23 (i.e. one measurement every 4°)

When angular scan is complete, press "GO" to execute similar angular scan. Perform this for a few hours.

Information obtained is Intensity ("Count rate") vs. angle and Q (ignore this).

Radius of gyration obtained is incorrect because various parameters were not specified.

## **SAMPLE PREP**

### **Notes**

All procedures involving Burchard sample cells best performed in laminar flow cabinet to avoid dust contamination. Seal Burchard cell with stopper before transferring from cabinet to spectrometer.

Use Burchard sample cells for samples. Glass walls of 10 mm round cuvettes (for size measurements at 90 degrees) give too much flare especially at angles below 30 degrees.

Rinse all equipment with particle free water (Fresenius Kabi).

Calibrate daily before experiments with pure toluene in Burchard cell (best to keep one cell apart for this purpose). Angular scan (e.g. 10 to 140 degrees) on toluene will give constant intensities at all angles (flat line) because toluene is an isotropic scatterer.

Minimum sample volume for laser beam to pass through sample in Burchard cell is 3.8 ml.

Before transferring sample (in Burchard cell) to holder in water vat, clean its outside walls (from fingerprints, dust, etc.). Breathe on its outside walls and polish with tissues. Put into spectrometer and run pump for a few seconds to get rid of any bubbles on Burchard cell.

### **Procedure**

Calibrate with toluene.

Fill Burchard cell with particle free water.

Perform angle scan on water sample to ensure cleanliness of cell and water in vat. Count rates at forward (small) angles should be less than 5000 (5 KCts/sec).

Empty Burchard cell and fill with sample (e.g. addition of 2 ml DNA to 2 ml PLL in cell).

Transfer to spectrometer and perform angular scan.

Ensure count rates at forward (small) angles from samples are always less than 1 m (1000 KCts/sec).

## Papers









































